

University of Nebraska - Lincoln

DigitalCommons@University of Nebraska - Lincoln

Mechanical (and Materials) Engineering --
Dissertations, Theses, and Student Research

Mechanical & Materials Engineering,
Department of

Summer 8-2013

PAN Nanofibers and Nanofiber Reinforced Composites

Cheng Ren

University of Nebraska-Lincoln, chengren@huskers.unl.edu

Follow this and additional works at: <https://digitalcommons.unl.edu/mechengdiss>



Part of the [Mechanics of Materials Commons](#), [Nanoscience and Nanotechnology Commons](#), [Other Engineering Science and Materials Commons](#), and the [Polymer and Organic Materials Commons](#)

Ren, Cheng, "PAN Nanofibers and Nanofiber Reinforced Composites" (2013). *Mechanical (and Materials) Engineering -- Dissertations, Theses, and Student Research*. 59.
<https://digitalcommons.unl.edu/mechengdiss/59>

This Article is brought to you for free and open access by the Mechanical & Materials Engineering, Department of at DigitalCommons@University of Nebraska - Lincoln. It has been accepted for inclusion in Mechanical (and Materials) Engineering -- Dissertations, Theses, and Student Research by an authorized administrator of DigitalCommons@University of Nebraska - Lincoln.

PAN NANOFIBERS AND NANOFIBER REINFORCED COMPOSITES

by

Cheng Ren

A THESIS

Presented to the Faculty of

The Graduate College at the University of Nebraska

In Partial Fulfillment of Requirements

For the Degree of Master of Science

Major: Mechanical Engineering and Applied Mechanics

Under the Supervision of Professor Yuris Dzenis

Lincoln, Nebraska

August, 2013

PAN NANOFIBERS AND NANOFIBER REINFORCED COMPOSITES

Cheng Ren, M.S.

University of Nebraska, 2013

Adviser: Yuris Dzenis

Nanomaterials play an important role in the development of nanotechnology. They possess unique mechanical, physical, and chemical properties coupled with small size and ultrahigh surface area that can provide critical advantages for applications. Continuous nanofibers attract special interest due to their dual nano-macro nature and ability to bridge scales. Nanofibers are being considered for a broad range of applications spanning advanced filters, separation membranes, ultrasensitive sensors, micro/nano actuators, nanoprobe, tissue engineering scaffolds, protective and smart closing, and multifunctional composites. Most of these applications require certain mechanical properties and robustness. However, the literature on the mechanical behavior of nanofibers and their assemblies and composites is very sparse. The objective of this thesis was to manufacture and study the mechanical behavior of nanofiber networks and nanofiber reinforced composites with several nanofiber orientation distributions. Uniform diameter polyacrylonitrile (PAN) nanofibers were manufactured using electrospinning technique. In order to find the optimum manufacturing conditions, the effects of several electrospinning process parameters on PAN nanofiber diameters and orientation distributions were analyzed systematically experimentally. Nanofiber morphologies were examined and statistically quantified by scanning electron microscopy. Non-linear mechanical properties of single nanofibers and aligned and random nanofiber networks

were investigated and compared. Aligned and random PAN nanofiber reinforced composites were fabricated and their anisotropic fracture properties were evaluated experimentally for the first time. It was shown that a small amount of nanofiber reinforcement produced significant improvements in fracture toughness of epoxy-based nanocomposites. The results of this study can be used in the development of nanofibrous materials and applications requiring a degree of mechanical robustness.

ACKNOWLEDGEMENTS

There are many friends, colleagues and family that I would like to thank for their continued support and guidance during my graduate studies.

First and foremost, I would like to express my sincere appreciation to my adviser, Prof. Yuris Dzenis, for his guidance, advice and support of this research over the past few years. I would like to thank Prof. Li Tan, Prof. Jung Yul Lim for serving on my supervisory committee. Their thoughtful suggestions of this thesis are greatly appreciated.

Specially, I would like to thank Dr. Xiangfa Wu, Dr. Yongkui Wen, Dr. Xi Ren and Dr. Alexander Goponenko for their patient training and help to setup experiments. I would like to thank Ms. Yan Zou and Mr. Yong Liu for their assistance in this research. I would also like to thank all the past and current members of Prof. Dzenis' group: Dr. Zhenyu Li, Dr. Yong Chen, Dr. Lihua Liu, Dr. Anastasia Desyatova, Dr. Alexey Kamenskiy, Dr. Yury Salkovskiy, Mr. Mikhail Kartashov, Mr. Chad Peterson, Mr. John Hannappel, Ms. Kazi Israt Jahan, Mr. Mohammad Nahid Andalib, Mr. Dimitry Papkov, and Mr. Kaspars Maleckis. You have had an impact on my graduate experience both individually and collectively.

Many thanks go to all faculty, staff, and students in the Department of Mechanical and Materials Engineering at University of Nebraska-Lincoln.

I would like to thank all of the grants and findings for making the research in this thesis possible. This research was supported by NSF, ARO, AFOSR, and NRI grants to

Prof. Dzenis.

Last but not least, I dedicate this work to my family. For my parents Xingwu Ren and Anyang Li, who supported and encouraged me throughout the process of my pursuing the M.S. degree. For my husband Zhen Li, I never would have achieved this without his love. He has always been there for me when I needed it most.

TABLE OF CONTENTS

List of Figures	ix
List of Tables	xv
Chapter 1: Introduction	1
1.1 Nanotechnology	1
1.2 Nanomaterials.....	3
1.3 Nanocomposites	4
1.4 Electrospinning.....	6
1.4.1 History	7
1.4.2 Electrospinning Process.....	8
1.4.3 Mechanisms of Electrospinning	10
1.4.4 Advantages of Electrospinning.....	11
1.5 Electrospun Nanofibers	11
1.5.1 Applications of Electrospun Nanofibers	13
1.5.2 Aligned Electrospun Nanofibers	15
1.5.3 Mechanical Properties of Nanofibers, Nanofiber Assemblies, and Nanofiber Reinforced Composites	16
1.6 Summary and Problem Formulation	18
Chapter 2: PAN Nanofiber Manufacturing.....	20
2.1 Experimental	20
2.1.1 PAN Solution Preparation	20
2.1.2 Electrospinning Setup.....	22
2.2 Evaluation of Electrospun Nanofiber Morphologies	23
2.2.1 SEM Sample Preparation	24
2.2.2 SEM Images	24
2.3 Electrospinning Parameters.....	39

2.3.1 Spinnability and Diameter of PAN Nanofibers in Different Manufacturing Conditions.....	39
2.3.2 Effects of Electrospinning Parameters on Nanofiber Diameter	43
2.3.2.1 Applied Voltage.....	43
2.3.2.2 PAN Solution Concentration.....	46
2.4 Thermal Analysis of Electrospun Nanofibers	49
2.5 Conclusions	53
 Chapter 3: PAN Nanofiber Networks	54
3.1 Aligned Nanofibers Manufacturing	54
3.2 Effects of Electrospinning Parameters	56
3.2.1 Effect of Collector Gap Size on Diameter and Orientation of Aligned Nanofibers	56
3.2.1.1 Effect of Collector Gap Size on Aligned Nanofibers Diameter	56
3.2.1.2 Effect of Collector Gap Size on Aligned Nanofibers Orientation Distribution.....	62
3.2.2 Effect of Manufacturing Duration on Aligned Nanofiber Orientation.....	67
3.2.3 Calculation of Orientation Parameters	68
3.3 Equivalent Thickness Measurement of Polymer Nanofiber Sheet	71
3.4 Mechanical Properties of PAN Nanofibers	72
3.4.1 Tensile Testing	72
3.4.2 Single PAN Nanofiber Testing.....	74
3.4.3 Aligned PAN Nanofiber Network Testing.....	77
3.4.3.1 Fiber Network Manufactured in 1 Hour.....	77
3.4.3.2 Fiber Network Manufactured in 2 Hours	79
3.4.4 Random Nanofiber Networks.....	80
3.4.5 Comparison of Mechanical Properties of Nanofiber Networks	83
3.5 Conclusions	85
 Chapter 4: PAN Nanofiber Reinforced Composites	86

4.1 Composites Manufacturing	86
4.1.1 Materials	86
4.1.2 Molding	87
4.1.3 Curing Cycle.....	88
4.1.4 PAN Nanofiber Reinforced Composites	89
4.1.4.1 Aligned PAN Nanofiber Reinforced Composites	89
4.1.4.2 Random PAN Nanofiber Reinforced Composites.....	90
4.2 Evaluation of Fiber Mass Fraction: V_m	92
4.3 Fracture Analysis of PAN Nanofiber Reinforced Composites	93
4.3.1 Selected Specimen Geometry and Data Reduction Method.....	96
4.3.2 Tensile Testing	97
4.3.3 Fracture Properties of Testing Materials	98
4.3.3.1 [0] nanocomposites.....	98
4.3.3.2 [90] nanocomposites.....	99
4.3.3.3 Random Nanofiber Reinforced Composites.....	101
4.3.3.4 Pure Epoxy	103
4.3.4 Data Summary and Analysis	104
4.3.5 SEM Images of Fracture Surface	107
4.4 Conclusions	110
 Chapter 5: Summary and Conclusions.....	 112
 Bibliography	 114
 Appendix: Diameter Distributions of PAN Nanofibers.....	 122

LIST OF FIGURES

Figure 1.1: Publications related to nanotechnology from 2000 to 2012. Data is from Web of Science.

Figure 1.2: Smart clothing runway show and SEM image of cloth fiber with coated nanoparticles

Figure 1.3: Illustration of the usage of polymer nanocomposites parts

Figure 1.4: Publications related to electrospinning from 2000 to 2012. Data is from Web of Science.

Figure 1.5: A setup for electrospinning

Figure 1.6: Photographs illustrating the instability region of an electrospun liquid jet. The capture time was on two different time scales: A. 1/250 s, and B. 18 ns, respectively.

Figure 1.7: Publication search on “electrospun nanofiber/nanofibers” from the Web of Science

Figure 1.8: SEM images of nanofibers

Figure 1.9: Application of nanofibers in filtration

Figure 1.10: Nanoreinforcement between plies of the traditional composites laminates

Figure 1.11: Setup for generating aligned nanofibers

Figure 1.12: Comparison of specific strength and specific energy to failure of as-spun PAN nanofibers (diamonds) with typical values for commercial and developmental fibers and materials

Figure 2.1: DMF solution (left) and PAN powder (right)

Figure 2.2: PAN solution: (a) before stirring and heating; (b) after mixing

Figure 2.3: Electrospinning setup

Figure 2.4: SEM samples

Figure 2.5: SEM images of 10% PAN nanofibers manufactured in (a) 8kV; (b) 9kV; (c) 10kV; (d) 11kV; (e) 12kV; (f) 13kV

Figure 2.6: SEM images of 11% PAN nanofibers manufactured in (a) 9kV; (b) 10kV; (c) 11kV; (d) 12kV; (e) 13kV; (f) 14kV

Figure 2.7: SEM images of 12% PAN nanofibers manufactured in (a) 8kV; (b) 9kV; (c) 10kV

Figure 2.8: SEM images of 13% PAN nanofibers manufactured in (a) 11kV; (b) 12kV; (c) 13kV; (d) 14kV; (e) 15kV

Figure 2.9: SEM images of 14% PAN nanofibers manufactured in (a) 9kV; (b) 10kV; (c) 11kV; (d) 12kV

Figure 2.10: Beaded electrospun PAN nanofibers

Figure 2.11: Effect of applied voltage on nanofiber diameter (a) 10% PAN; (b) 11% PAN; (c) 12% PAN; (d) 13% PAN; (e) 14% PAN

Figure 2.12: Effect of PAN solution concentration on nanofiber diameter (a) 9kV; (b) 10kV; (c) 11kV; (d) 12kV; (e) 13kV

Figure 2.13: The Perkin-Elmer Pyris TGA-7

Figure 2.14: SEM image of electrospun PAN nanofibers tested in TGA

Figure 2.15: TGA curves of selected electrospun PAN nanofibers

Figure 3.1: Electrospinning setup for manufacturing aligned PAN nanofibers

Figure 3.2: An example of aligned PAN nanofibers produced by the gap method

Figure 3.3: SEM images of aligned PAN nanofibers manufactured with 2cm gap size

Figure 3.4: SEM images of aligned PAN nanofibers manufactured with 3cm gap size

Figure 3.5: SEM images of aligned PAN nanofibers manufactured with 4cm gap size

Figure 3.6: SEM images of aligned PAN nanofibers manufactured with 5cm gap size

Figure 3.7: SEM images of aligned PAN nanofibers manufactured with 6cm gap size

Figure 3.8: Diameter distribution of aligned PAN nanofibers manufactured with 2cm gap size

Figure 3.9: Diameter distribution of aligned PAN nanofibers manufactured with 3cm gap size

Figure 3.10: Diameter distribution of aligned PAN nanofibers manufactured with 4cm gap size

Figure 3.11: Diameter distribution of aligned PAN nanofibers manufactured with 5cm gap size

Figure 3.12: Diameter distribution of aligned PAN nanofibers manufactured with 6cm gap size

Figure 3.13: Diameter of aligned PAN nanofibers manufactured with different gap size

Figure 3.14: Schematic definition of 0 degree orientation of aligned nanofibers

Figure 3.15: An example of aligned PAN nanofibers with 0 degree direction indicated by an arrow

Figure 3.16: SEM image and orientation distribution of aligned PAN nanofibers manufactured with 2cm gap

Figure 3.17: SEM image and orientation distribution of aligned PAN nanofibers manufactured with 3cm gap

Figure 3.18: SEM image and orientation distribution of aligned PAN nanofibers manufactured with 4cm gap

Figure 3.19: SEM image and orientation distribution of aligned PAN nanofibers manufactured with 5cm gap

Figure 3.20: SEM image and orientation distribution of aligned PAN nanofibers manufactured with 6cm gap

Figure 3.21: SEM image of aligned PAN nanofibers manufactured in 1 hour (left) and 2 hours (right)

Figure 3.22: f_p values of aligned nanofibers with different manufacturing gap size

Figure 3.23: g_p values of aligned nanofibers with different manufacturing gap size

Figure 3.24: NANO UTM Testing System by Agilent

Figure 3.25: Representative strain-stress curves of single PAN nanofibers

Figure 3.26: SEM images of single PAN nanofibers with diameters: (a) 420 nm (b) 375 nm

Figure 3.27: Effect of single nanofiber diameter on strength

Figure 3.28: Tensile testing of aligned PAN nanofibers

Figure 3.29: Representative strain-stress curves of aligned PAN nanofiber network manufactured in 1 hour

Figure 3.30: Representative strain-stress curves of aligned PAN nanofiber network manufactured in 2 hours

Figure 3.31: SEM images of random PAN nanofiber network

Figure 3.32: Tensile testing of random PAN nanofiber network

Figure 3.33: Representative strain-stress curves of random PAN nanofiber network

Figure 3.34: Strength of aligned (manufactured in 1 hour and 2 hours) and random PAN nanofiber network

Figure 3.35: Young's Modulus of aligned (manufactured in 1 hour and 2 hours) and random PAN nanofiber network

Figure 3.36: Toughness of aligned (manufactured in 1 hour and 2 hours) and random PAN nanofiber network

Figure 4.1: Jeffamine D-400 (left) and EPON Resin 828 (right)

Figure 4.2: Hot-Press: CARVER; model 2699, S/N 2699-126

Figure 4.3: Example of aligned PAN nanofiber reinforced composites

Figure 4.4: Example of random PAN nanofiber reinforced composites

Figure 4.5: Fracture modes

Figure 4.6: Double edge notch test specimen

Figure 4.7: Specimen design of double edge notch test (left) and an experimental sample (right)

Figure 4.8: MICROTTEST 200N tensile stage

Figure 4.9: Representative strain-stress curves of [0] nanocomposites

Figure 4.10: Representative strain-stress curves of [90] nanocomposites

Figure 4.11: Representative strain-stress curves of random nanofiber reinforced composites

Figure 4.12: Representative strain-stress curves of pure epoxy

Figure 4.13: Fracture strength of [0] nanocomposites, [90] nanocomposites, random nanofiber reinforced composites and pure epoxy

Figure 4.14: Young's Modulus of [0] nanocomposites, [90] nanocomposites, random nanofiber reinforced composites and pure epoxy

Figure 4.15: Critical stress intensity factor of [0] nanocomposites, [90] nanocomposites,

random nanofiber reinforced composites and pure epoxy

Figure 4.16: SEM images of fracture surface of [0] nanocomposites

Figure 4.17: SEM images of fracture surface of [90] nanocomposites

Figure 4.18: SEM images of fracture surface of random nanofiber reinforced composites

Figure 6.1: 10% PAN nanofibers manufactured in (a) 8kV; (b) 9kV; (c) 10kV; (d) 11kV; (e) 12kV; (f) 13kV

Figure 6.2: 11% PAN nanofibers manufactured in (a) 9kV; (b) 10kV; (c) 11kV; (d) 12kV; (e) 13kV; (f) 14kV

Figure 6.3: 12% PAN nanofibers manufactured in (a) 8kV; (b) 9kV; (c) 10k

Figure 6.4: of 13% PAN nanofibers manufactured in (a) 11kV; (b) 12kV; (c) 13kV; (d) 14kV; (e) 15kV

Figure 6.5: Diameter distribution of 14% PAN nanofibers manufactured in (a) 9kV; (b) 10kV; (c) 11kV; (d) 12kV

LIST OF TABLES

Table 2.1: Spinnability and diameters of electrospun PAN nanofibers fabricated using different manufacturing conditions

Table 2.2: Diameter and standard deviation of 10% PAN nanofibers manufactured with different applied voltage

Table 2.3: Diameter and standard deviation of 11% PAN nanofibers manufactured with different applied voltage

Table 2.4: Diameter and standard deviation of 12% PAN nanofibers manufactured with different applied voltage

Table 2.5: Diameter and standard deviation of 13% PAN nanofibers manufactured with different applied voltage

Table 2.6: Diameter and standard deviation of 14% PAN nanofibers manufactured with different applied voltage

Table 2.7: Manufacturing conditions of electrospun PAN nanofibers tested in TGA

Table 3.1: Manufacturing conditions for aligned PAN nanofibers

Table 3.2: Average diameter and standard deviation of aligned PAN nanofibers manufactured with different gap size

Table 3.3: Manufacturing conditions for aligned PAN nanofibers

Table 3.4: f_p and g_p values of aligned nanofibers with different manufacturing gap size

Table 3.5: f_p and g_p values of aligned nanofibers with different manufacturing duration

Table 3.6: Weight/area and computed equivalent thickness of aligned PAN nanofibers manufactured during different durations

Table 3.7: Loading conditions of UTM tests

Table 3.8: Manufacturing conditions for single PAN nanofiber

Table 3.9: Mechanical properties of single PAN nanofiber

Table 3.10: Mechanical properties of aligned PAN nanofiber network manufactured in 1 hour

Table 3.11: Mechanical properties of aligned PAN nanofiber network manufactured in 2 hours

Table 3.12: Manufacturing conditions for random PAN nanofiber network

Table 3.13: Mechanical properties of random PAN nanofiber network

Table 3.14: Mechanical properties of aligned (manufactured in 1 hour and 2 hours) and random PAN nanofiber network

Table 4.1: Manufacturing conditions for aligned PAN nanofibers

Table 4.2: Manufacturing conditions of random PAN nanofibers

Table 4.3: Fracture properties of [0] nanocomposites

Table 4.4: Fracture properties of [90] nanocomposites

Table 4.5: Fracture properties of random nanofiber reinforced composites

Table 4.6: Fracture properties of pure epoxy

Table 4.7: Fracture properties of [0] nanocomposites, [90] nanocomposites, random nanofiber reinforced composites and pure epoxy

CHAPTER 1

INTRODUCTION

1.1 Nanotechnology

Nanoscale science and technology is a relatively new area of research. It focuses on things that are measured in nanometers. In the past several decades, scientists have developed tools and methods that help better understanding the fundamental aspects of the world [1-3].

A nanometer is a billionth of a meter. The great potential of nanoscale objects stems from their tiny size. Things have different properties at the nanoscale, which allows scientists and engineers to create new materials and devices [4-7].

“Nanotechnology is the manipulation of matter with at least one dimension sized from 1 to 100 nanometers (nm)”, as defined by the National Nanotechnology Initiative [10]. The structures at nanoscale behave differently from atoms or bulk materials. The reasons are quantum effects, size effects, and large surface-to-volume ratio or interface-to-volume ratio [11-13]. It is possible to control properties of materials (mechanical, thermal, electrical, magnetic, optical etc.) by changing their nanoscale structure. Materials which are developed at nanoscale usually have some superior properties as compared with general materials. These high-performance materials can be used in a variety of new products. For example, the high surface-to-volume ratio of nanomaterials

can be used in composites, chemical reactions, drug delivery, and energy storage. Nanosized catalysts will increase the efficiency of chemical reactions [14-16].

Nanotechnology is expected to significantly redevelop existing technologies and create new industries. The fields of science that are involved in nanotechnology are diverse and very broad and include surface science, organic chemistry, molecular biology, semiconductor physics, microfabrication, etc. [17]. Major research areas are synthesis, characterization and integration of nanomaterials. A great demand for the nanotechnology research (Figure 1.1) and development of new nanomaterials is fueled by the broad variety of potential applications in both industry and military [18-20]. Governments have invested billions of dollars in research on nanotechnology [21-24]. As reported in April 2012, the USA has invested 3.7 billion dollars through its National Nanotechnology Initiative, while the European Union has invested 1.2 billion and Japan has invested 750 million dollars [25].

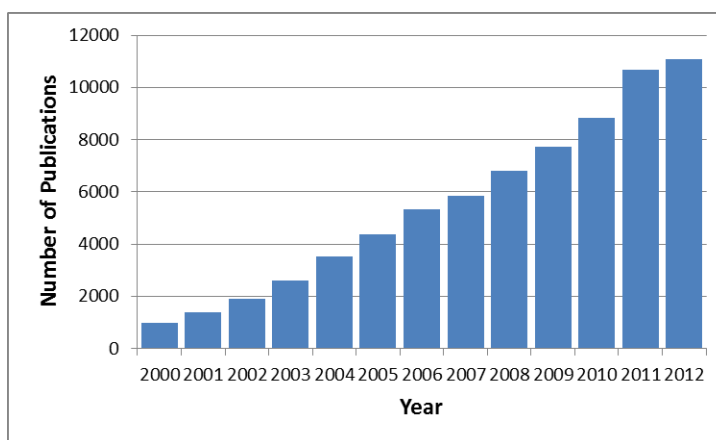


Figure 1.1: Publications related to nanotechnology from 2000 to 2012. Data is from Web of Science.

1.2 Nanomaterials

Nanomaterials are an important subset of nanotechnology. A nanomaterial is a material with at least one dimension less than 100 nm [26]. The definition of a nanomaterial from European Commission on 18 October 2011 is as follows: “A natural, incidental or manufactured material containing particles, in an unbound state or as an aggregate or as an agglomerate and where, for 50% or more of the particles in the number size distribution, one or more external dimensions is in the size range 1 nm to 100 nm. In specific cases and where warranted by concerns for the environment, health, safety or competitiveness the number size distribution threshold of 50% may be replaced by a threshold between 1 and 50%.” [27]

Nanomaterials have many unique features such as unique physical and chemical properties, small size coupled with high specific surface area, and quantum confinement. Scientists create useful materials, devices and systems through control of matter in the nanometer length scale and explore novel properties and phenomena developed at that scale [32].

Nanomaterials can be classified as zero-dimensional nanomaterials (i.e. nanoparticles, nanoclusters and nanodots), one-dimensional nanomaterials (i.e. nanofibers, nanotubes and nanowires) and two-dimensional nanomaterials (i.e. nanoplatelets and nanofilms) [28-30].

Figure 1.2A shows models wearing garments made of fibers coated with nano-sized bits of metal. SEM image of these fibers is shown in Figure 1.2B. As a result of the nanoparticle coating, the clothes were resistant to dirt, allergens and even broke down

harmful pollution before it reaches the wearer's skin [31].



Figure 1.2: Smart clothing runway show and SEM image of cloth fiber with coated nanoparticles [31]

1.3 Nanocomposites

Conventional composites are solid materials composed of two or more constituents combined to offer users the specific properties they required. Usually, they are composed of a matrix and reinforcements of different types.

Nanocomposites are composites where at least one constituent has at least one dimension smaller than 100 nm [33]. Natural nanocomposites can be found in the

structure of the abalone shell and bone. Nanocomposites can be classified as polymer matrix nanocomposites, metal matrix nanocomposites and ceramic matrix nanocomposites, based on the type of matrix. Compared to conventional composites, interphases in nanocomposites play a dominant role and affect their macroscopic properties. The reinforcing material can be made up of nanomaterial in zero, one or two dimensional form [34,35]. The area of the interface between the matrix and reinforcement phase(s) is significantly larger than that of conventional composites.

The applications of nanocomposites include structural materials with improved mechanical properties, electronic materials, magnetic materials, biomedical materials, photonics, high-performance coating and catalysts [36-39].

Figure 1.3 illustrates the usage of polymer nanocomposites parts in a Toyota motor vehicle. The main advantages for using polymer nanocomposite parts in the automotive industry are: reducing vehicle's weight, improving engine efficiency, saving fuel, increasing safety [41].



Figure 1.3: Illustration of the usage of polymer nanocomposites parts [41]

Currently, one-dimensional (1D) and two-dimensional (2D) nanomaterials attract high interest for use as nanoreinforcement in nanocomposites. 1D carbon nanotubes show high promise, but their processing into nanocomposites has not yet been successful due to their discontinuity [40]. Polymer nanofibers can be continuous and their high mechanical and other properties show big advantages over nanoreinforcement [39].

The current experimental and theoretical works on polymer nanocomposites mainly focus on relationships between effective properties (such as modulus and thermomechanical characteristics) and properties of constituents (polymer matrix and reinforcement), volume fraction of components, shape and arrangement of reinforcement, and interaction between matrix and reinforcement [42]. Limited research has been performed on mechanical properties of random nanofiber reinforced polymer nanocomposites, however aligned nanofiber reinforced polymer nanocomposites have not yet been investigated.

1.4 Electrospinning

Electrospinning, also known as electrostatic spinning, is a method to produce superfine fibers with diameters from less than 10 nm to over 1 μm [43]. Conventional mechanical fiber spinning techniques cannot produce fibers with diameters smaller than 2 μm [56]. Electrospinning has gained increased attention in the last decade due to a surging interest in nanotechnology (Figure 1.4). With the help of electrical charge, this process can draw very fine fibres from a liquid and does not require the use of

coagulation chemistry or high temperatures. It is considered the simplest and most effective technology to produce continuous polymer nanofibers from polymer solutions or melts in high electric fields [44-46].

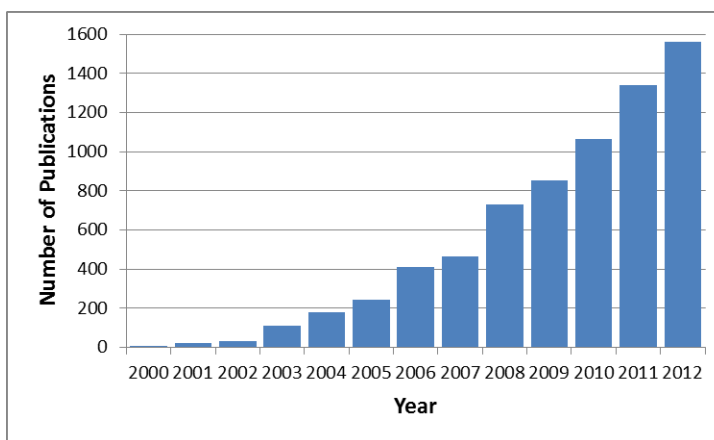


Figure 1.4: Publications related to electrospinning from 2000 to 2012. Data is from Web of Science.

1.4.1 History

The origin of electrospinning as a viable fiber spinning technique can be traced back to 1900s. In 1914, John Zeleny published an article on electrified jet [47]. A series of patents from Anton Formhals were awarded later. The first patent related to the process for producing polymer filaments using electric charges appeared in 1934 [48]. In 1939, Formhals refined the previous method to give more drying time for the electrospun fibers [49-51]. In 1940, he patented another approach to produce composite fiber webs from multiple polymers and fiber substrates by electrostatically spinning polymer fibers on a moving base substrate [52]. In the 1960s, fundamental studies on the jet forming process

were initiated by Taylor. His finding was later referred to by other researchers as the “Taylor Cone”. In 1971, electrospun acrylic nanofibers with diameters ranging from 500 to 1100 nm were produced by Baumgarten [53]. However, it was not until two decades later that the great application potential of nanofibers in different areas has been realized [54]. Research on nanofibers gained a milestone with the work of Doshi and Reneker [55]. Recently, over 200 universities and research institutes were studying various aspects of the electrospinning process worldwide [60]. In Dzenis’ group, there is intensive ongoing research work on electrospinning, including process analysis and modeling, nanofiber testing and optimization, design, modeling, and experimental evaluation of nanofiber applications [56-59].

1.4.2 Electrospinning Process

A typical electrospinning process setup is shown in Figure 1.5. It consists of three major components: a high-voltage power supply, a spinneret (a metallic needle) and a collector (a grounded conductor) [61]. The polymer solution is contained in a syringe. In order to get a constant and controllable solution feed rate, a syringe pump should be used. The collector can be made of any shape for specific requirements, such as a flat plate, rotating drum, etc.

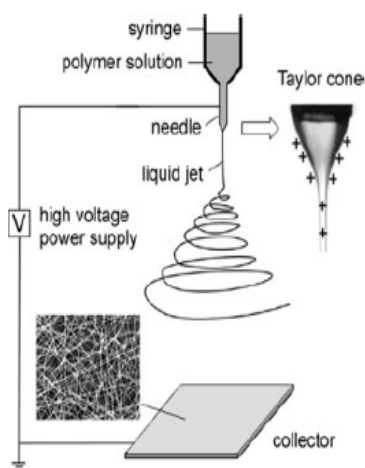


Figure 1.5: A setup for electrospinning [61]

The drop of polymer solution at the nozzle will become highly electrified, when a high voltage is applied. The range of voltage is usually from 1 kV to 30 kV. There are two types of electrostatic forces involved in electrospinning: the electrostatic Coulombic repulsion between the charges embedded in different jet segments and the guiding electric force applied by the external electric field [62-64]. When the strength of electric field reaches a critical value required to overcome the surface tension of the liquid, a jet of liquid is ejected from the nozzle. As the jet travels through the atmosphere, the solvent evaporates. As a result, a long and thin thread can be generated on the collecting device [65-67]. The charged fibers are often in a random nonwoven mat form.

The following parameters and processing variables affect the electrospinning process [68]:

(1) System parameters such as molecular weight, molecular-weight distribution and conformation (branched, linear, etc.) of the polymer and various properties of solution

like concentration, conductivity and surface tension.

(2) Process parameters such as strength of applied electric field, feeding rate, concentration of polymer solution, distance between the needle and collector, needle gauge, spinning environment (temperature, humidity and air velocity in the chamber) and finally motion of target screen.

1.4.3 Mechanisms of Electrospinning

Although the setup for electrospinning is straightforward, the spinning mechanism is rather complicated [61]. As the techniques improved, recent experimental observations demonstrated that the thinning of a jet during electrospinning is mainly caused by the bending instability [72-75]. However, before 1999, it was believed that a single jet splitting or splaying into multiple thin fiber filaments due to radial charge repulsion was the spinning mechanism [69-71].

Figure 1.6A illustrates the photograph of a spinning jet [76]. It shows that the jet flew away from the droplet in a nearly straight line and then became unstable. The instability region appears to be composed of multiple jets that led early researchers to believe that the original liquid jet splits into multiple branches. Figure 1.6B establishes however that the conical envelope contains only a single bending thread [77]. This photo was taken by using high-speed photography, while conventional photography (Fig. 1.6A) could not properly resolve this due to high velocities of the moving bent jet segments [61].

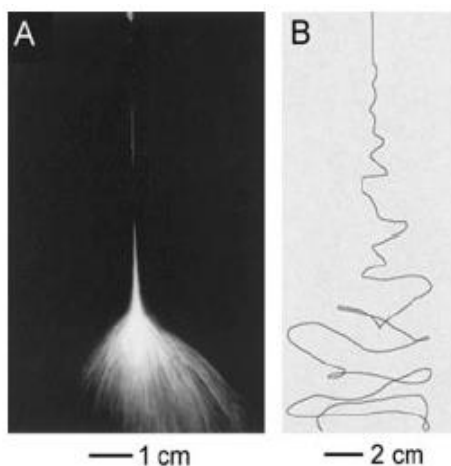


Figure 1.6: Photographs illustrating the instability region of an electrospun liquid jet [61]. The capture time was on two different time scales: A. 1/250 s, and B. 18 ns, respectively.

1.4.4 Advantages of Electrospinning

Compared to most bottom-up methods, the major advantage of this top-down process is relatively low cost. The resulting nanofibers are often uniform and continuous. Electrospinning can be used to generate nanofibers from hundreds of polymers. So, this process has unique potential for producing cost-effective continuous nanofibers and manufacturing of two- and three-dimensional nanofiber assemblies [56].

1.5 Electrospun Nanofibers

Fiber mechanical properties are known to substantially improve with a decrease in the fiber diameter [79-83]. Nanofibers prepared by electrospinning are continuous fibers with diameters between 2 nm and 5000 nm. They are usually characterized by solid

interior and smooth surface and are expected to possess high axial strength. Nanofibres provide a connection between the nanoscale world and the macroscale world, since their diameters are in the nanometer range and the length is continuous (i.e. theoretically infinite) [84]. At present, nanofibers are attracting very high interest (Figure 1.7) due to their remarkable micro and nano structural characteristics, high porosity and inherently large total surface area.

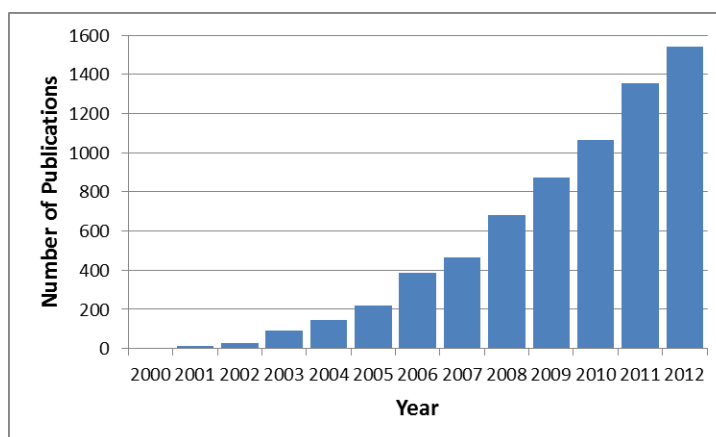


Figure 1.7: Publication search on “electrospun nanofiber/nanofibers” from the Web of Science

Figure 1.8 SEM images illustrate various types of electrospun nanofibers: (A) comparison of commercial advanced carbon fiber (one of the smallest advanced fibers) and electrospun continuous nanofibers, (B) vapor-grown carbon nanofibers, (C) uniform electrospun carbon nanofibers, (D) highly aligned nanofibers, (E) aligned and orthogonal nanofibers, (F) cross section of nanocrystalline zirconia nanofiber. [56]

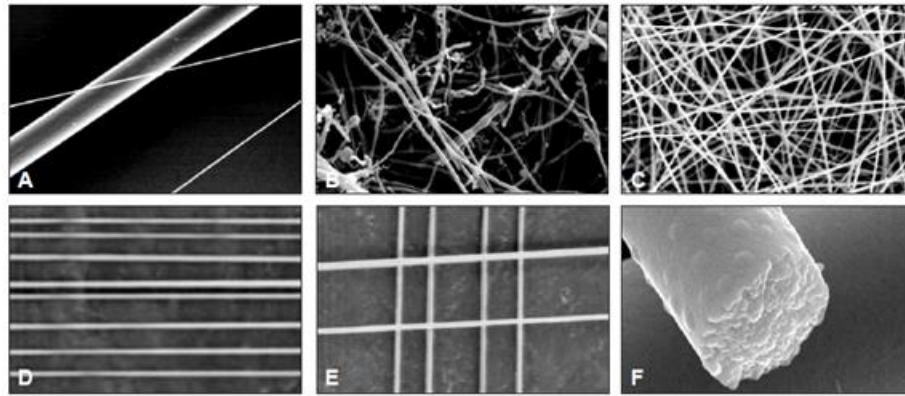


Figure 1.8: SEM images of nanofibers [56]

1.5.1 Applications of Electrospun Nanofibers

Electrospun nanofibers are currently considered for a broad variety of applications.

The following applications are examples:

- Medical: artificial organ components, tissue engineering [85,86], implant material [87,88], drug delivery [89,90], wound dressing, medical textile materials.
- Protective materials: sound absorption materials, protective clothing [91,92] for chemical and biological warfare agents protection, sensor applications [93] for detecting chemical agents.
- Textile: sport apparels, sport shoes, climbing, rainwear, outerwear garments, baby diapers.
- Filtration (Figure 1.9): air, oil, fuel filters for automotive, filters for beverage, pharmacy, medical applications. [94]
- Energy generation: electrostatic dissipation, solar sails, electromagnetic interference shielding, photovoltaic device, fabrication of tiny electronic devices.

[47]

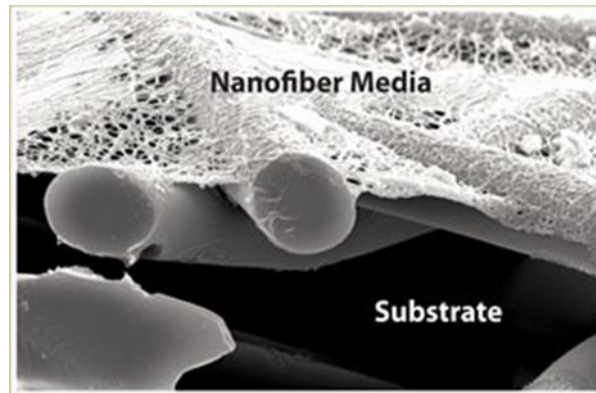


Figure 1.9: Application of nanofibers in filtration

In limited laboratory studies to date, nanofibers have been used as reinforcement in composite materials. Because of the high surface to volume ratio, use of nanofibers in composites may significantly increase the interaction between the fibers and the matrix material [73]. In Dzenis' group, nanofibers were applied as nanoreinforcement between plies of the traditional advanced composites laminates to improve interlaminar fracture toughness and suppress delamination (Figure 1.10). It was reported that nanofibers could significantly reinforce and toughen interfaces in advanced laminated composites [95].

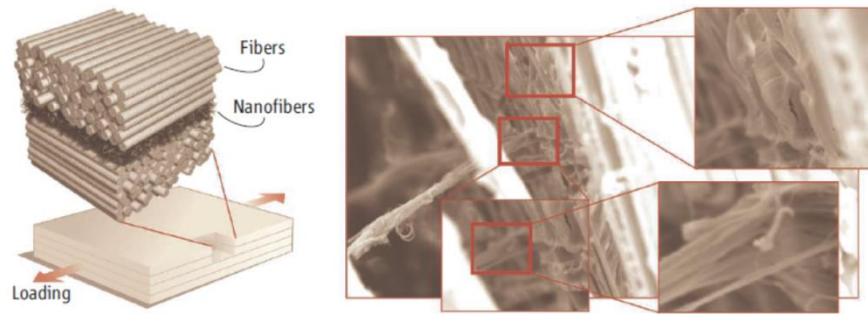


Figure 1.10: Nanoreinforcement between plies of the traditional composites laminates [95]

1.5.2 Aligned Electrospun Nanofibers

Because of the jet bending instability, electrospun nanofibers are normally produced as randomly oriented structures in the form of nonwoven mats. As discussed earlier, these nanofibers can be applied in many areas, such as: medical, textile, filtration, protective materials, and energy generation. However, in many applications, such as composite reinforcement and device manufacture, highly ordered structures are desired. Recent studies have shown that aligned nanofiber sheets have improved mechanical properties compared to randomly oriented nanofibers [96-98].

Several approaches have been tried to generate aligned electrospun fibers, including: spinning onto a rotating drum or onto the sharp edge of a thin rotating wheel, using an auxiliary electrode or electrical field, quickly oscillating a grounded frame within the jet, and using a metal frame as a collector [99,100]. These methods still need to be further developed to optimize the degree of alignment. In Xia's group, a simple method for producing aligned nanofibers was demonstrated [101]. The grounded collector was

replaced by two conductive collectors separated by a gap as shown in Figure 1.11.

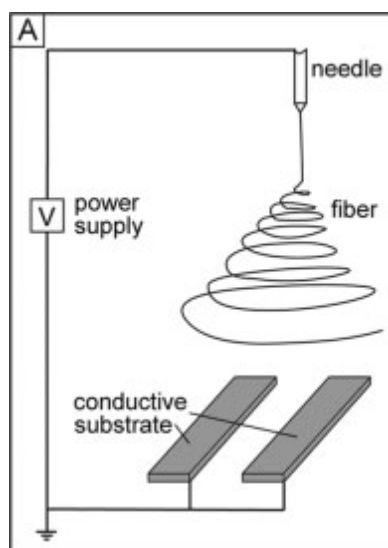


Figure 1.11: Setup for generating aligned nanofibers [101]

The mechanism of alignment in the latter method can be ascribed to electrostatic interactions [102]. The gap changes the structure of the external electric field and creates electrostatic forces promoting jet segment orientation and resulting in nanofibers spanning the gap.

1.5.3 Mechanical Properties of Nanofibers, Nanofiber Assemblies, and Nanofiber Reinforced Composites

Mechanical properties of nanofibers are important for many applications. So far, most studies focused on bundles of nanofibers [108]. Only limited numbers of studies were conducted on individual nanofibers.

In general, it can be expected that nanofiber strength and modulus would increase with their diameter decrease. This is due to better structural alignment and reduced size and probability of flaws in finer fibers. In most structural materials and fibers, the properties of strength and toughness are mutually exclusive [109]. Usually, increased strength is accompanied with decreased toughness. In a recent breakthrough from Dzenis' group, it was shown that nanofibers toughness can also increase [108].

Figure 1.12 compares strength and toughness of as-spun PAN nanofibers with properties of some commercial and developmental fibers and structural materials [108]. It can be seen that the properties of most structural materials and fibers are within the shaded area, showing the trade-off relationship between strength and toughness. Ultrafine electrospun nanofibers exhibited extremely high strength, modulus and toughness simultaneously. (The arrow color density indicates nanofiber diameter values.) This discovery has high potential for structural and composite applications of nanofibers.

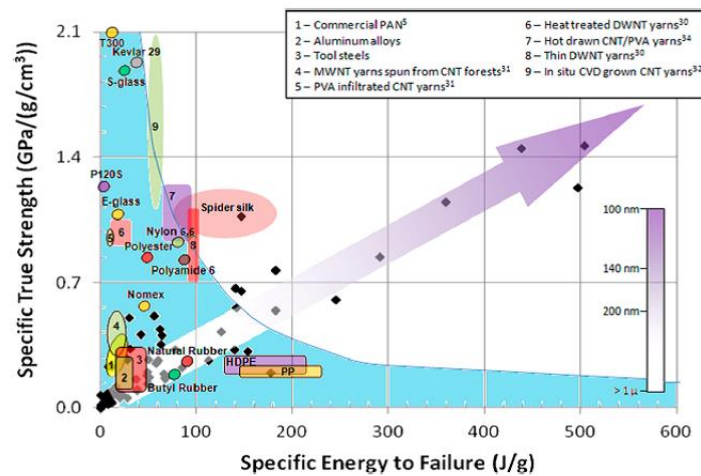


Figure 1.12: Comparison of specific strength and specific energy to failure of as-spun

PAN nanofibers (diamonds) with typical values for commercial and developmental fibers and materials [108]

Despite the importance, mechanical properties of nanofiber networks and nanofiber reinforced composites have not yet been systematically studied. Mechanical behavior of networks, although builds on single fiber properties, is much more complex as it may involve several non-linear effects such as evolution of nanofiber orientation, contact and nanofiber breaks accumulation, etc. This behavior needs to be better understood for nanofiber applications.

1.6 Summary and Problem Formulation

Electrospinning provides a simple, straightforward, effective method for producing continuous nanofibers. Electrospun nanofibers have attracted large attention in recent years, due to their remarkable micro and nano structural characteristics, high porosity and inherently large total surface area. They are being considered for many applications including medical, textile, filtration, protective materials, and energy generation. Research interest in aligned oriented nanofibers is growing because of the requirements for highly ordered nanofiber assemblies in many applications.

However, reaching high alignment degree is still a big challenge for electrospinning and nanofiber researchers. Also, there is limited published work focused on mechanical properties of nanofiber mats and no comparative studies of random and aligned nanofiber

assemblies have been found in the literature. Mechanical properties of nanofibers and nanofiber reinforced composites are important for most applications and need to be better understood. So far, there was no systematic experimental study of nanofiber composites. In particular, there have been no studies on their anisotropic fracture properties.

Based on the review above, the following objectives of this research were formulated:

- Fabricate continuous, uniform diameter polyacrylonitrile (PAN) nanofibers using electrospinning technique.
- Study effects of electrospinning process parameters on nanofiber diameter, uniformity, and orientation.
- Analyze and compare mechanical behavior of single nanofibers, and aligned and random nanofiber networks.
- Investigate fracture properties of aligned and random nanofiber reinforced nanocomposites.

CHAPTER 2

PAN NANOFIBER MANUFACTURING

There are several parameters affecting electrospinning process. In order to find the optimal manufacturing conditions for electrospinning, we need to better understand the effects of these parameters.

In this chapter, fine, continuous, uniform diameter polyacrylonitrile (PAN) nanofibers without beads were manufactured using electrospinning technique. The effect of the electrospinning process parameters on PAN nanofiber diameter was analyzed systematically experimentally.

2.1 Experimental

2.1.1 PAN Solution Preparation

Because of its good properties, PAN is one of the most extensively used polymers in many areas such as in composite fabrics and materials, tissue engineering, protective clothing, filtration, and biomedical application [43]. In this study, PAN solution was prepared by mixing PAN powder with dimethylformamide (DMF). Both PAN and DMF were products of SIGMA-ALDRICH with product numbers 181315 and D158550.

Average molecular weight of PAN was 150,000. Solutions were prepared in the range of concentrations from 6% to 16%. Corning stirrer hot plate with stirring-level 5 and heating-level 2.5 was used and mixing duration was 12 hours. The well dissolved solutions were transparent and had a light yellow color as shown in Figure 2.2(b).



Figure 2.1: DMF solution (left) and PAN powder (right)



(a)



(b)

Figure 2.2: PAN solution: (a) before stirring and heating; (b) after mixing

2.1.2 Electrospinning Setup

The basic setup for electrospinning consists of three major components: a high-voltage power supply, a spinneret and a collector. The spinneret is connected to syringe in which the polymer solution is hosted. With the use of a syringe pump, the solution can be fed through the spinneret at a constant and controllable rate.

In this study, the setup included a direct current (DC) power supply, a high voltage transformer, a syringe with a metallic needle, and a large aluminum plate collector

(Figure 2.3). The DC supply was connected to high voltage transformer with the output voltage ranging from 0 to 30 kV. Positive high voltage source was used to charge the spinneret, whereas the negative voltage was used to charge the collector. The range of applied voltage in this study was from 7 kV to 20 kV. The distance between the spinneret and the collector was 24 cm. The feed rate of the solution was kept constant at 5 ml/h using the controlled syringe micropump.



Figure 2.3: Electrospinning setup

2.2 Evaluation of Electronspon Nanofiber Morphologies

Nanofiber morphologies were examined by scanning electron microscopy (JEOL JSM-840A SEM).

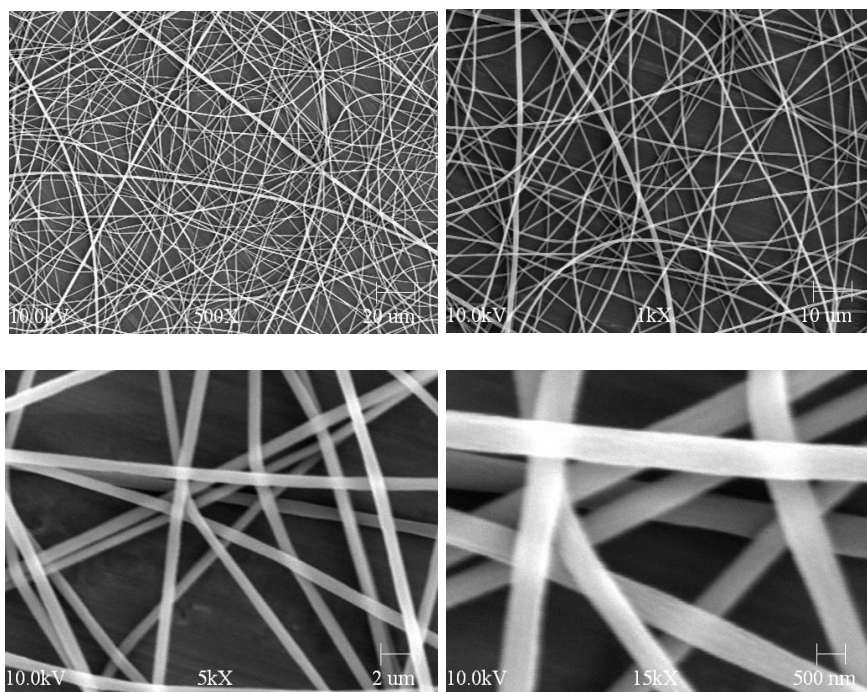
2.2.1 SEM Sample Preparation

A piece of nanofiber sheet was adhered onto the SEM stage with conductive tape (Figure 2.4). To observe nanofiber clearly, a thin gold layer was deposited on the surface of each nanofiber sample.

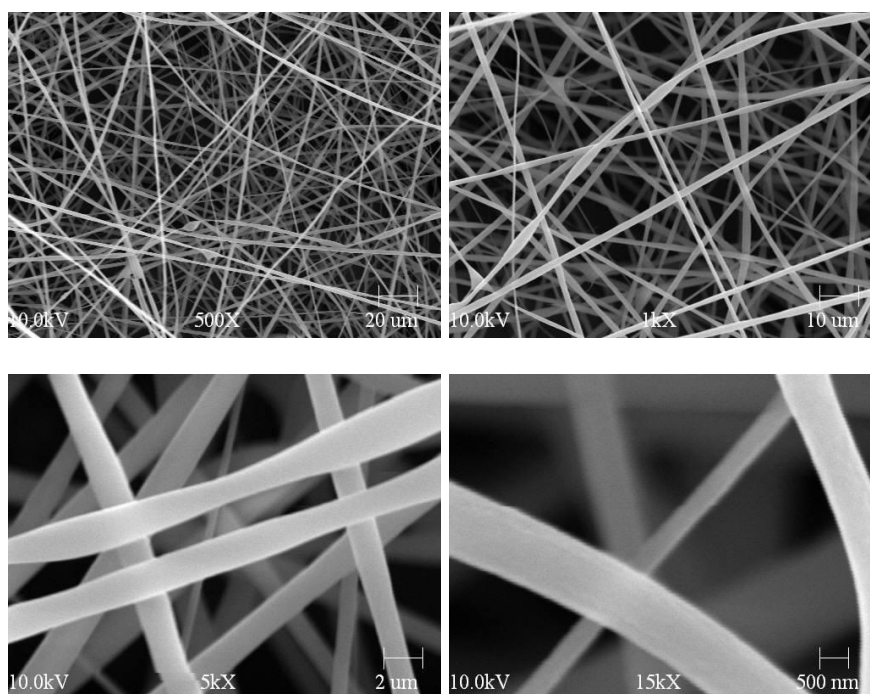


Figure 2.4: SEM samples

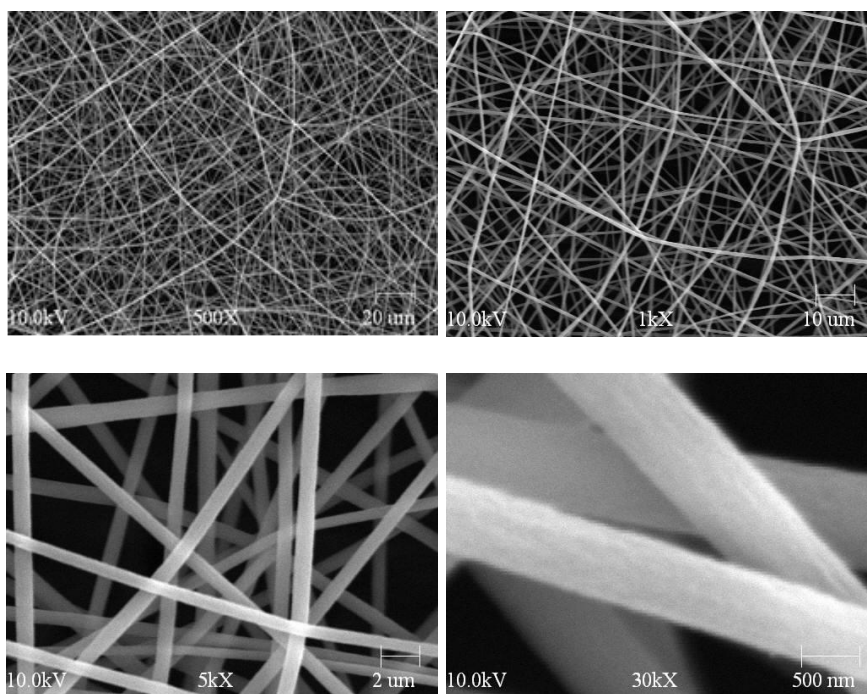
2.2.2 SEM Images



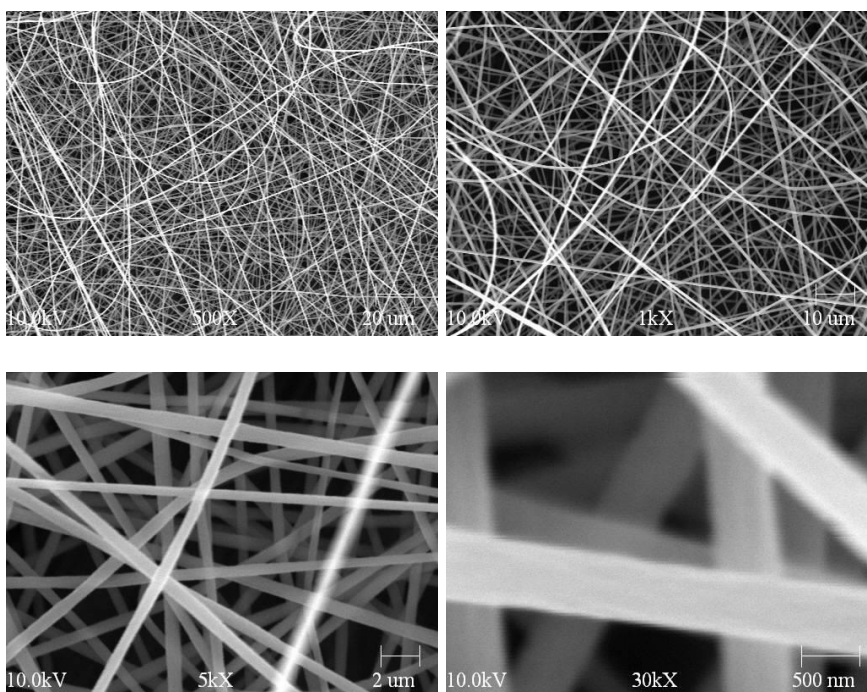
(a)



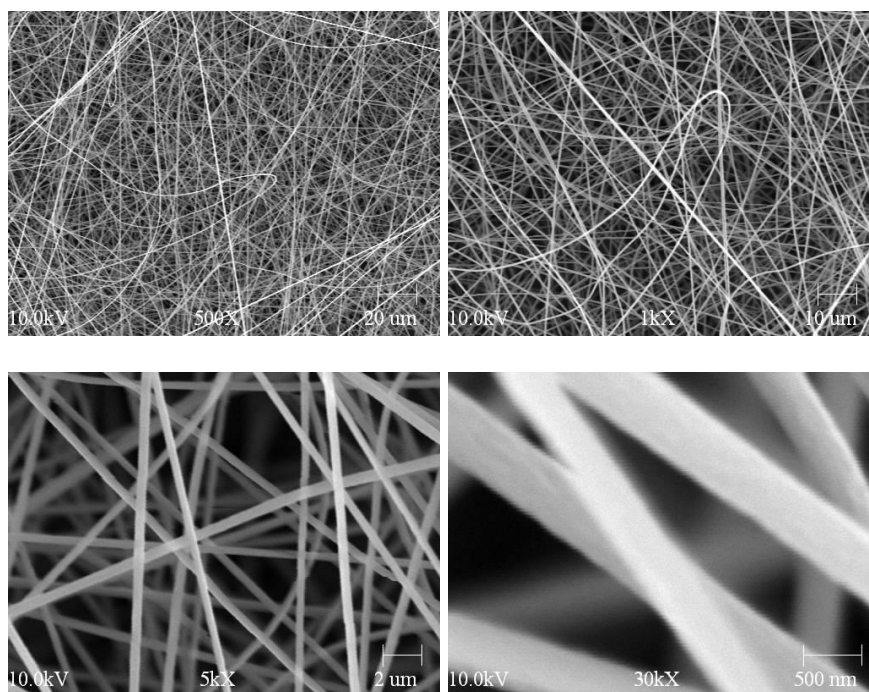
(b)



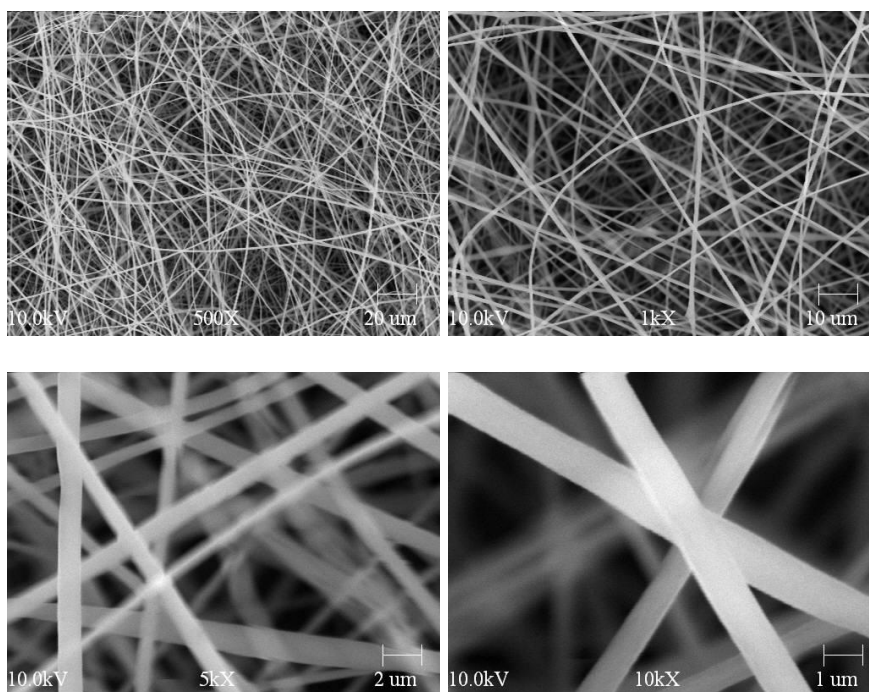
(c)



(d)

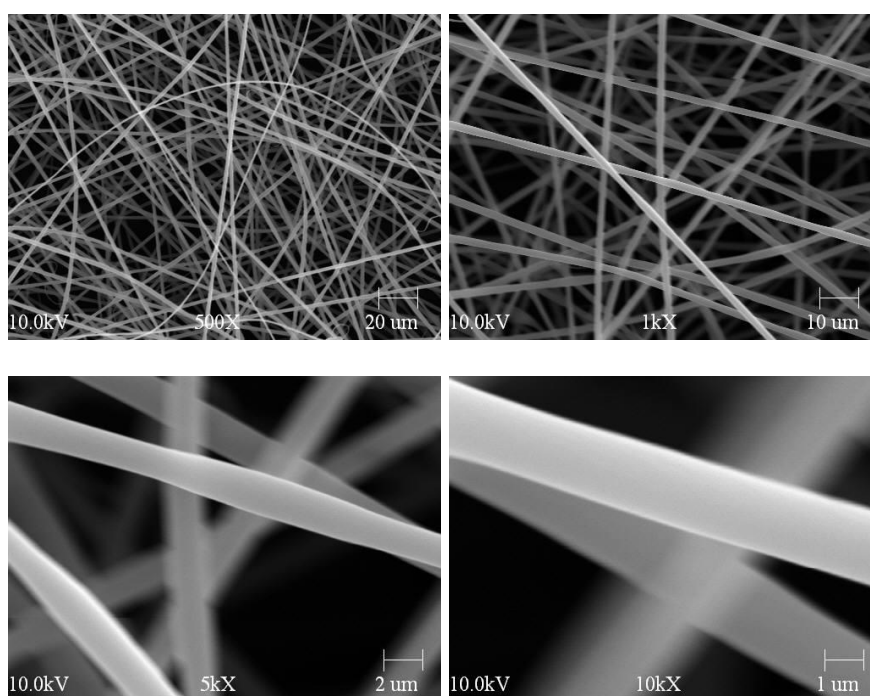


(e)

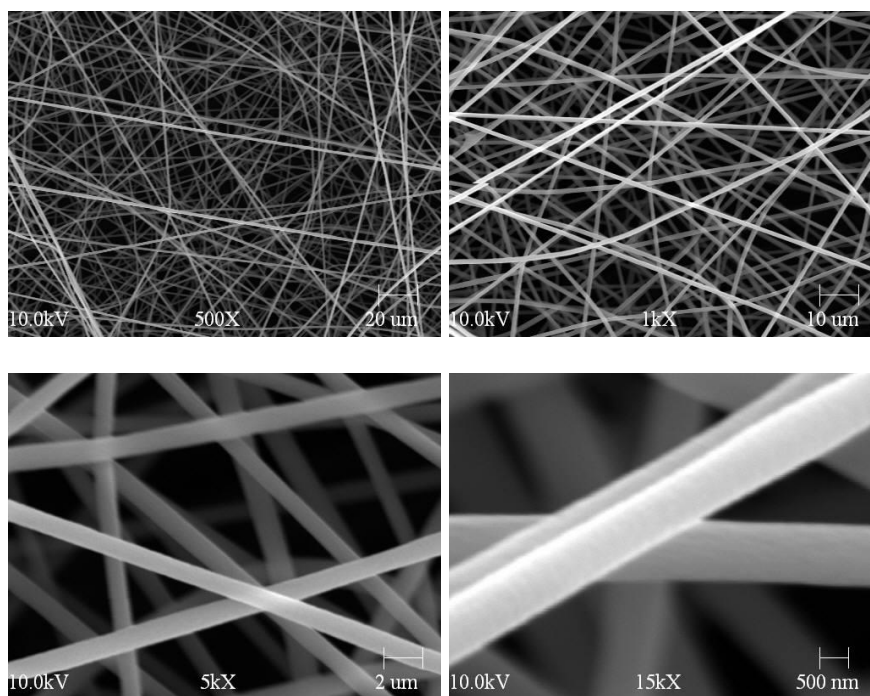


(f)

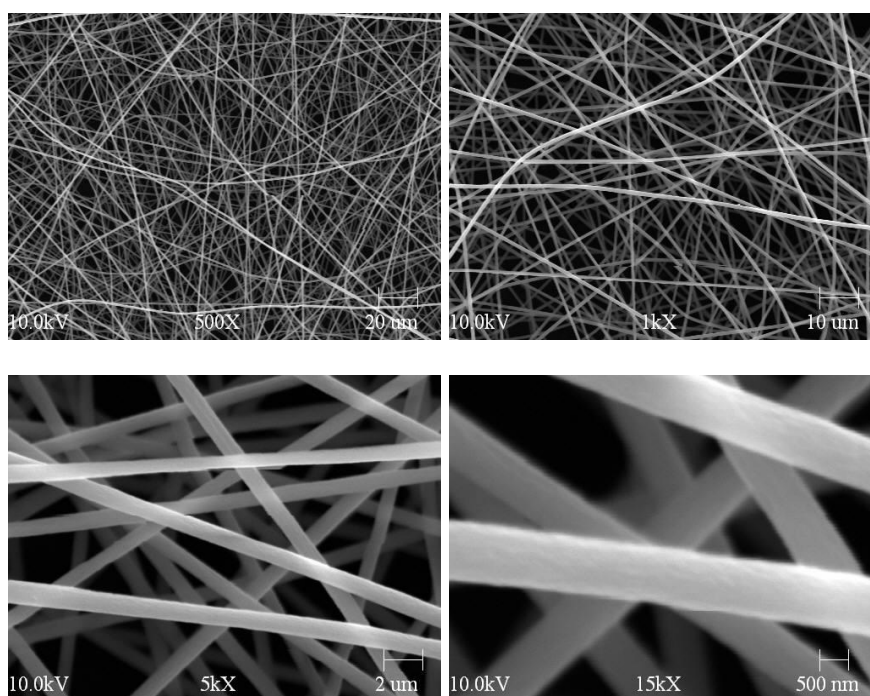
Figure 2.5: SEM images of 10% PAN nanofibers manufactured in (a) 8kV; (b) 9kV; (c) 10kV; (d) 11kV; (e) 12kV; (f) 13kV



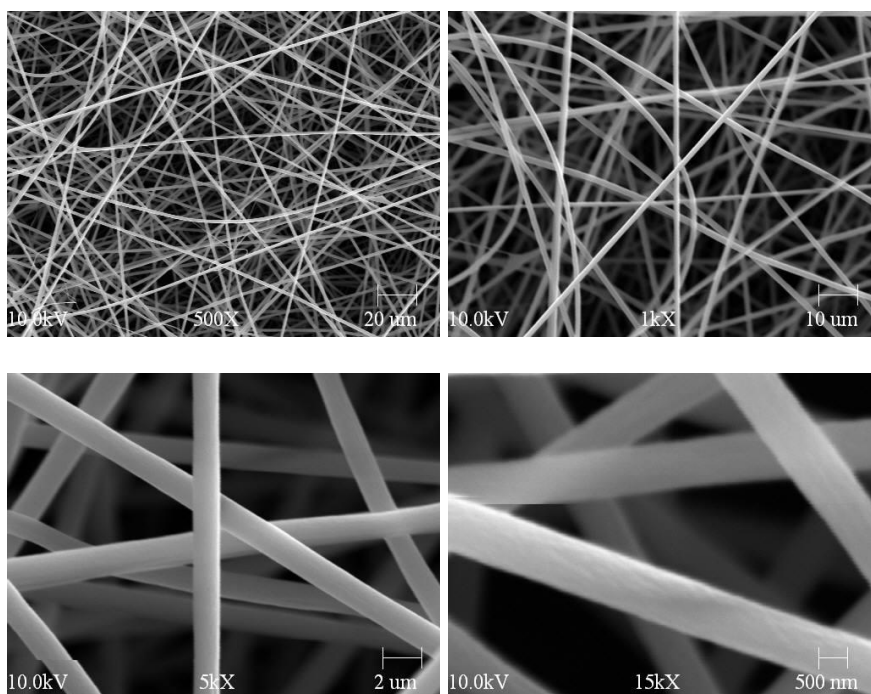
(a)



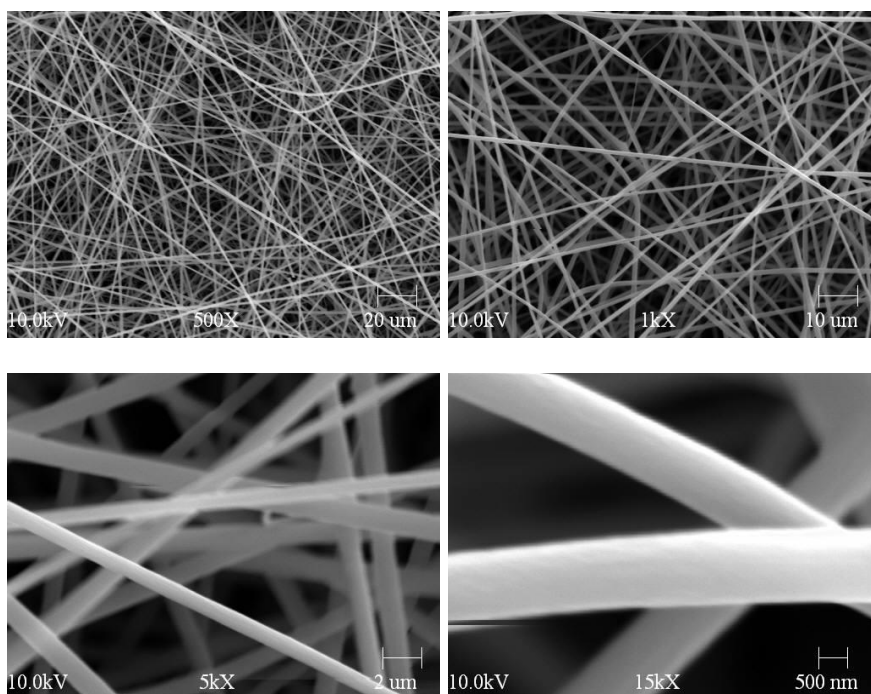
(b)



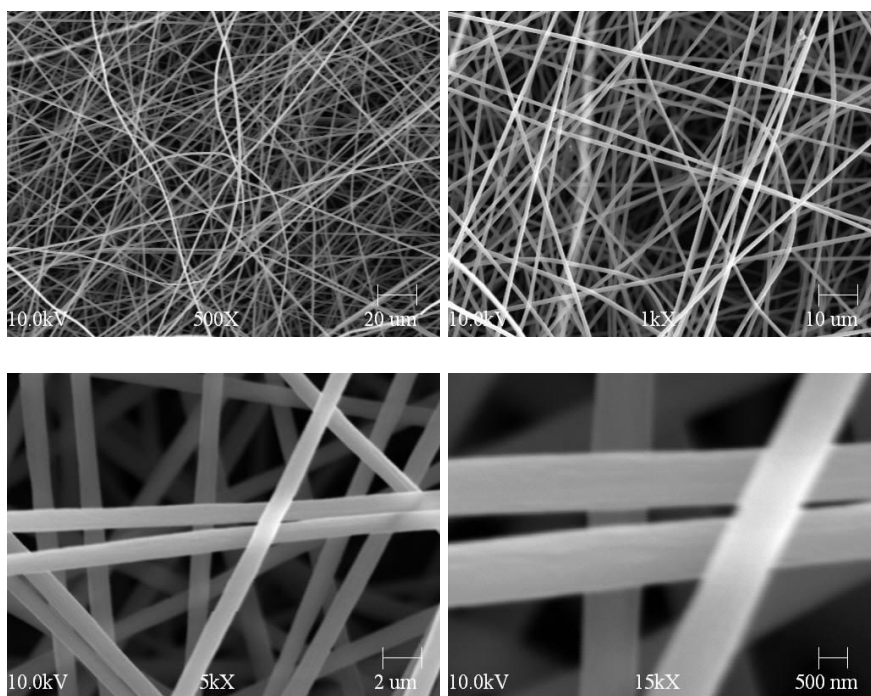
(c)



(d)

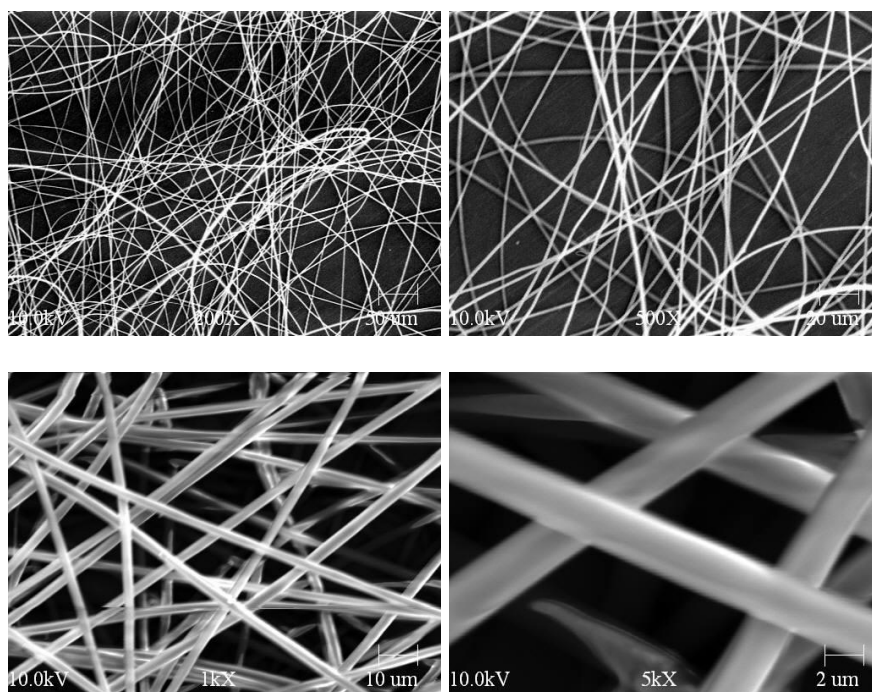


(e)

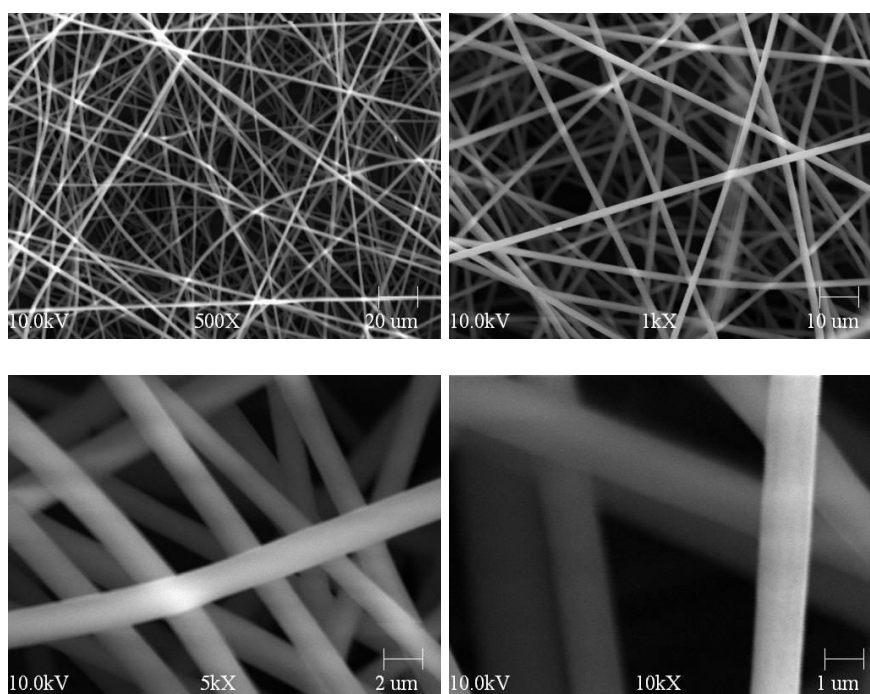


(f)

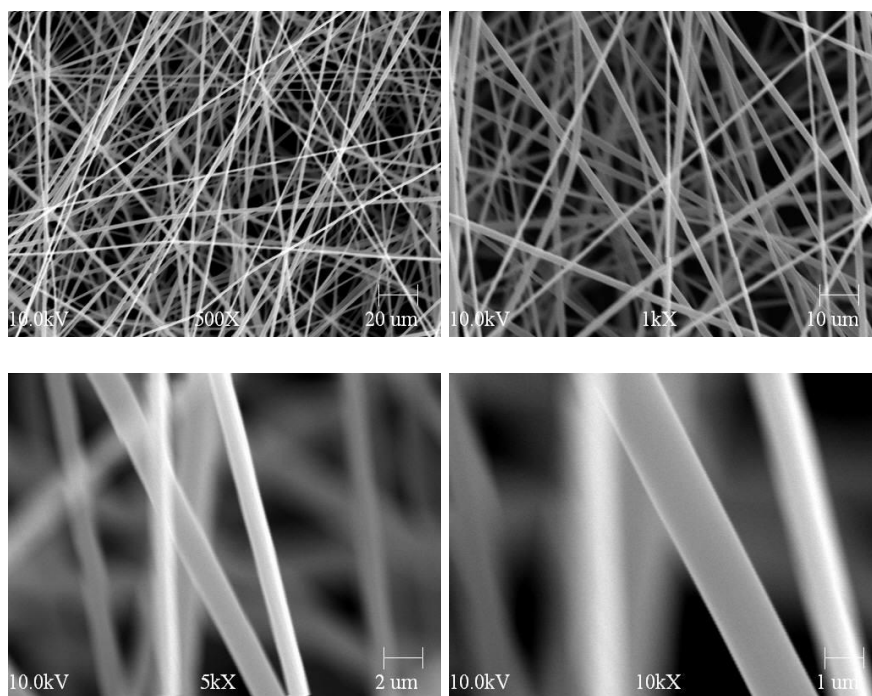
Figure 2.6: SEM images of 11% PAN nanofibers manufactured in (a) 9kV; (b) 10kV; (c) 11kV; (d) 12kV; (e) 13kV; (f) 14kV



(a)

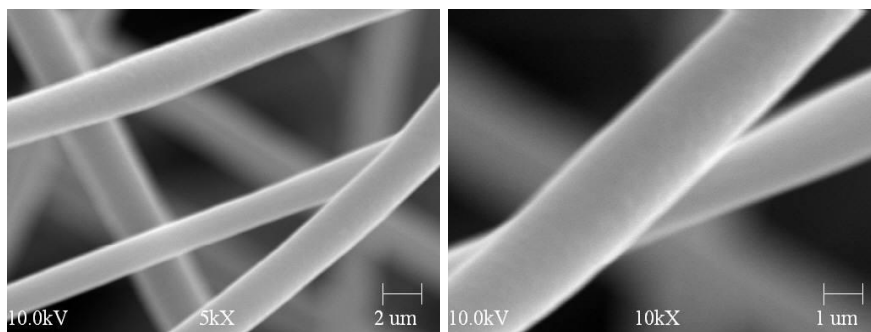
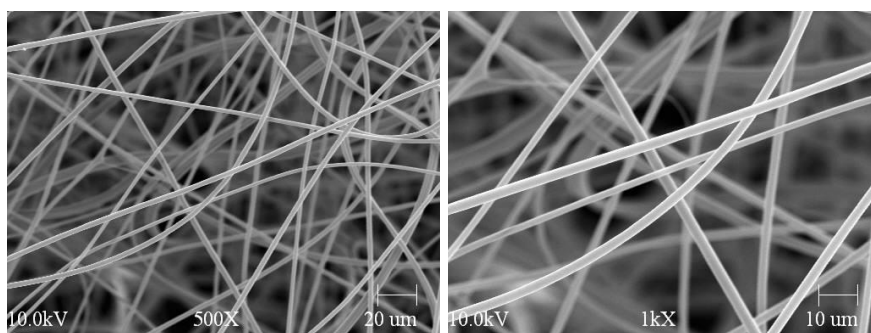


(b)

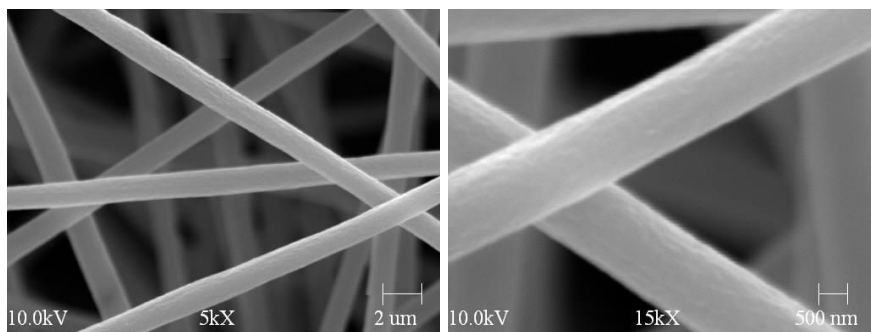
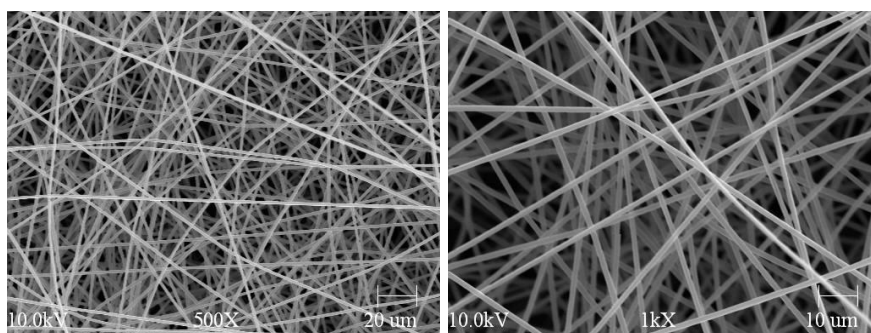


(c)

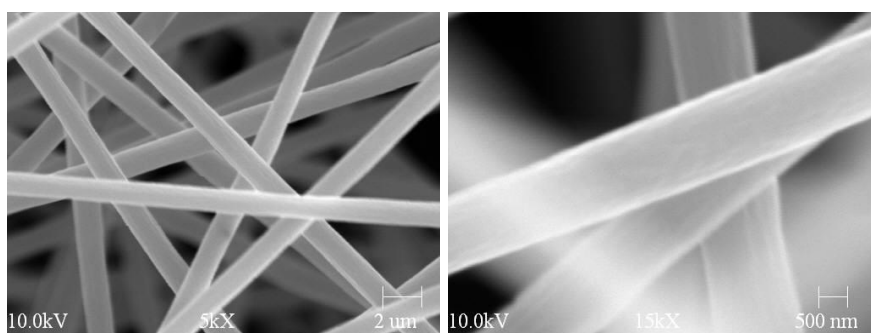
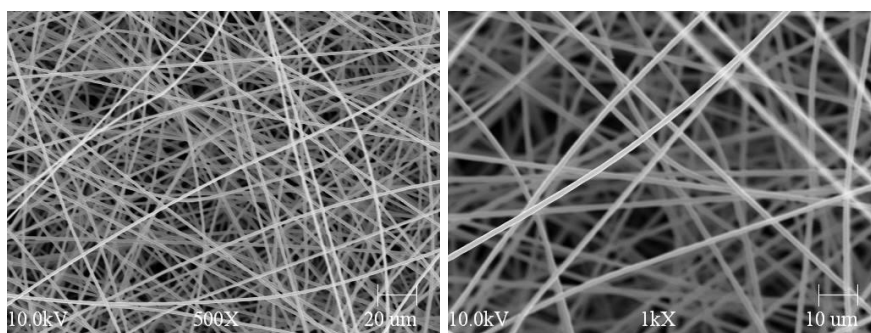
Figure 2.7: SEM images of 12% PAN nanofibers manufactured in (a) 8kV; (b) 9kV; (c) 10kV



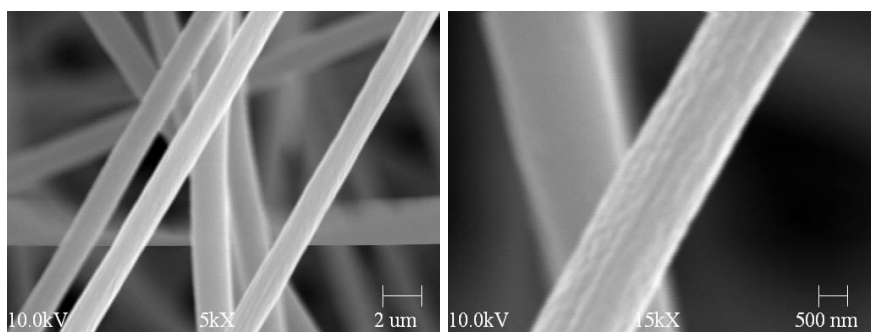
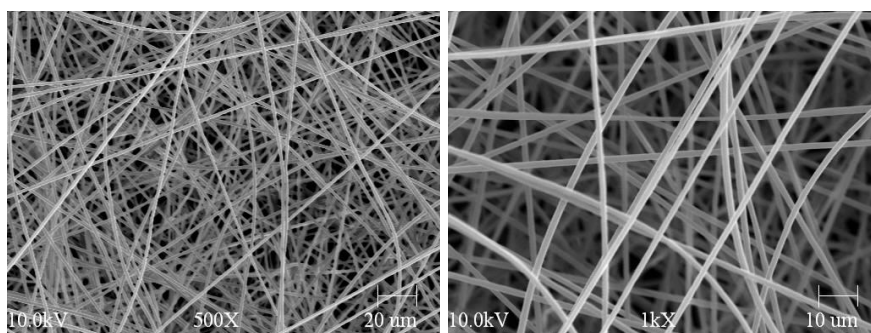
(a)



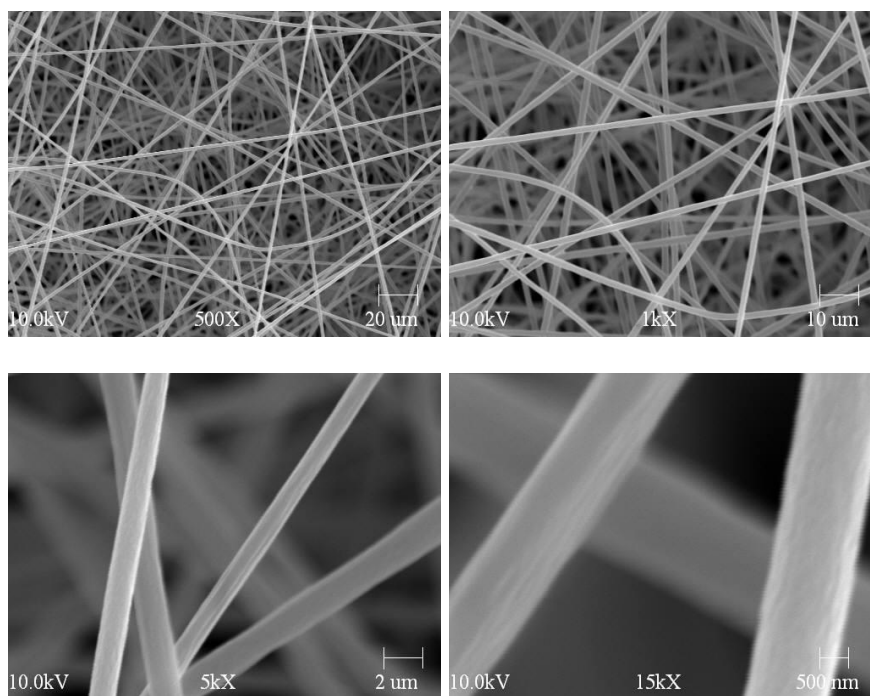
(b)



(c)

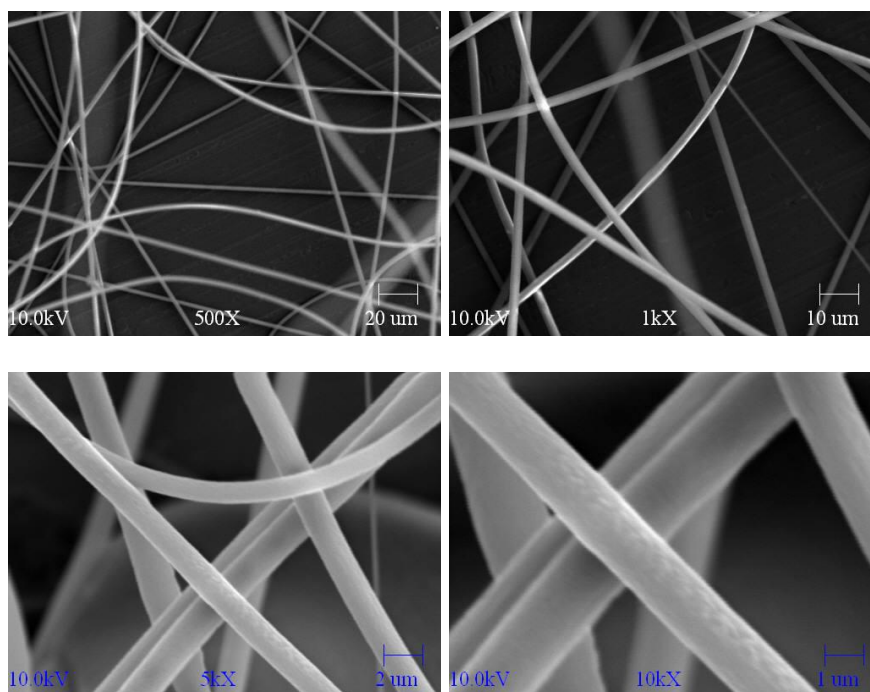


(d)

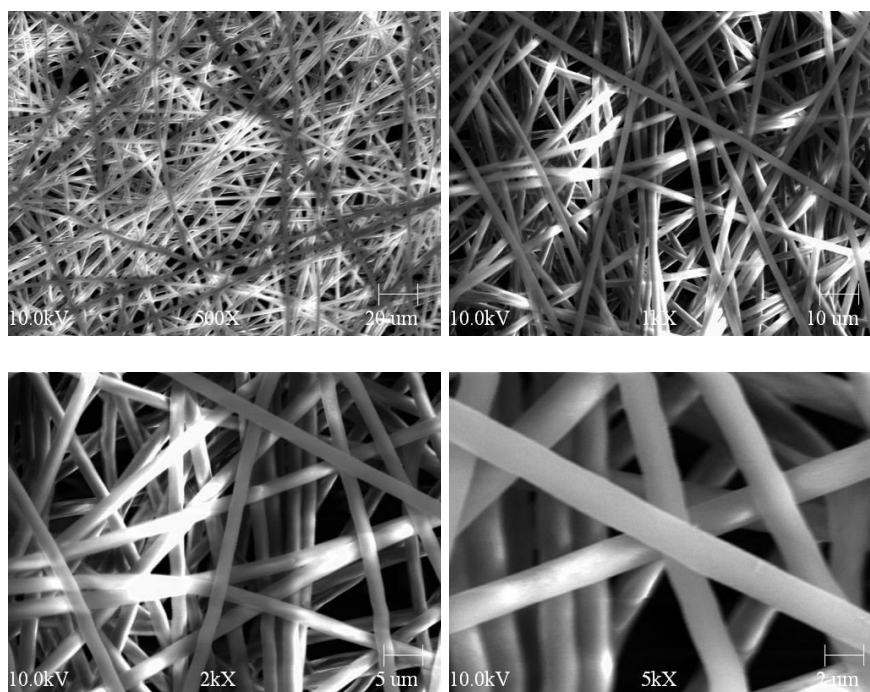


(e)

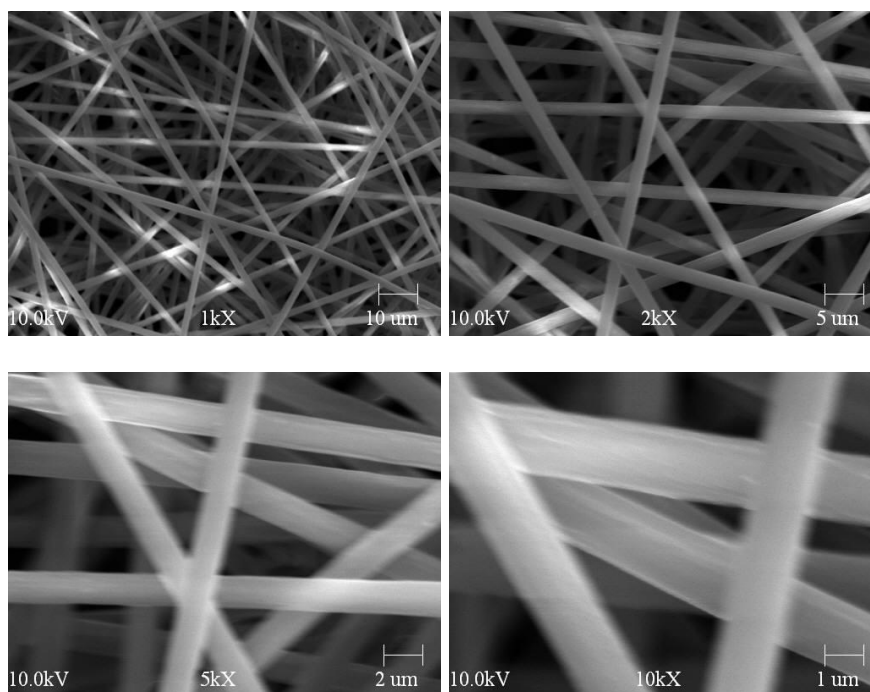
Figure 2.8: SEM images of 13% PAN nanofibers manufactured in (a) 11kV; (b) 12kV; (c) 13kV; (d) 14kV; (e) 15kV



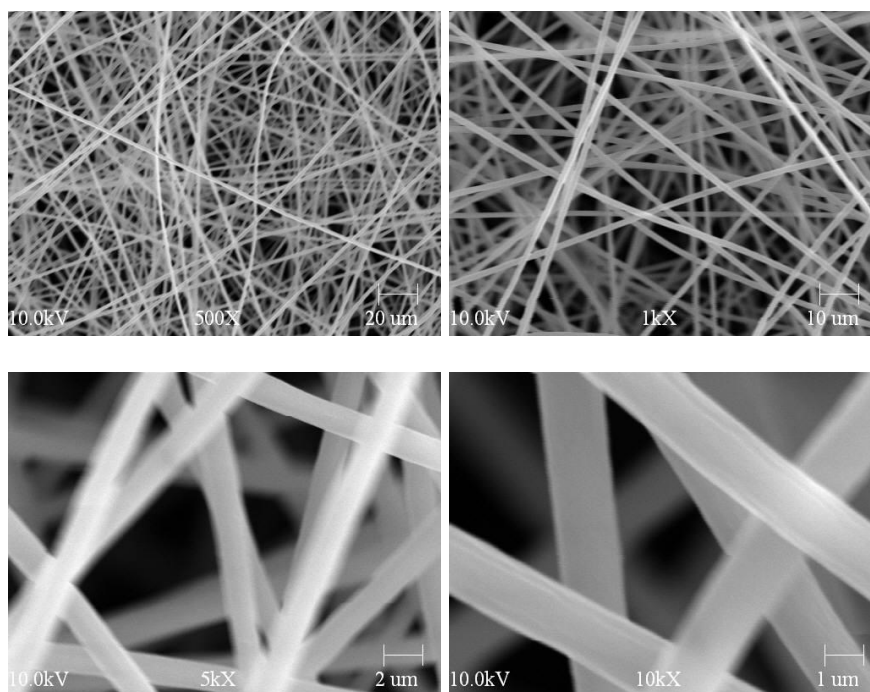
(a)



(b)



(c)



(d)

Figure 2.9: SEM images of 14% PAN nanofibers manufactured in (a) 9kV; (b) 10kV; (c) 11kV; (d) 12kV

2.3 Electrospinning Parameters

There are several parameters which can effect on the electrospinning process and resulting nanofibers. These include distance between the needle and collector, solution feed rate, solution concentration and applied voltage. Nanofiber diameter can vary depending on the nanomanufacturing conditions.

2.3.1 Spinnability and Diameter of PAN Nanofibers in Different Manufacturing Conditions

In this study, two parameters were fixed. One was the distance between needle and collector which was 24 cm. Another was PAN solution feed rate which was 5 ml/h. Two parameters were varied. The PAN solution concentration varied form 6 % to 16 % and the applied voltage varied from 7 kV to 20 kV. Spinnability and diameters of electrospun PAN nanofibers produced in different manufacturing conditions are summarized in Table 2.1. Average diameters with standard deviations are shown in Table 2.2 to Table 2.6 respectively. And computed diameter distributions are shown in Appendix.

	7kV	8kV	9kV	10kV	11kV	12kV	13kV	14kV	15kV	16kV	17kV	18kV	19kV	20kV
6%	Difficult to Collect							Beaded Fibers						
8%	Difficult to Collect					Beaded Fibers								
9%	Difficult to Collect				Beaded Fibers									
10%	D C	680	1370	730	590	480	830	Beaded Fibers		Beaded Fibers		Fluffy Fibers		
11%	Difficult to Collect		1840	1060	830	1390	1110	1010	Beaded Fibers		Fluffy Fibers			
12%	D C	2650	1670	1230	Fluffy Fibers									
13%	Difficult to Collect			2450		1320	1360	1610	1510	Fluffy Fibers				
14%	Difficult to Collect			1870	1770	1560	1890	Fluffy Fibers						
15%	Difficult to Collect					Fluffy Fibers								
16%	Difficult to Collect													

Table 2.1: Spinnability and diameters of electrospun PAN nanofibers fabricated using different manufacturing conditions

In the Table 2.1, “Difficult to collect” means liquid jet could not reach the collector due to the low applied voltage. When applied voltage was too high, “fluffy fibers” were observed. When fibers had some beads as illustrated in Figure 2.10, we considered the fibers to be “not good” (for our study). It has been stated that the formation of beads is influenced mainly by the viscoelasticity of the solution, charge density carried by the jet, and the surface tension of the solution [110].

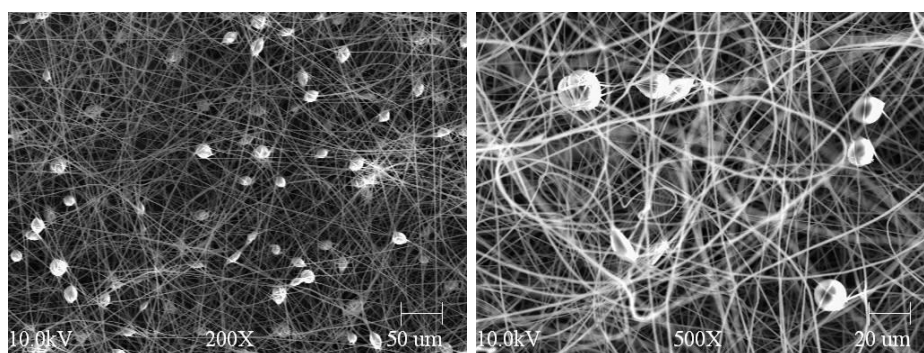


Figure 2.10: Beaded electrospun PAN nanofibers

	8kV	9kV	10kV	11kV	12kV	13kV
Diameter (nm)	680	1370	730	590	480	830
Standard Deviation	50	460	130	110	60	210

Table 2.2: Diameter and standard deviation of 10% PAN nanofibers manufactured with different applied voltage

	9kV	10kV	11kV	12kV	13kV	14kV
Diameter (nm)	1840	1060	830	1390	1110	1010
Standard Deviation	170	120	50	90	150	70

Table 2.3: Diameter and standard deviation of 11% PAN nanofibers manufactured with different applied voltage

	8kV	9kV	10kV
Diameter (nm)	2650	1670	1230
Standard Deviation	290	250	160

Table 2.4: Diameter and standard deviation of 12% PAN nanofibers manufactured with different applied voltage

	11kV	12kV	13kV	14kV	15kV
Diameter (nm)	2450	1320	1360	1610	1510
Standard Deviation	3140	70	50	170	180

Table 2.5: Diameter and standard deviation of 13% PAN nanofibers manufactured with different applied voltage

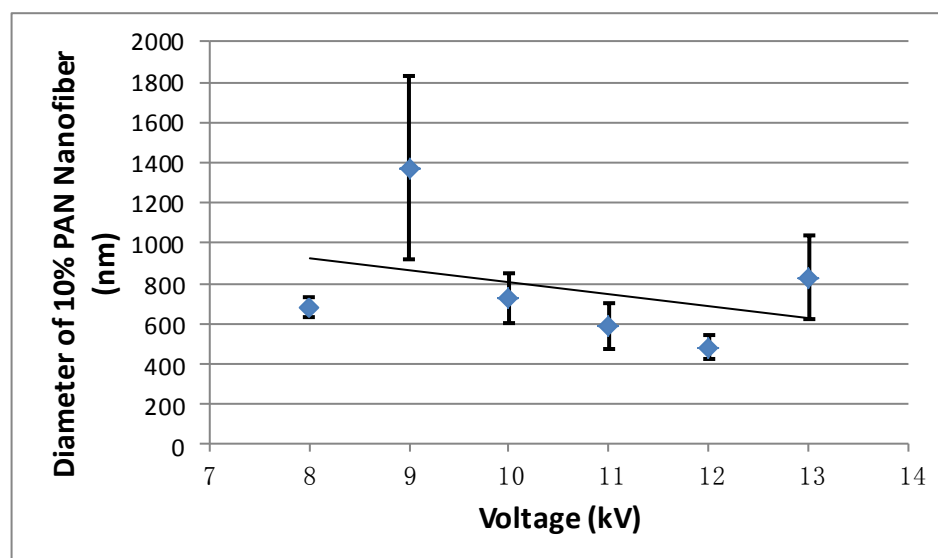
	10kV	11kV	12kV	13kV
Diameter (nm)	1870	1770	1560	1890
Standard Deviation	130	70	110	120

Table 2.6: Diameter and standard deviation of 14% PAN nanofibers manufactured with different applied voltage

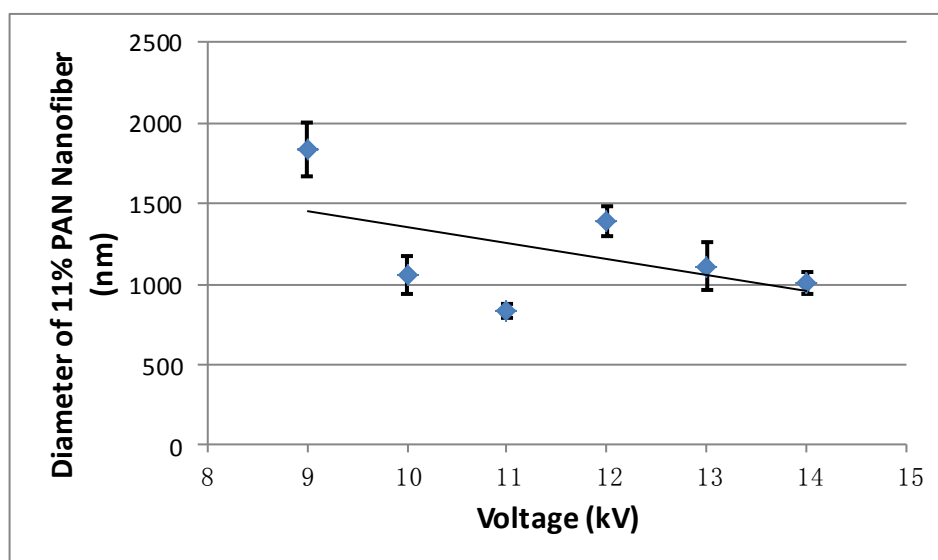
2.3.2 Effects of Electrospinning Parameters on Nanofiber Diameter

2.3.2.1 Applied Voltage

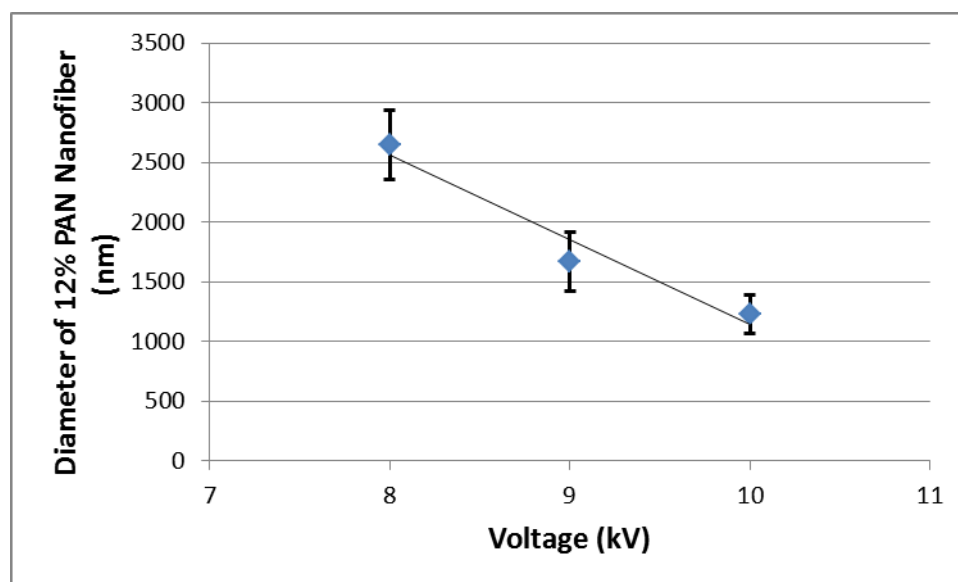
We manufactured good quality PAN nanofibers with PAN solution concentrations ranging from 10% to 14% and found that when keeping other parameters constant, diameter of PAN nanofibers decreased when the applied voltage increased.



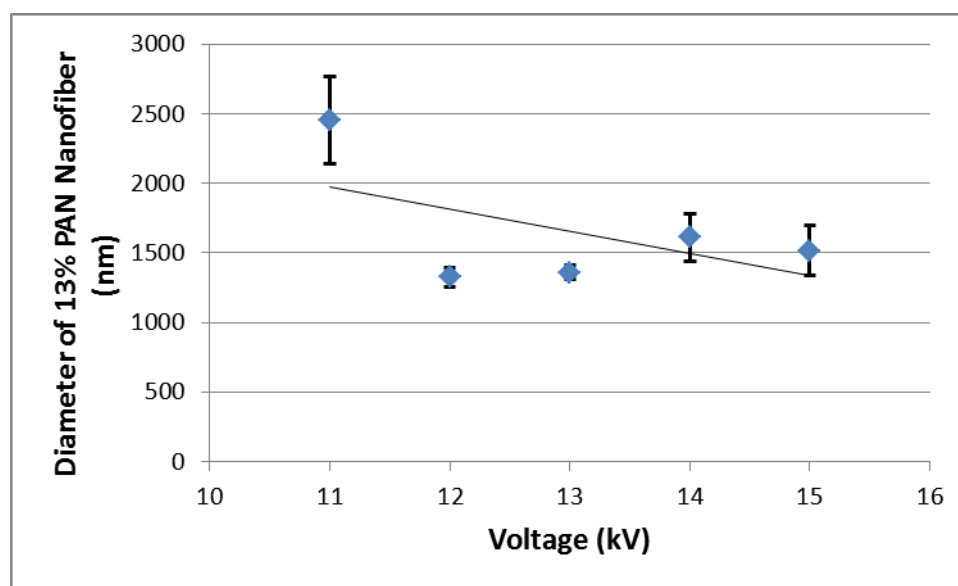
(a)



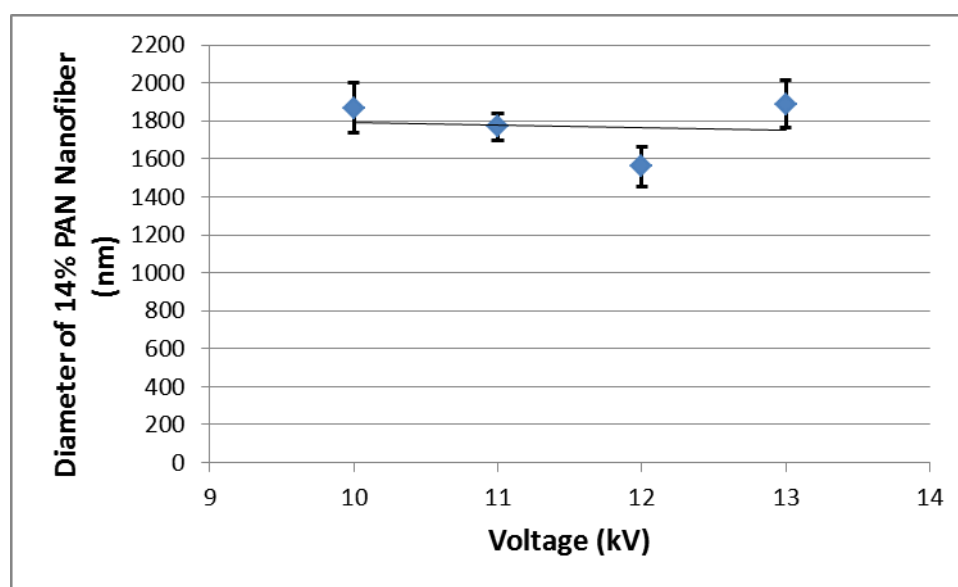
(b)



(c)



(d)

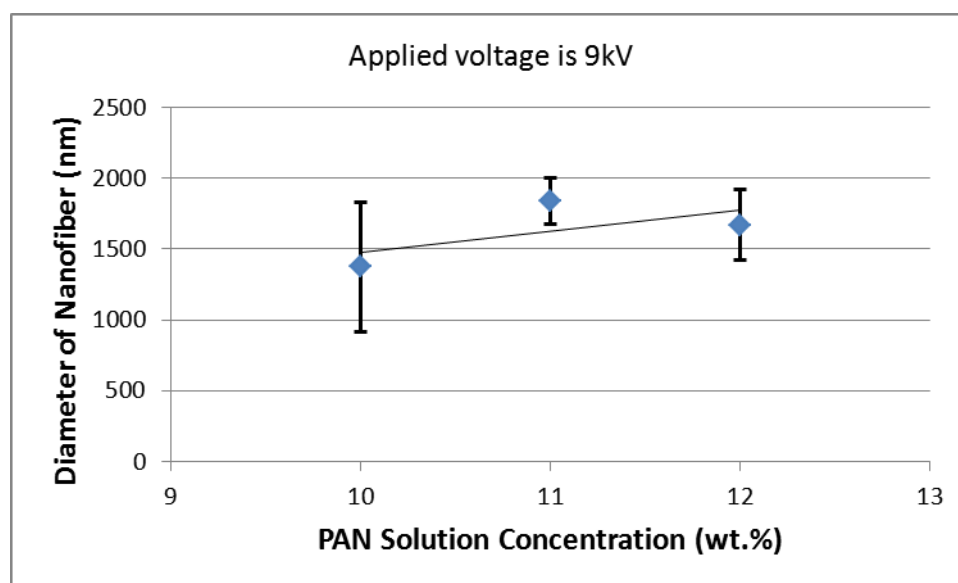


(e)

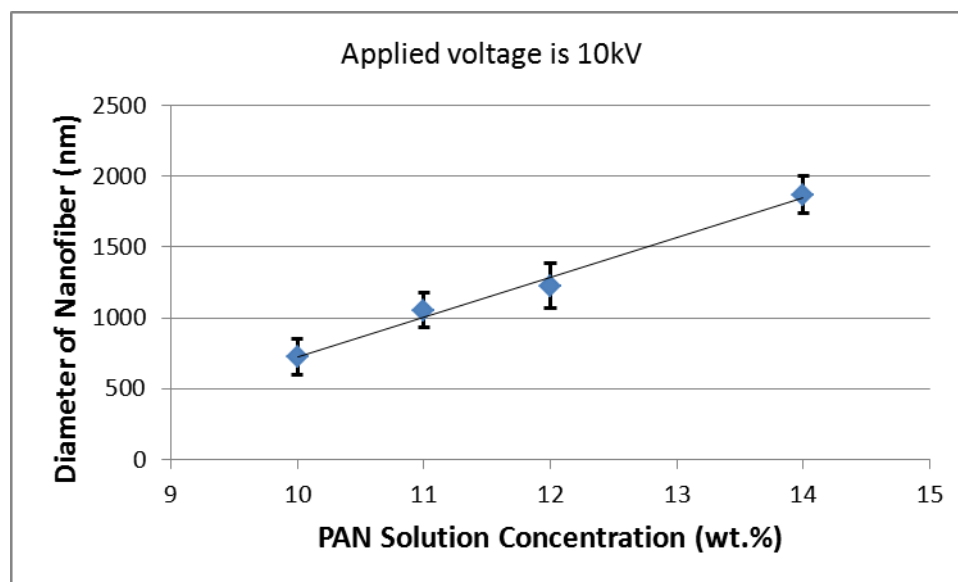
Figure 2.11: Effect of applied voltage on nanofiber diameter (a) 10% PAN; (b) 11% PAN; (c) 12% PAN; (d) 13% PAN; (e) 14% PAN

2.3.2.2 PAN Solution Concentration

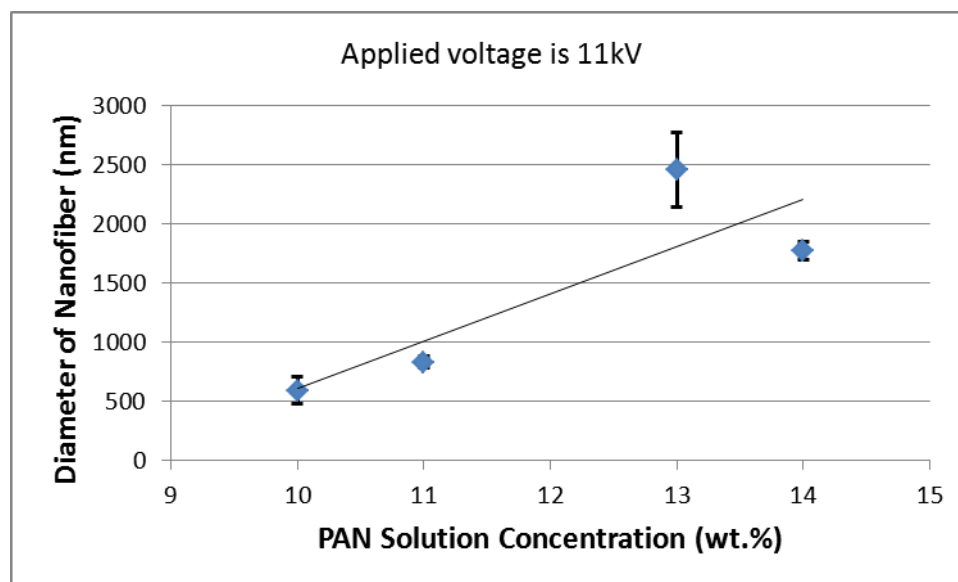
We manufactured good quality PAN nanofibers under applied voltage ranging from 9 kV to 13 kV and found that when keeping other parameters constant, diameter of PAN nanofiber increased as PAN solution concentration increased.



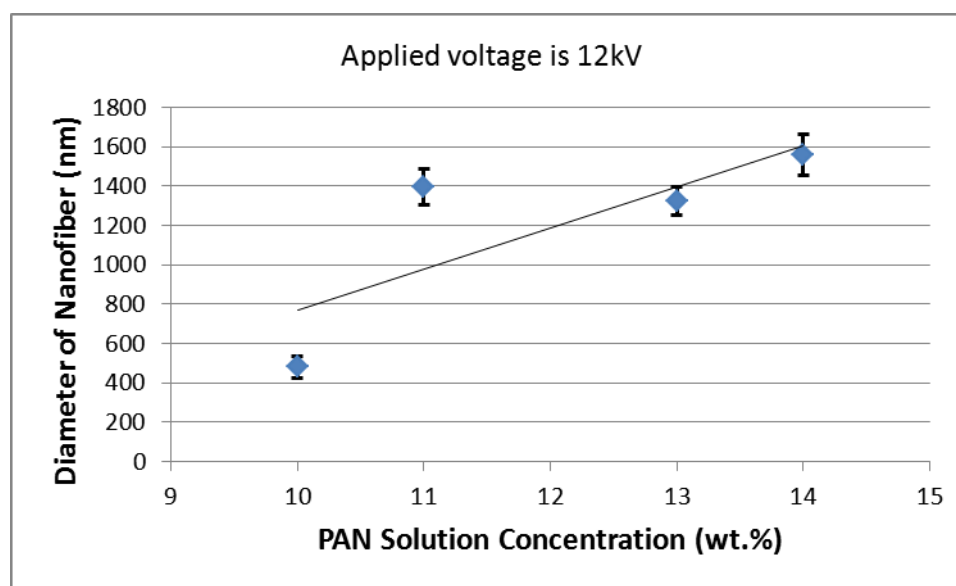
(a)



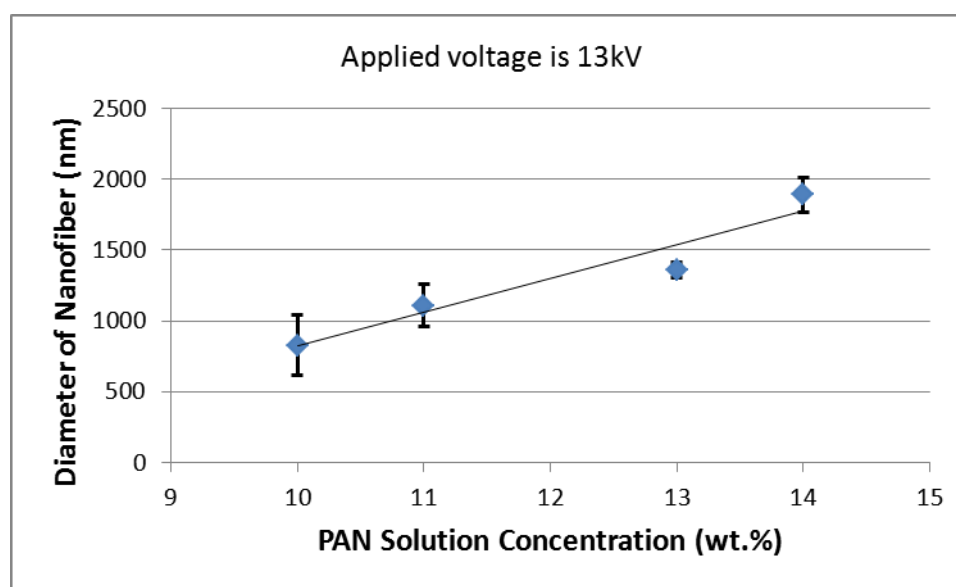
(b)



(c)



(d)



(e)

Figure 2.12: Effect of PAN solution concentration on nanofiber diameter (a) 9kV; (b) 10kV; (c) 11kV; (d) 12kV; (e) 13kV

2.4 Thermal Analysis of Electrospun Nanofibers

Thermogravimetric analysis was used to determine residual solvent concentration in electrospun nanofibers. The Perkin-Elmer Pyris TGA-7 shown in Figure 2.13 was used for thermogravimetric analysis.



Figure 2.13: The Perkin-Elmer Pyris TGA-7

The following testing method was used in this analysis:

1. Hold for 10 min at 25°C
2. Heat from 25°C to 100°C at 10°C/min
3. Heat from 100°C to 250°C at 2°C/min
4. Cool from 250°C to 25°C at 20°C/min

We selected electrospun PAN nanofiber manufactured in 12 kV and with 10% PAN solution as our samples in this test. Manufacturing conditions are shown in Table 2.7. Because PAN nanofibers manufactured in these conditions have the smallest diameter and smallest standard deviation. According to the previous diameter studies, average diameter of the PAN nanofiber was 480 nm with standard deviation 58 nm.

These selected electrospun PAN nanofibers with manufacturing conditions shown in Table 2.7 were further used in the experimental research described in Chapters 3 and 4 below.

Distance between Needle and Collector	24 cm
Speed of Jet	5 ml/h
PAN Solution Concentration	10%
Applied Voltage	12 kV

Table 2.7: Manufacturing conditions of electrospun PAN nanofibers tested in TGA

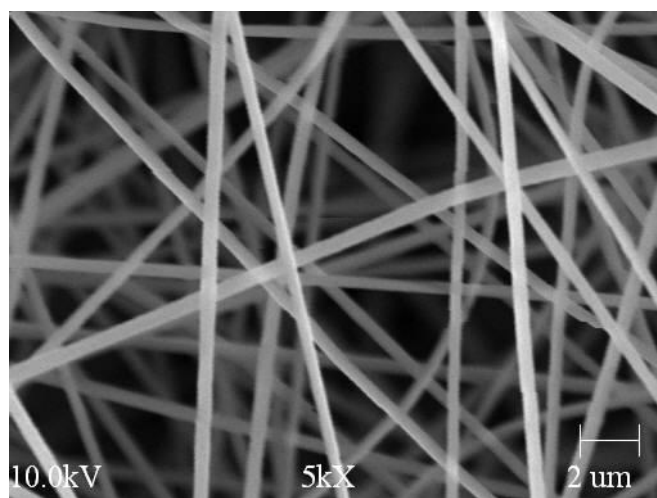
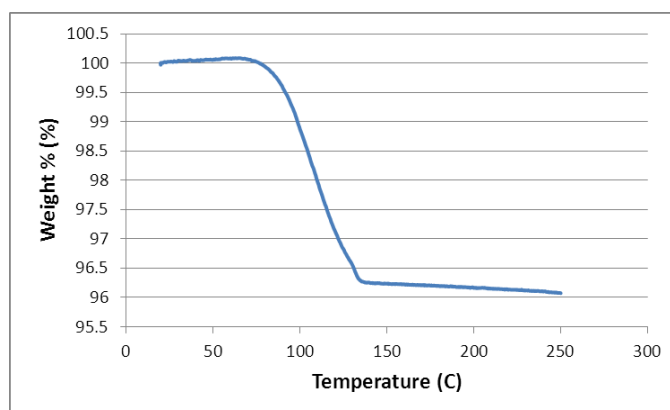
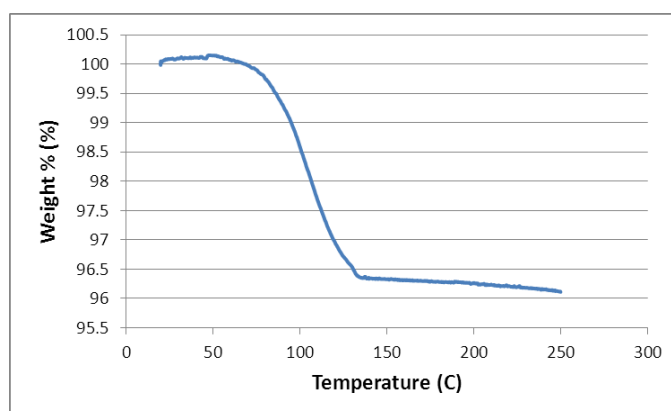


Figure 2.14: SEM image of electrospun PAN nanofibers tested in TGA

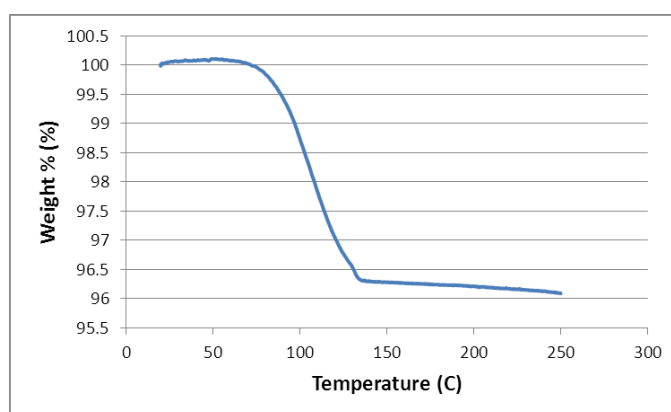
TG curves of as-spun electrospun PAN nanofibers recorded in nitrogen atmosphere are shown in Figure 2.16.



(a)



(b)



(c)

Figure 2.15: TGA curves of selected electrospun PAN nanofibers

The average weight percentage of solvent is 3.69% with standard deviation 0.05% as shown in Figure 2.15. There are 3.69% solvent (DMF) in PAN as-spun nanofibers. So, the portion of PAN is $100\% - 3.69\% = 96.31\%$. Therefore, we can find that the PAN nanofiber has extremely small amount of residual solvent (DMF).

2.5 Conclusions

In this chapter, continuous, uniform diameter PAN nanofibers were manufactured using electrospinning technique. Systematic experimental studies of the effects of process parameters on nanofiber spinnability and diameter were conducted. Range of parameters producing good quality fibers was identified. The following conclusions are drawn based on these studies:

- Higher applied voltage and lower PAN solution concentration produced electrospun nanofibers with smaller diameters.
- Thermal analysis showed that a small amount of solvent (3.69%) was present in PAN nanofibers.

Best processing conditions were selected for the subsequent studies described in the following chapters.

CHAPTER 3

PAN NANOFIBER NETWORKS

3.1 Aligned Nanofibers Manufacturing

In many applications, well aligned and highly ordered materials are required. It is therefore desirable to control the orientation of nanofibers. Our group has been involved in related research topics since 1999. Aligned nanofibers were successfully collected by several methods, including the gap method utilized further in this Chapter.

In the gap method setup for manufacturing aligned PAN nanofibers, the single collector used in Chapter 2 was replaced by two plates (Figure 3.1). All other devices were the same as in the electrospinning setup for random PAN nanofibers production described in Chapter 2. An example of aligned PAN nanofibers is given in Figure 3.2.

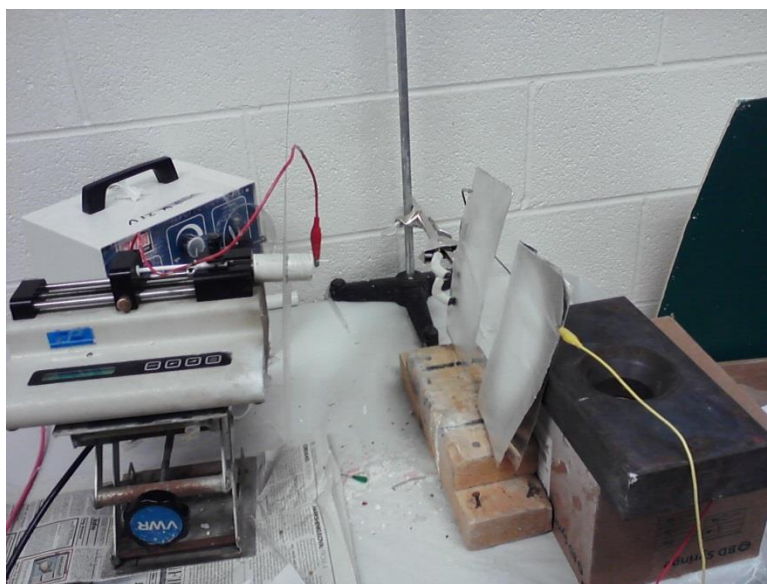


Figure 3.1: Electrospinning setup for manufacturing aligned PAN nanofibers



Figure 3.2: An example of aligned PAN nanofibers produced by the gap method

3.2 Effects of Electrospinning Parameters

In this research, effects of two manufacturing parameters were investigated: one was collector gap size and another was manufacturing duration.

3.2.1 Effect of Collector Gap Size on Diameter and Orientation of Aligned Nanofibers

The gap size between two collector parts can vary in the electrospinning process for manufacturing aligned nanofibers. In general, both diameters and orientation of nanofibers can be affected. Variation of these two outputs with the gap size is examined separately below.

3.2.1.1 Effect of Collector Gap Size on Aligned Nanofibers Diameter

In this study, gap size between the two collector parts was varied in the range from 2cm to 6cm. All other process parameters were kept constant (Table 3.1). Resulting PAN nanofibers were examined by SEM, their diameters were measured, and diameter distributions computed.

Distance between Needle and Collector	24 cm
Solution Feed Rate	5 ml/h
PAN Solution Concentration	10%
Applied Voltage	12 kV
Manufacturing Duration	1 hour
Collector Gap Size	2 cm to 6 cm

Table 3.1: Manufacturing conditions for aligned PAN nanofibers

SEM images of aligned PAN nanofibers manufactured with different gap size are shown in Figures 3.3 to 3.7. More than 200 nanofibers were measured for diameters of each gap size. Computed diameter distributions are presented in Figures 3.8 to 3.12.

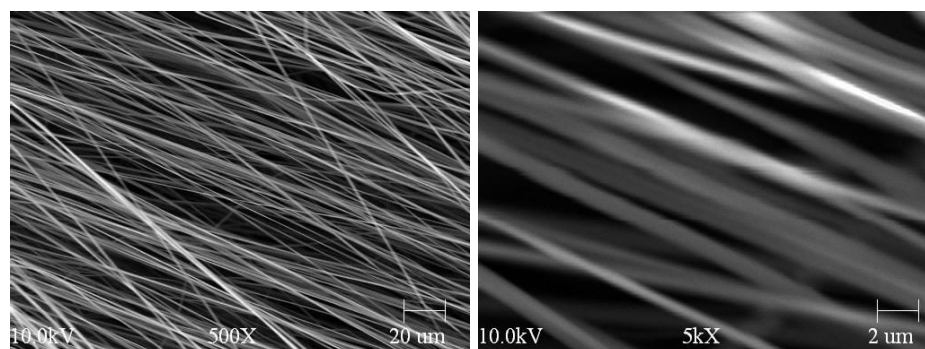


Figure 3.3: SEM images of aligned PAN nanofibers manufactured with 2cm gap size

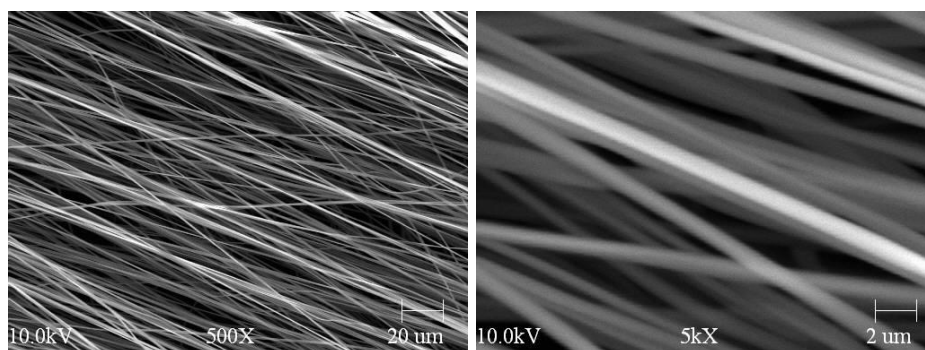


Figure 3.4: SEM images of aligned PAN nanofibers manufactured with 3cm gap size

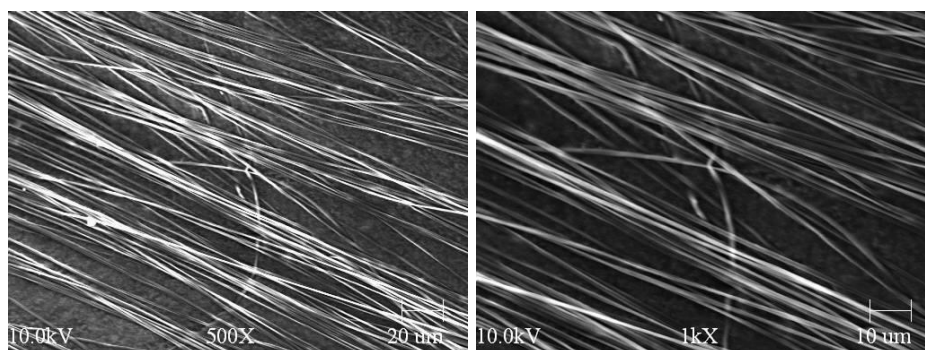


Figure 3.5: SEM images of aligned PAN nanofibers manufactured with 4cm gap size

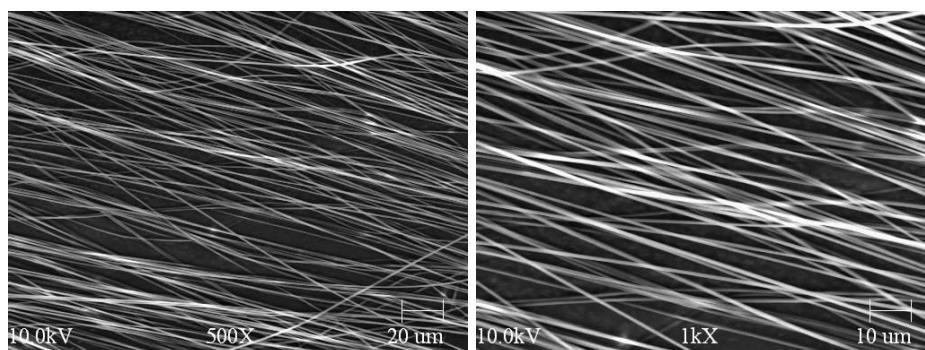


Figure 3.6: SEM images of aligned PAN nanofibers manufactured with 5cm gap size

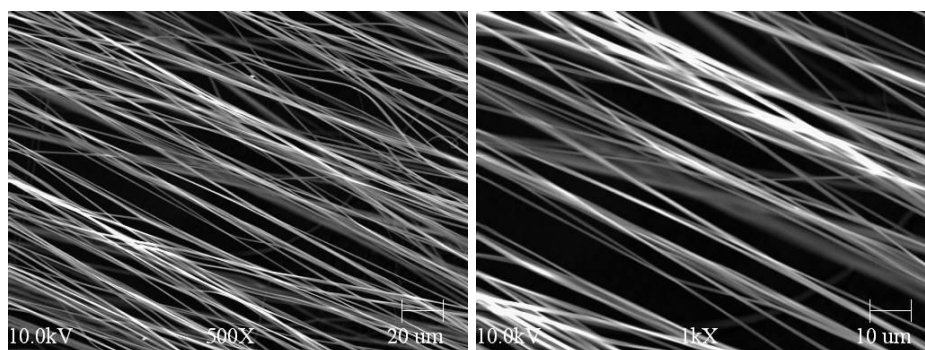


Figure 3.7: SEM images of aligned PAN nanofibers manufactured with 6cm gap size

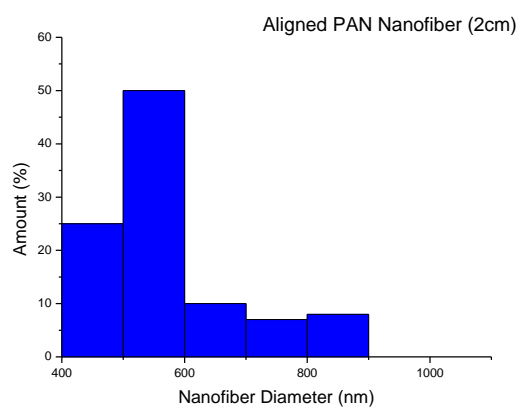


Figure 3.8: Diameter distribution of aligned PAN nanofibers manufactured with 2cm gap size

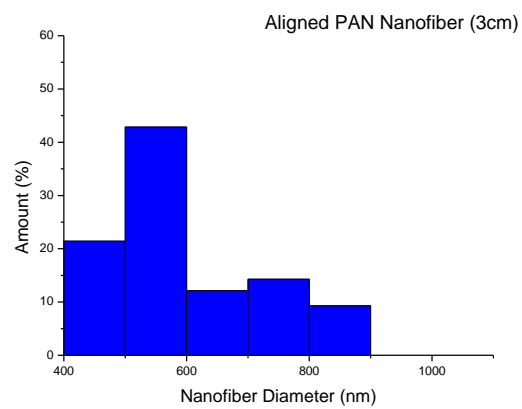


Figure 3.9: Diameter distribution of aligned PAN nanofibers manufactured with 3cm gap size

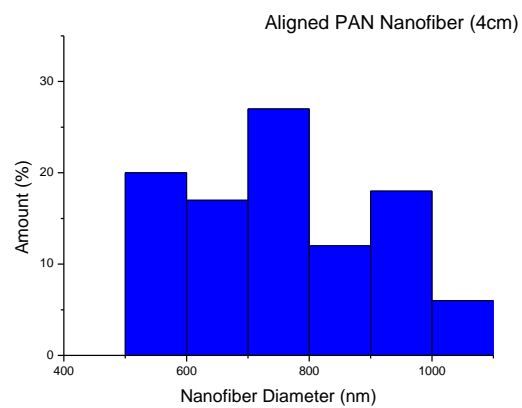


Figure 3.10: Diameter distribution of aligned PAN nanofibers manufactured with 4cm gap size

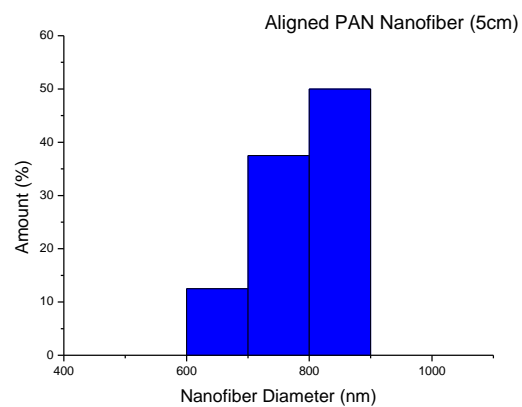


Figure 3.11: Diameter distribution of aligned PAN nanofibers manufactured with 5cm gap size

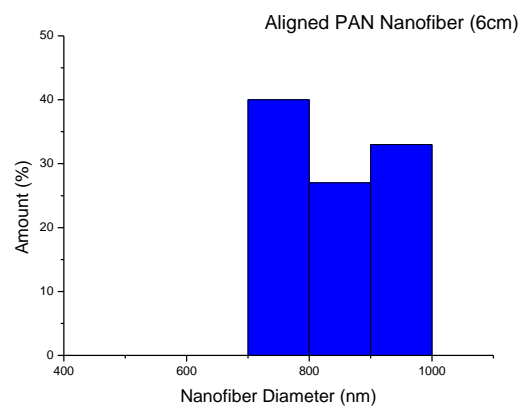


Figure 3.12: Diameter distribution of aligned PAN nanofibers manufactured with 6cm gap size

Average diameters and corresponding standard deviations are given in Table 3.2. As the gap size between the two collector parts increased, aligned nanofiber diameter increased (Figure 3.13).

	2cm	3cm	4cm	5cm	6cm
Diameter (nm)	630	640	760	810	850
Standard Deviation	150	110	300	70	90

Table 3.2: Average diameter and standard deviation of aligned PAN nanofibers manufactured with different gap size

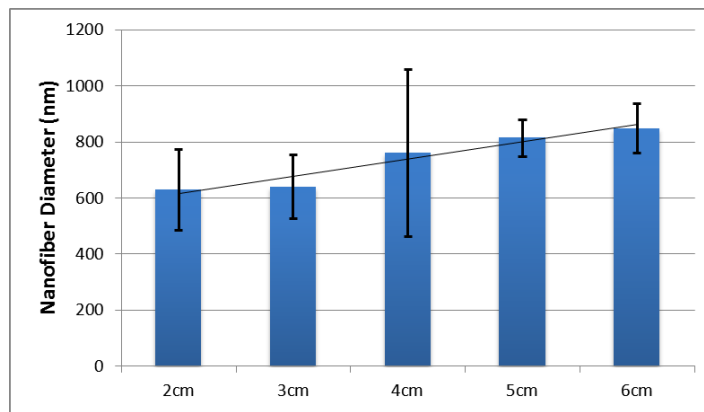


Figure 3.13: Diameter of aligned PAN nanofibers manufactured with different gap size

3.2.1.2 Effect of Collector Gap Size on Aligned Nanofibers Orientation Distribution

Various gap sizes produce different electric field distributions, which can result in different degrees of nanofiber alignment.

In the gap methods for manufacturing aligned nanofibers, two rectangular plates act as a collector. Most nanofibers would align between the two plates. To determine fiber orientation distribution, 0 degree was defined as shown below in Figure 3.14. An example SEM image of aligned PAN nanofibers with the 0 direction indicated by an arrow is presented in Figure 3.15.

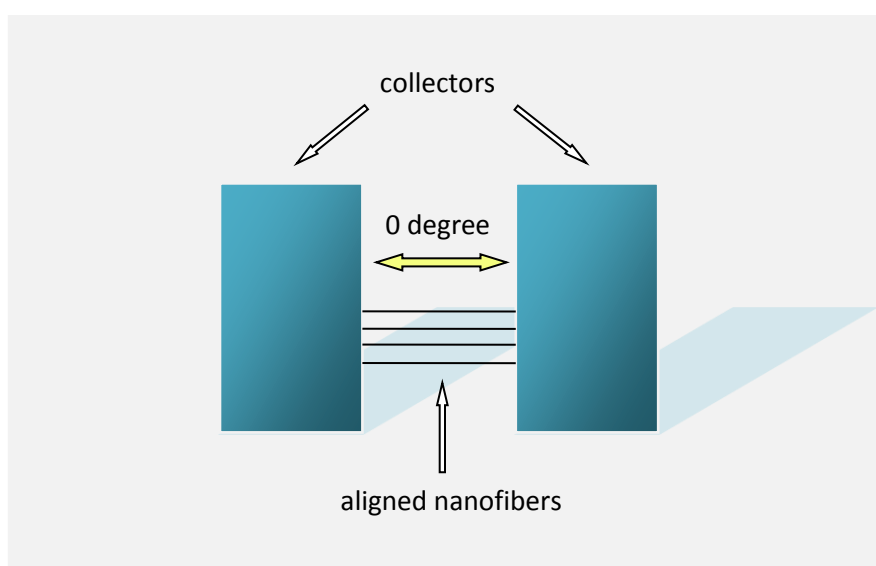


Figure 3.14: Schematic definition of 0 degree orientation of aligned nanofibers

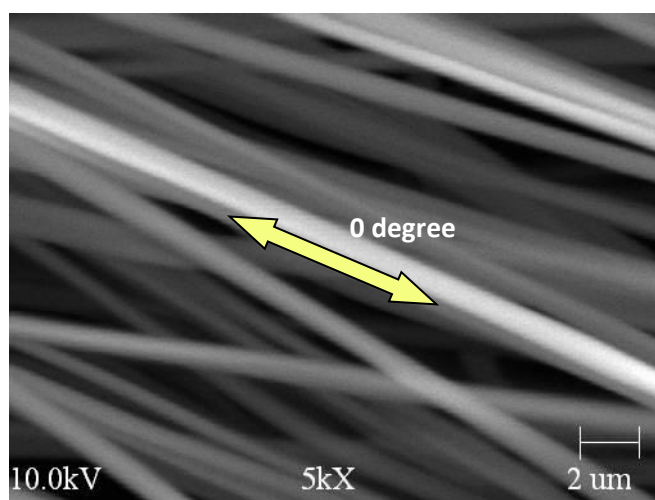


Figure 3.15: An example of aligned PAN nanofibers with 0 degree direction indicated by an arrow

SEM images similar to the one shown in Figure 3.15 were analyzed and orientation distributions of aligned PAN nanofibers manufactured with different gap size were calculated. For each gap size, more than 250 nanofibers were measured to get the orientation distribution. The results are presented in Figures 3.16 to 3.20.

Based on the analysis of SEM images, we found that nanofiber alignment increased with the increasing gap size. A quantitative evaluation of nanofiber alignment would be introduced in section 3.2.3.

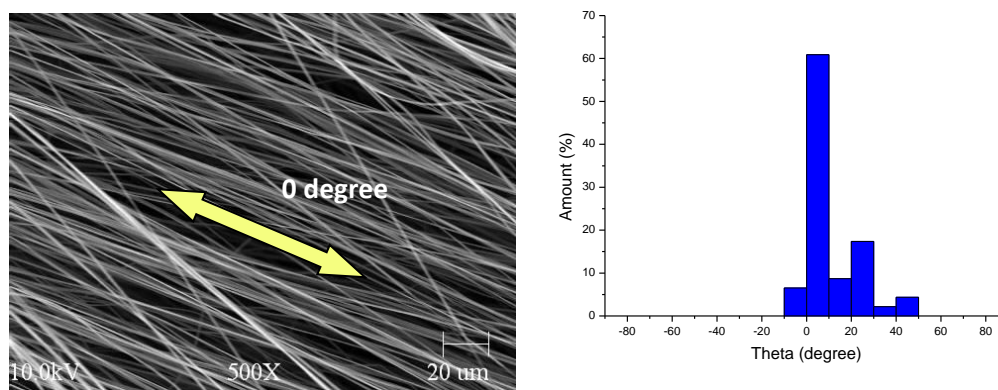


Figure 3.16: SEM image and orientation distribution of aligned PAN nanofibers manufactured with 2cm gap

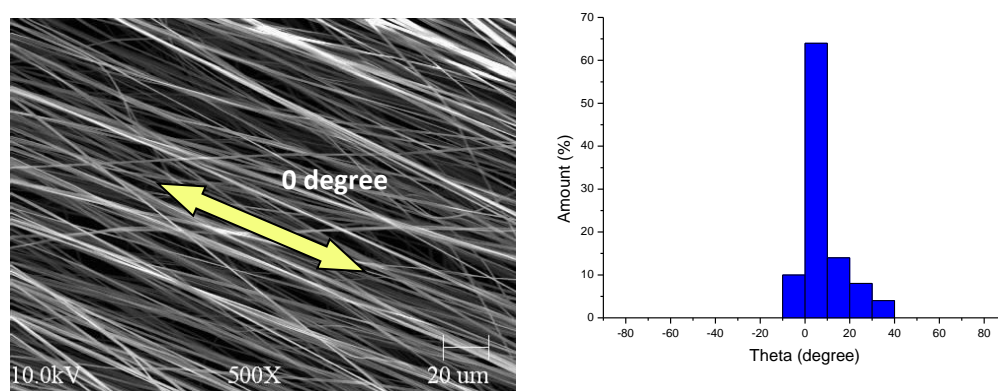


Figure 3.17: SEM image and orientation distribution of aligned PAN nanofibers manufactured with 3cm gap

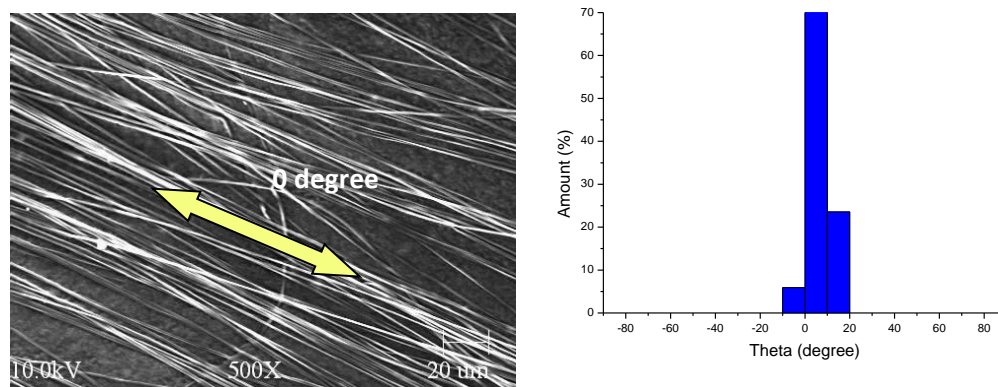


Figure 3.18: SEM image and orientation distribution of aligned PAN nanofibers manufactured with 4cm gap

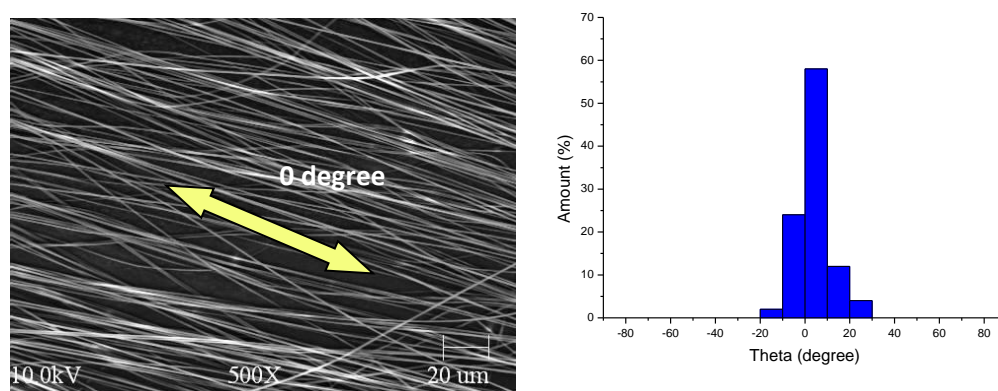


Figure 3.19: SEM image and orientation distribution of aligned PAN nanofibers manufactured with 5cm gap

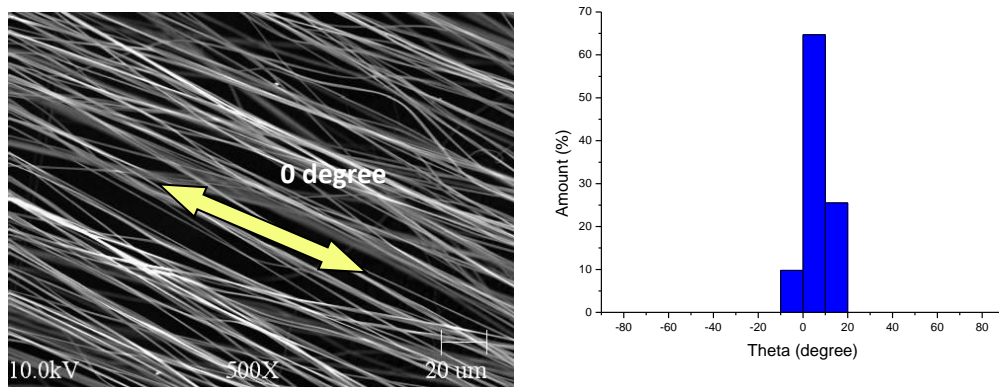


Figure 3.20: SEM image and orientation distribution of aligned PAN nanofibers manufactured with 6cm gap

3.2.2 Effect of Manufacturing Duration on Aligned Nanofiber Orientation

Due to non-perfect conductivity of electrospun nanofibers, they carry residual charges after deposition onto collector. These residual charges will interact with the charges carried by the upcoming jets/fibers during continuous deposition. These charge interactions can disturb the static external electric field configuration and can reduce the resulting nanofiber alignment. So far, no published work was found to study the relationship between manufacturing duration and nanofiber alignment.

SEM images of aligned PAN nanofibers manufactured in 1 hour and 2 hours are presented in Figure 3.21. Comparison shows that when other parameters are kept constant, increased manufacturing duration results in significantly reduced alignment. Quantitative evaluation of nanofiber alignment will be performed in section 3.2.3.

Distance between Needle and Collector	24 cm
Solution Feed Rate	5 ml/h
PAN Solution Concentration	10%
Applied Voltage	12 kV
Manufacturing Duration	1 hour & 2 hours, respectively
Collector Gap Size	3 cm

Table 3.3: Manufacturing conditions for aligned PAN nanofibers

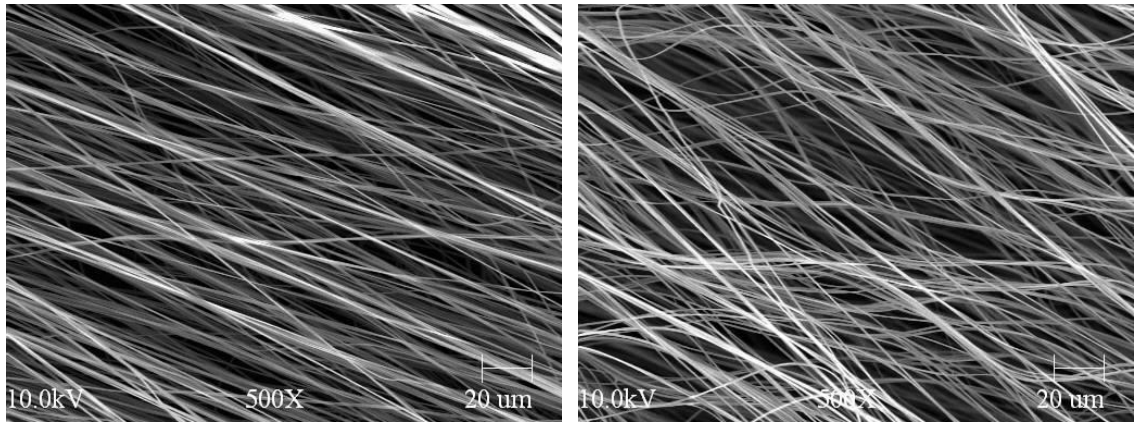


Figure 3.21: SEM image of aligned PAN nanofibers manufactured in 1 hour (left) and 2 hours (right)

3.2.3 Calculation of Orientation Parameters [103,107]

The orientation of fibers can be described by fiber orientation distribution function $\psi(\phi)$. This function defined as the probability, P , of finding a fiber between ϕ_1 and ϕ_2 is given by

$$P(\phi_1 \leq \phi \leq \phi_2) = \int_{\phi_1}^{\phi_2} \psi(\phi) d\phi$$

In order to describe the orientation of nanofibers quantitatively, two orientation parameters were introduced:

$$f_p = 2\langle \cos^2 \phi \rangle - 1$$

$$g_p = (8\langle \cos^4 \phi \rangle - 3)/5$$

where

$$\langle \cos^m \phi \rangle = \int_0^\pi \cos^m \phi \cdot \psi(\phi) d\phi \quad m=2,4$$

These orientation parameters vary from $f_p = g_p = 1$ for perfect alignment of nanofibers to $f_p = g_p = 0$ for random nanofiber distribution.

Orientation parameters, f_p and g_p , calculated based on experimental observations are shown in Table 3.4 and Table 3.5. Orientation parameters increased with the increasing gap size. Conversely, orientation parameters decreased with the increasing manufacturing duration. These results matched the qualitative observation on SEM images in 3.2.1.2 and 3.2.2.

	2 cm	3 cm	4 cm	5 cm	6 cm
f_p	0.9343	0.9598	0.9699	0.9643	0.9787
g_p	0.9014	0.9384	0.9535	0.9446	0.9664

Table 3.4: f_p and g_p values of aligned nanofibers with different manufacturing gap size

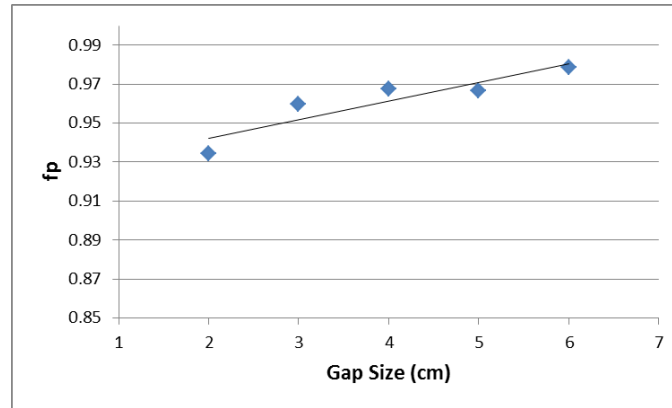


Figure 3.22: f_p values of aligned nanofibers with different manufacturing gap size

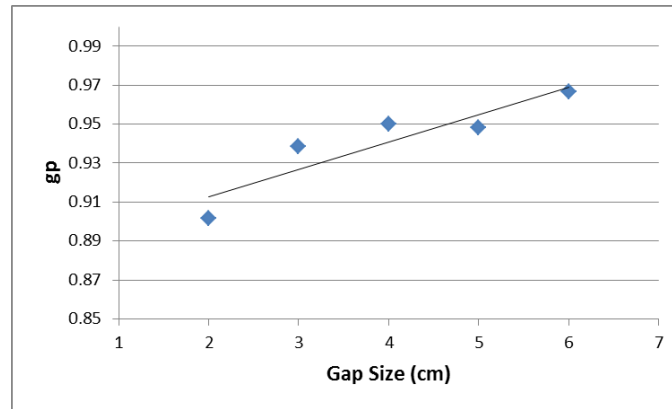


Figure 3.23: g_p values of aligned nanofibers with different manufacturing gap size

	1 hour	2 hours
f_p	0.9598	0.8265
g_p	0.9384	0.7540

Table 3.5: f_p and g_p values of aligned nanofibers with different manufacturing duration

3.3 Equivalent Thickness Measurement of Polymer Nanofiber Sheet

The thickness of nanofiber sheets is in the micron scale. It is challenging to measure it as the nanofiber layer is soft and the boundaries of the sheet are not well defined for application of optical methods. At the same time, sheet thickness is necessary for evaluation of mechanical characteristics, such as average macroscopic stress. In this research, equivalent thickness of polymer layer was introduced and used for that purpose. This parameter was calculated using following equation:

$$t = \frac{\text{weight} / \text{area}}{\rho_{PAN}}$$

where t is equivalent (solid) thickness of PAN nanofiber sheet

ρ_{PAN} is density of PAN powder

weight/area ratio of aligned PAN nanofiber sheet manufactured in 1 hour was $0.778 \times 10^{-6} \text{ g/mm}^2$

weight/area ratio of aligned PAN nanofiber sheet manufactured in 2 hours was $1.600 \times 10^{-6} \text{ g/mm}^2$

Computed equivalent thickness of aligned nanofiber networks is presented in Table 3.6.

These results were applied to determine cross-sectional area for stress analysis in the following tensile testing study.

	1 hour	2 hours
weight/area (g/mm ²)	0.778×10^{-6}	1.600×10^{-6}
thickness (mm)	0.662×10^{-3}	1.362×10^{-3}

Table 3.6: Weight/area and computed equivalent thickness of aligned PAN nanofibers manufactured during different durations

3.4 Mechanical Properties of PAN Nanofibers

3.4.1 Tensile Testing

The NANO UTM Testing System shown in Figure 3.24 was used in the tensile testing. This universal testing machine (UTM) provides a superior means of nanomechanical characterization. This state-of-the-art UTM offers high sensitivity over a large strain. Mechanical properties such as strain, tensile strength and yield stress, were captured. The system software allowed real-time experimental data analysis and visualization.

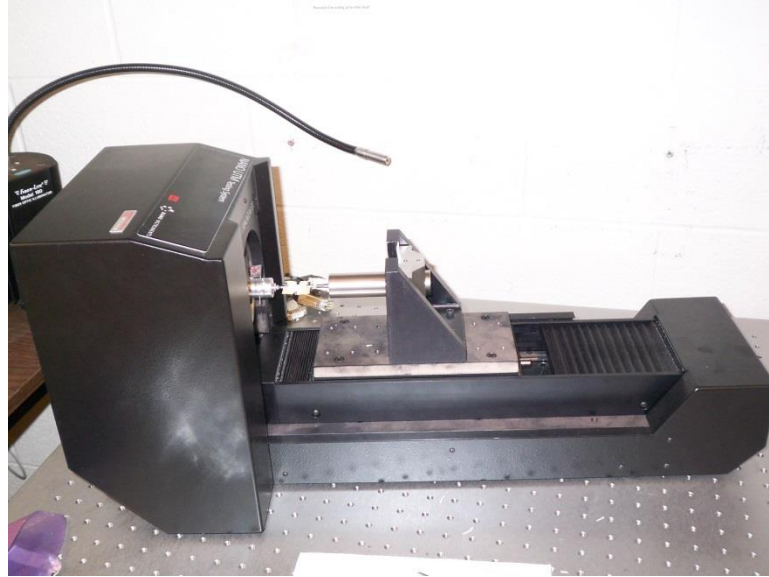


Figure 3.24: NANO UTM Testing System by Agilent

Same loading conditions were applied in all tensile testing by using UTM, as shown in Table 3.7.

Delta Extension for Data	0.01 mm
Strain Rate	5×10^{-3} 1/s
Relaxation Hold Time	5 s
Nominal Gage Length	15 mm for networks
Tension Trigger	5 μ N
Max. Strain	3 mm/mm

Table 3.7: Loading conditions of UTM tests

In the following study, single PAN nanofibers, aligned PAN nanofiber networks and random PAN nanofiber networks were tested to compare their mechanical properties.

3.4.2 Single PAN Nanofiber Testing

Manufacturing conditions for single nanofiber are shown in Table 3.8.

Distance between Needle and Collector	24 cm
Solution Feed Rate	5 ml/h
PAN Solution Concentration	10%
Applied Voltage	12 kV

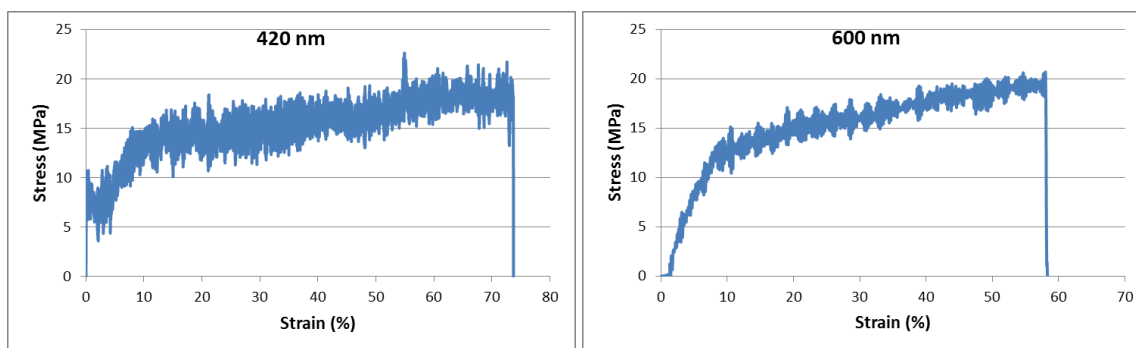
Table 3.8: Manufacturing conditions for single PAN nanofiber

40 tests were applied to calculate the average and standard deviation.

	Strength (MPa)	Young's Modulus (MPa)	Toughness (MPa)
Average	21.5	815.1	8.9
Standard Deviation	2.4	217.3	3.1

Table 3.9: Mechanical properties of single PAN nanofiber

Strain-Stress curves:



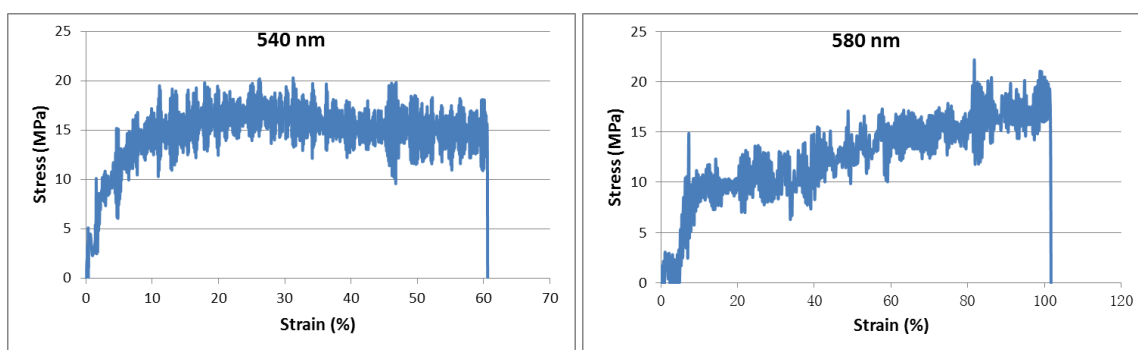
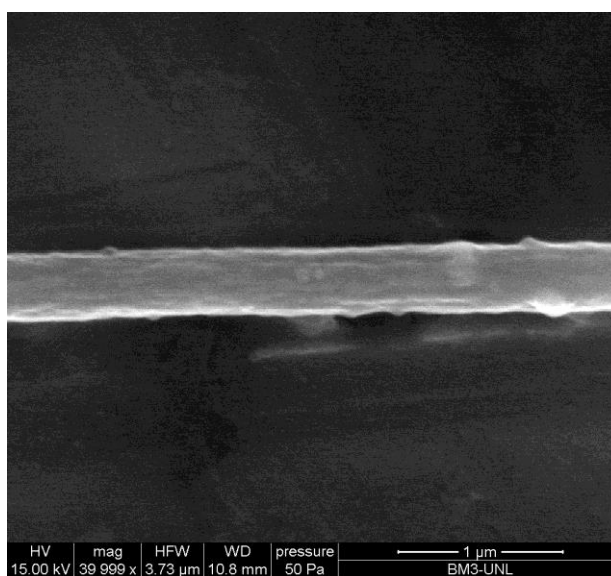
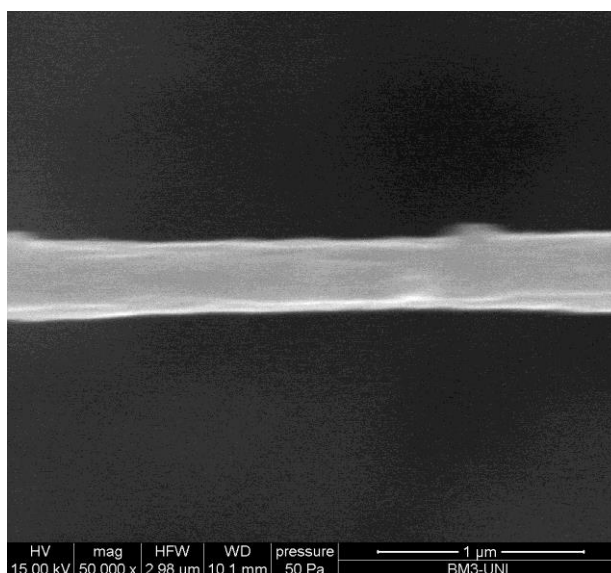


Figure 3.25: Representative strain-stress curves of single PAN nanofibers

SEM images were used to determine diameters of single nanofibers.



(a)



(b)

Figure 3.26: SEM images of single PAN nanofibers with diameters: (a) 420 nm (b) 375 nm

As presented in Figure 3.27, strength of single nanofiber increased, when nanofiber diameter decreased.

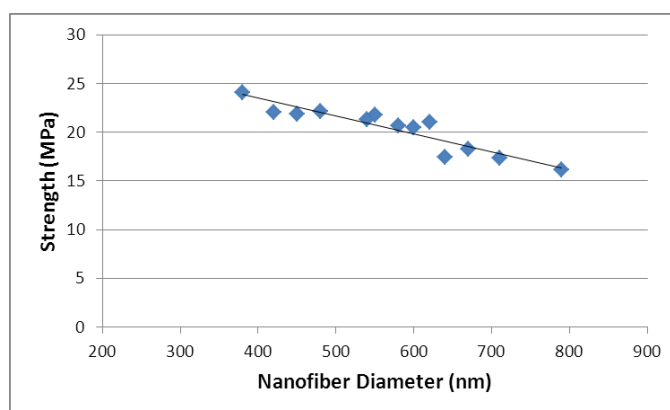


Figure 3.27: Effect of single nanofiber diameter on strength

3.4.3 Aligned PAN Nanofiber Network Testing

In this study, aligned PAN nanofiber networks manufactured in 1 hour and 2 hours respectively were tested. These were the same networks in previous section 3.2.2. Same manufacturing and testing conditions were applied for two types of nanofiber sheets. Figure 3.34 illustrates the process of tensile testing using UTM.

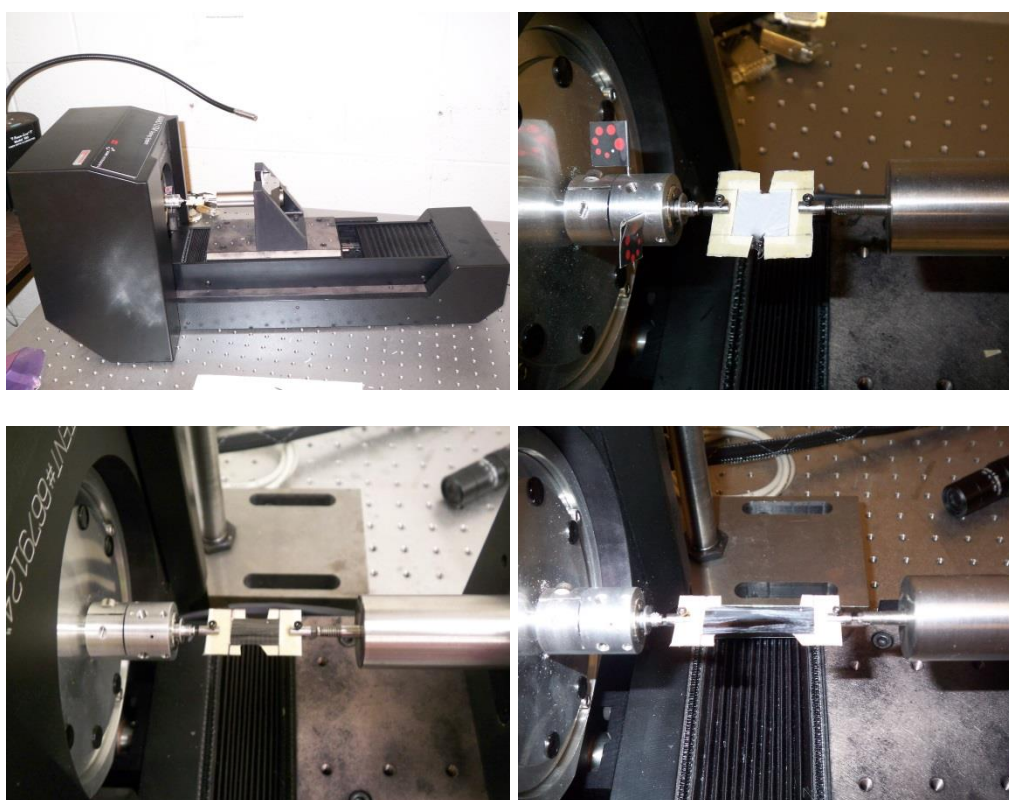


Figure 3.28: Tensile testing of aligned PAN nanofibers

3.4.3.1 Fiber Network Manufactured in 1 Hour

Tensile testing results of aligned nanofiber network are presented in Table 3.10. 50 tests were applied to calculate the average and standard deviation. Strain-stress curves are

shown in Figure 3.29.

	Strength (MPa)	Young's Modulus (MPa)	Toughness (MPa)
Average	20.9	541.4	9.4
Standard Deviation	3.0	102.8	2.3

Table 3.10: Mechanical properties of aligned PAN nanofiber network manufactured in 1 hour

Strain-Stress curves:

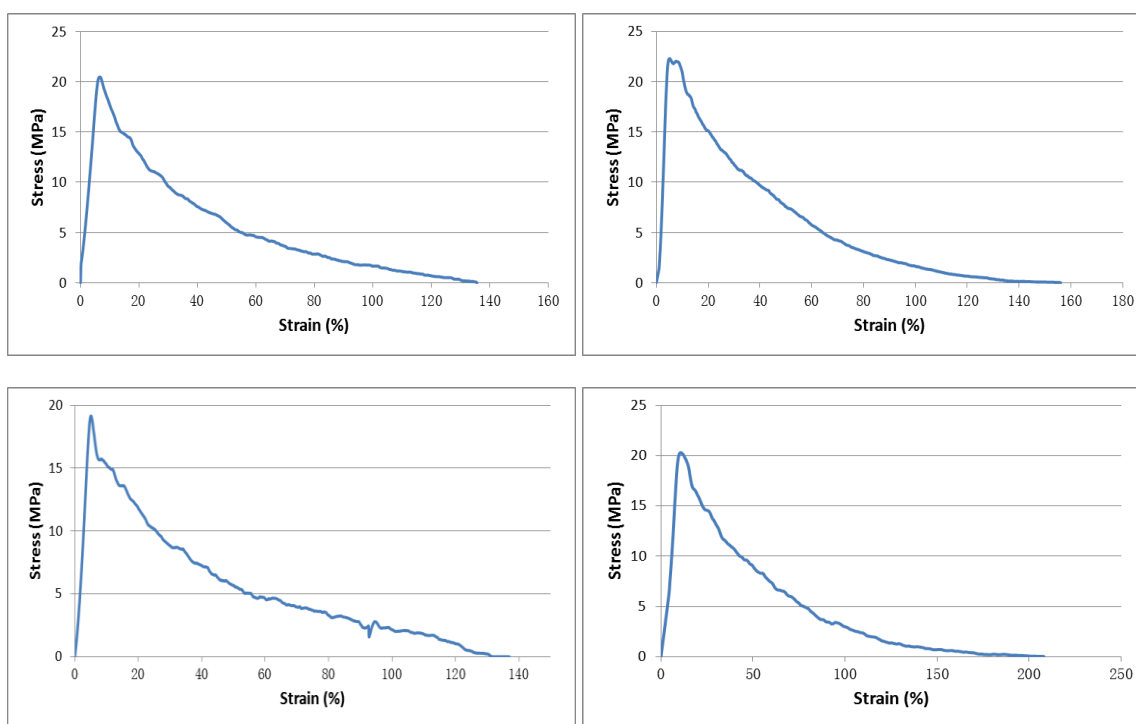


Figure 3.29: Representative strain-stress curves of aligned PAN nanofiber network manufactured in 1 hour

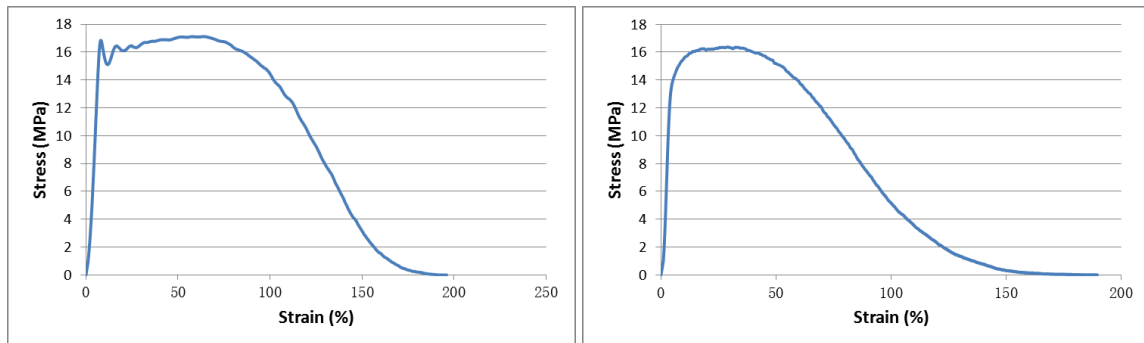
3.4.3.2 Fiber Network Manufactured in 2 Hours

Tensile testing results of aligned nanofiber network are presented in Table 3.11. 40 tests were applied to calculate the average and standard deviation. Strain-stress curves are shown in Figure 3.36.

	Strength (MPa)	Young's Modulus (MPa)	Toughness (MPa)
Average	17.9	329.6	13.2
Standard Deviation	3.3	67.9	2.4

Table 3.11: Mechanical properties of aligned PAN nanofiber network manufactured in 2 hours

Strain-Stress curves:



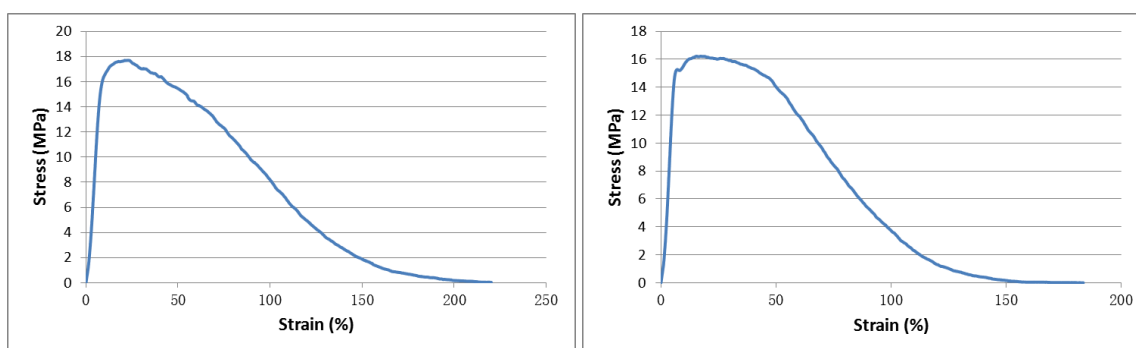


Figure 3.30: Representative strain-stress curves of aligned PAN nanofiber network manufactured in 2 hours

3.4.4 Random Nanofiber Networks

Manufacturing conditions for random nanofibers networks are shown in Table 3.12. Manufacturing conditions were the same as for single nanofibers and aligned nanofiber networks fabrication.

Distance between Needle and Collector	24 cm
Solution Feed Rate	5 ml/h
PAN Solution Concentration	10%
Applied Voltage	12 kV

Table 3.12: Manufacturing conditions for random PAN nanofiber network

SEM images of tested random nanofiber network are shown in Figure 3.31. Average diameter of nanofiber is 480 nm with standard deviation 60.

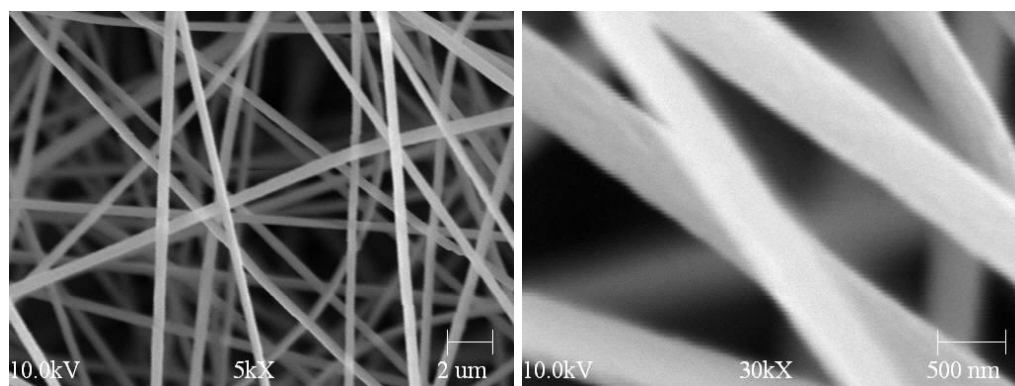


Figure 3.31: SEM images of random PAN nanofiber network

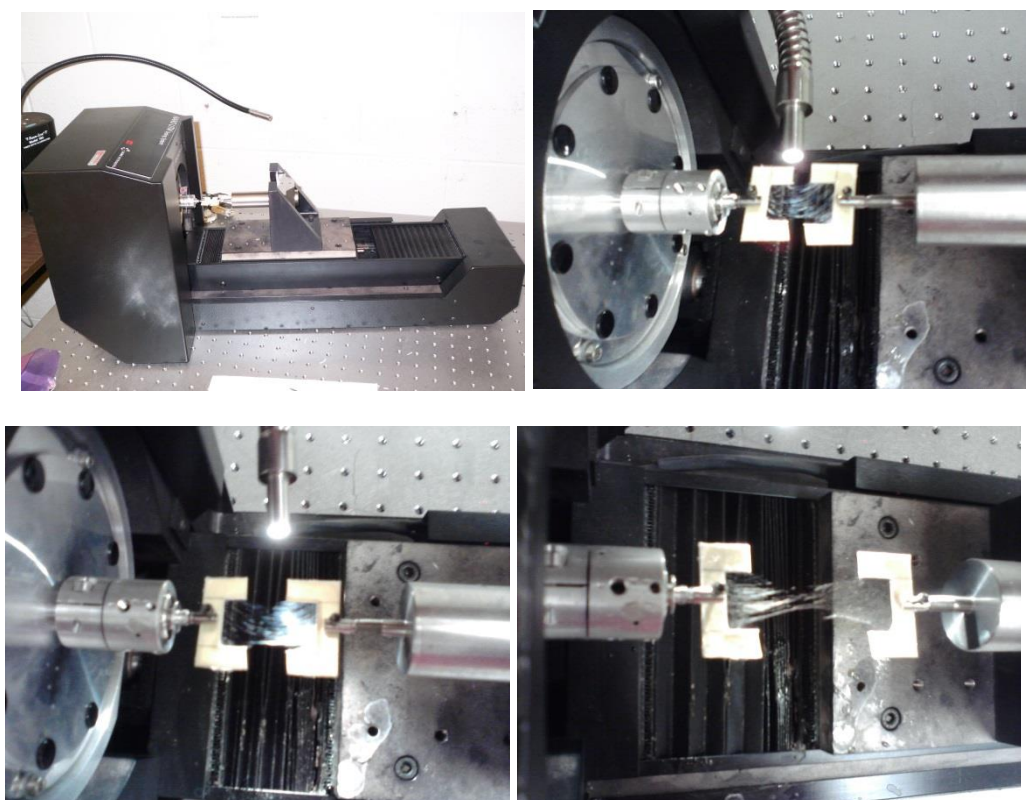


Figure 3.32: Tensile testing of random PAN nanofiber network

Tensile testing results for random nanofiber network are presented in Table 3.13. 40 tests were applied to calculate the average and standard deviation. Strain-stress curves are shown in Figure 3.33.

	Strength (MPa)	Young's Modulus (MPa)	Toughness (MPa)
Average	9.9	150.1	14.0
Standard Deviation	2.4	72.6	3.2

Table 3.13: Mechanical properties of random PAN nanofiber network

Strain-Stress curves:

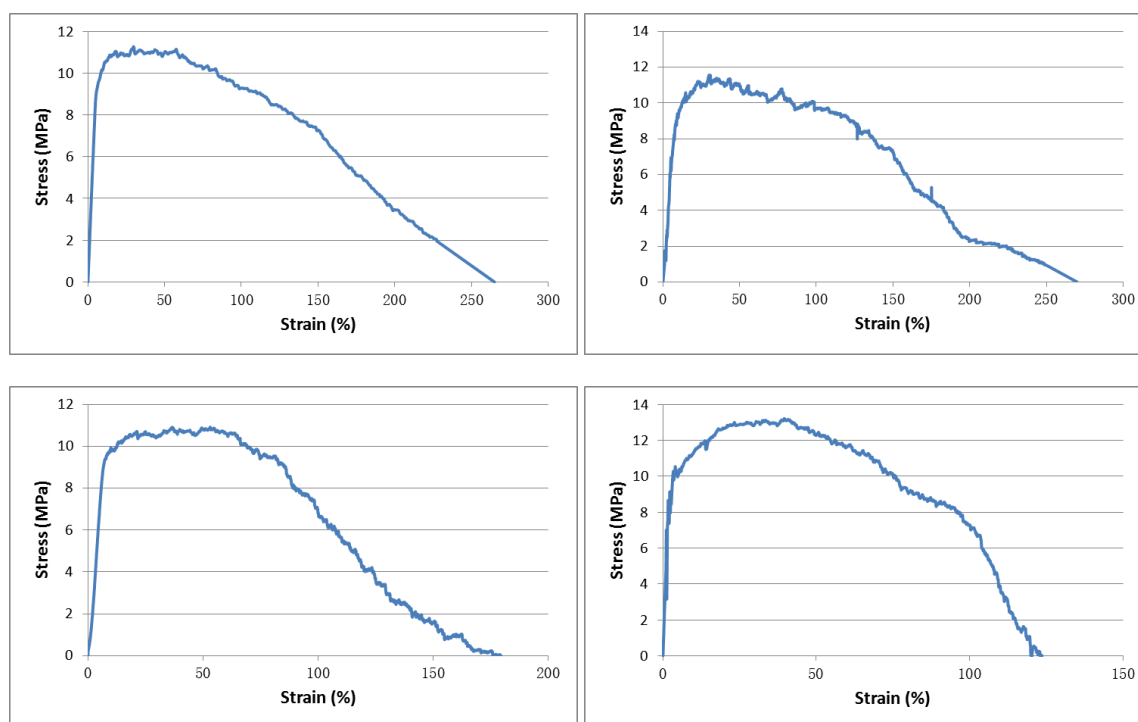


Figure 3.33: Representative strain-stress curves of random PAN nanofiber network

3.4.5 Comparison of Mechanical Properties of Nanofiber Networks

Tensile testing results are presented in Table 3.14 for three types of nanofiber networks. Aligned nanofiber network manufactured in 1 hour has the highest value of strength and Young's modulus, while lowest value of toughness. On the contrary, random nanofiber network has the highest value in toughness, but lowest value in both strength and Young's modulus.

	Strength (MPa)	Young's Modulus (MPa)	Toughness (MPa)
Aligned – 1hour	20.9	541.4	9.4
Aligned – 2hours	17.9	329.6	13.2
Random	9.9	150.1	14.0

Table 3.14: Mechanical properties of aligned (manufactured in 1 hour and 2 hours) and random PAN nanofiber network

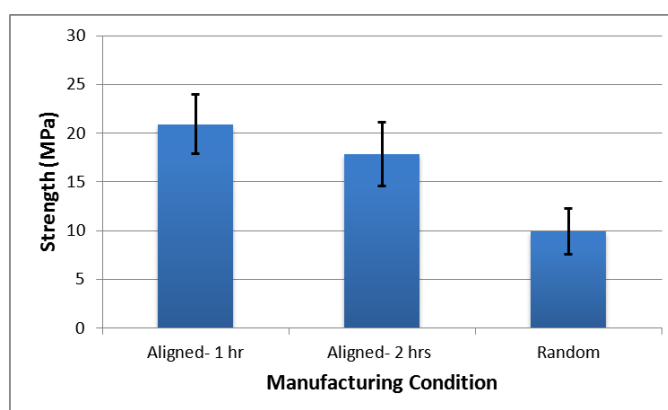


Figure 3.34: Strength of aligned (manufactured in 1 hour and 2 hours) and random PAN

nanofiber network

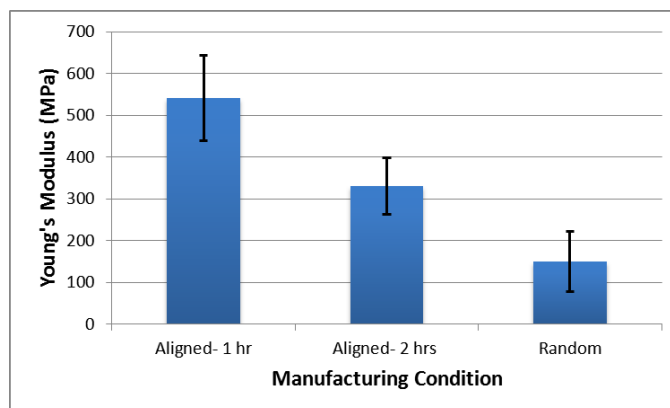


Figure 3.35: Young's Modulus of aligned (manufactured in 1 hour and 2 hours) and random PAN nanofiber network

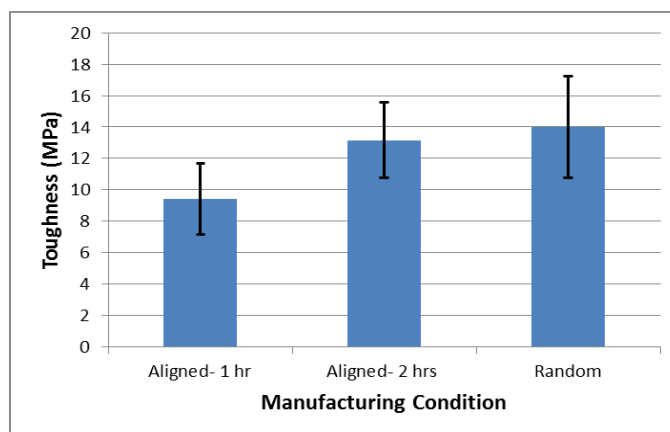


Figure 3.36: Toughness of aligned (manufactured in 1 hour and 2 hours) and random PAN nanofiber network

3.5 Conclusions

In this chapter, aligned electrospun PAN nanofibers were manufactured using gap method. Effects of manufacturing parameters on nanofiber diameters and alignment were studied. Mechanical properties of single nanofibers and nanofiber networks were evaluated by tensile testing using NANO UTM nanomechanics testing system. Main conclusions are as follows:

- Smaller gap distance between two collectors resulted in smaller diameters of aligned nanofibers.
- Nanofiber alignment decreased with the gap size decrease or manufacturing duration increase.
- Aligned PAN nanofiber networks had highest mechanical strength and modulus along the fiber direction. However, random network exhibited highest toughness.

CHAPTER 4

PAN NANOFIBER REINFORCED COMPOSITES

4.1 Composites Manufacturing

4.1.1 Materials

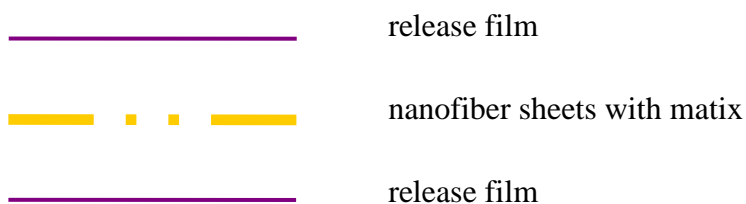
In this study, nanofibers were used as nanoreinforcement in polymer composites. Epoxy Resin EPON 828 was used as a matrix for composite fabrication. This resin has extended curing cycle and moderate viscosity. Jeffamine D-400 was used as curing agent [29]. The weight ratio of EPON Resin 828 and Jeffamine D-400 was 5/3. For example, 5 g EPON Resin 828 mixed with 3 g Jeffamine D-400. Corning stirrer with stirring-level 1 and no heat was used for 30 minutes to mix the matrix components.



Figure 4.1: Jeffamine D-400 (left) and EPON Resin 828 (right)

4.1.2 Molding

Nanocomposites were manufactured by curing nanofiber sheets infiltrated by liquid epoxy resin. The process started with assembling a molding stack consisting of a layer of release film, infiltrated PAN nanofiber sheets, and another layer of release film. In this study, Teflon films were used as release films. Number of nanofiber sheets was 2 for random and 10 for aligned nanofiber reinforced composites.



4.1.3 Curing Cycle

The Hot-Press: CARVER (model 2699, S/N 2699-126; CARVER, INC) shown in Figure 4.2 was used for curing.



Figure 4.2: Hot-Press: CARVER; model 2699, S/N 2699-126

In the manufacturing process, the following curing sequence was used.

- (1) Assemble the infiltrated nanofiber sheets and insert the stack into the hot-press.
- (2) Turn air and vacuum on to establish the contact pressure of 75 psi.
- (3) Set the temperature to 176 F.
- (4) When 176 F is reached, wait for 2 hours.
- (5) Ramp temperature to 248 F.
- (6) When 248 F is reached, wait for 2 hours.
- (7) Turn off the heat, air and vacuum.

(8) Remove the composite the next day.

4.1.4 PAN Nanofiber Reinforced Composites

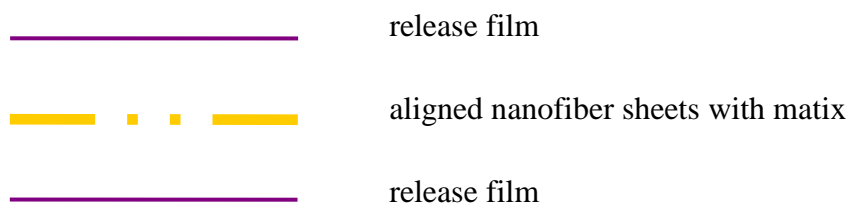
4.1.4.1 Aligned PAN Nanofiber Reinforced Composites

In the aligned PAN nanofiber reinforced composites, aligned PAN nanofibers were used as reinforcement material. The manufacturing conditions for the aligned PAN nanofibers are shown in Table 4.1.

Distance between Needle and Collector	24 cm
Solution Feed Rate	5 ml/h
PAN Solution Concentration	10%
Applied Voltage	12 kV
Manufacturing Duration	1 hour
Collector Gap Distance	3 cm

Table 4.1: Manufacturing conditions for aligned PAN nanofibers

The molding stack for manufacturing aligned PAN nanofiber reinforced composites was:



An example of aligned PAN nanofiber reinforced composites is shown in Figure 4.3. The sample is a thin film (Average of thickness was 0.146 mm), nearly transparent.

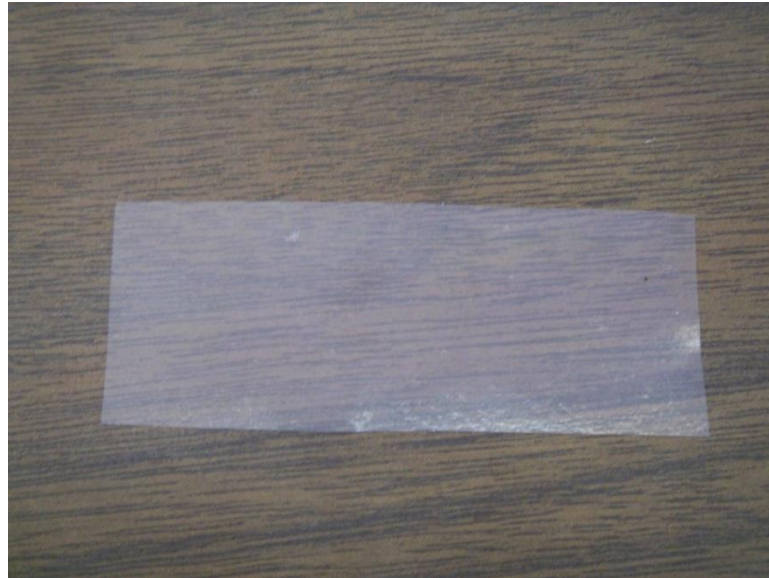


Figure 4.3: Example of aligned PAN nanofiber reinforced composites

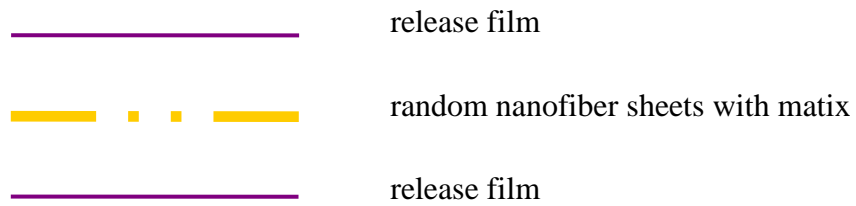
4.1.4.2 Random PAN Nanofiber Reinforced Composites

In the random PAN nanofiber reinforced composites, random PAN nanofibers were used as reinforcement material. The manufacturing conditions of the random PAN nanofiber are shown in Table 4.2 below.

Distance between Needle and Collector	24 cm
Speed of Jet	5 ml/h
PAN Solution Concentration	10%
Applied Voltage	12 kV
Manufacturing Duration	30 min

Table 4.2: Manufacturing conditions of random PAN nanofibers

The molding stack for manufacturing random PAN nanofiber reinforced composites was:



An example of random PAN nanofiber reinforced composite is shown in Figure 4.4. The sample was a thin film (Average thickness was 0.197 mm), nearly transparent similar to the aligned PAN nanofiber reinforced composite shown previously in Figure 4.3.



Figure 4.4: Example of random PAN nanofiber reinforced composites

4.2 Evaluation of Fiber Mass Fraction: V_m

Fiber mass fraction is the weight of fiber in a cured composite. It is one of the most important factors which determine the mechanical characteristics of a composite material.

In this research, the fiber volume fraction was calculated as:

$$V_m = (\text{weight/area of nanofibers}) / (\text{weight/area of composites})$$

Weight/area ratios for PAN nanofibers and composites were measured on at least twenty samples and average values were calculated.

For aligned PAN nanofiber reinforced composites, the average weight/area of nanofibers was $7.778 \times 10^{-6} \text{ g/mm}^2$, and the average weight/area of composites was

$1.429 \times 10^{-4} \text{ g/mm}^2$. So, according to the formula, $V_m = 5.44\%$ was obtained.

For random PAN nanofiber reinforced composites, the average weight/area of nanofibers was $4.784 \times 10^{-6} \text{ g/mm}^2$, and the average weight/area of composites was $2.206880 \times 10^{-4} \text{ g/mm}^2$. So, $V_m = 2.39\%$ for random PAN nanofiber reinforced composites.

In this study, aligned and random PAN nanofiber reinforced composites were manufactured under the same manufacturing conditions, however, aligned nanofiber reinforced composites had higher fiber mass fraction than random nanofiber reinforced composites. The difference is most likely due to the difference in packing density of the two nanofiber families. It was shown that aligned fibers have higher packing density (and volume fraction in composites) compared to random fibers. [104,105]

4.3 Fracture Analysis of PAN Nanofiber Reinforced Composites

Opening or Peel Mode (Mode I), Forward Sliding Shear Mode (Mode II) and Tearing Mode (Mode III), are three basic fracture modes (Figure 4.5).

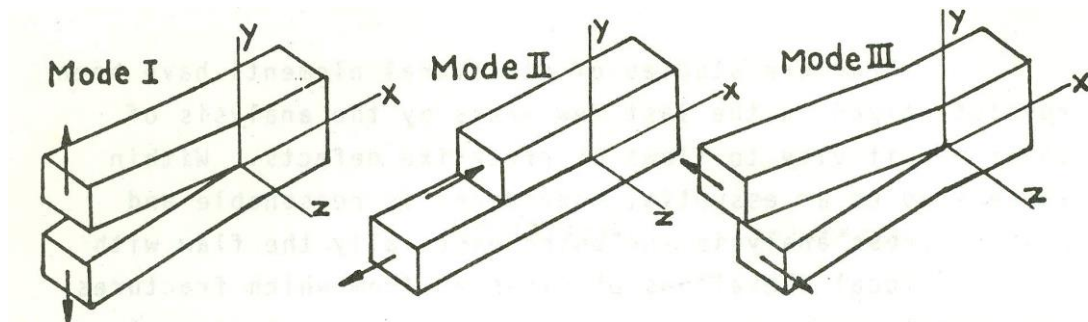


Figure 4.5: Fracture modes

Double edge notch test [106] was used in this fracture analysis, which is Mode I test.

The specimen in the test is shown in Figure 4.6.

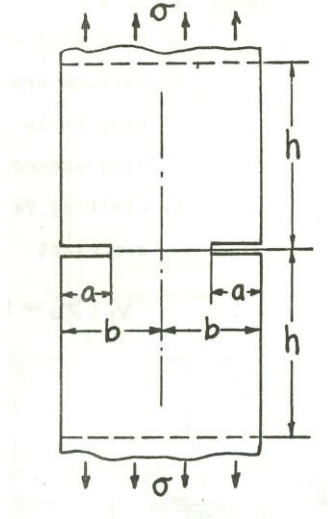


Figure 4.6: Double edge notch test specimen [106]

In this test, Critical Stress Intensity Factor K_I can be calculated as

$$K_I = \sigma_{\max} \sqrt{\pi a} * F(a/b)$$

$$\text{where } F(a/b) = \sqrt{\frac{2b}{\pi a} \tan \frac{\pi a}{2b}}$$

The stress is in the cross-section between two notches.

I. Numerical values of $F(a/b)$

Bowie's results ($h/b = 3.0$, mapping function method) have 1% accuracy and Yamamoto's results ($h/b = 2.75$, finite element method) have 0.5% accuracy for $0.2 < a/b$

< 0.9 (Figure 4.7). (Bowie 1964a, Yamamoto 1972)

II. Empirical Formulas

The following review of empirical models lists the proposed formulas and presents brief evaluation of their a) Accuracy and b) Method of derivation and reference.

$$F(a/b) = \sqrt{\frac{2b}{\pi a} \tan \frac{\pi a}{2b}}$$

- a. Better than 5% for $a/b > 0.4$
- b. Approximation by periodic crack solution, Irwin 1957

$$F(a/b) = 1.12 + 0.203(a/b) - 1.197(a/b)^2 + 1.930(a/b)^3$$

- a. Better than 2% for $a/b < 0.7$
- b. Least square fitting to Bowie's results, Brown 1966

$$F(a/b) = \frac{1.122 - 0.561(a/b) - 0.015(a/b)^2 + 0.091(a/b)^3}{\sqrt{1 - a/b}}$$

- a. Better than 2% for any a/b
- b. Asymptotic Approximation, Benthem 1972

$$F(a/b) = (1 + 0.122 \cos^4 \frac{\pi a}{2b}) \sqrt{\frac{2b}{\pi a} \tan \frac{\pi a}{2b}}$$

- a. 0.5% for any a/b
- b. Modification of Irwin's interpolation formula, Tada 1973

$$F(a/b) = \frac{1.122 - 0.561(a/b) - 0.205(a/b)^2 + 0.471(a/b)^3 - 0.190(a/b)^4}{\sqrt{1 - a/b}}$$

a. 0.5% for any a/b

b. Modification of Benthem's formula, Tada 1973

4.3.1 Selected Specimen Geometry and Data Reduction Method

The specimen was designed as shown in Figure 4.7 (left). Specimens were cut by an extremely sharp scissors. Compare to Figure 4.6, in the specimen, $a = 2$ mm, $b = 4$ mm. A sample of testing specimen is shown in Figure 4.7 (right).

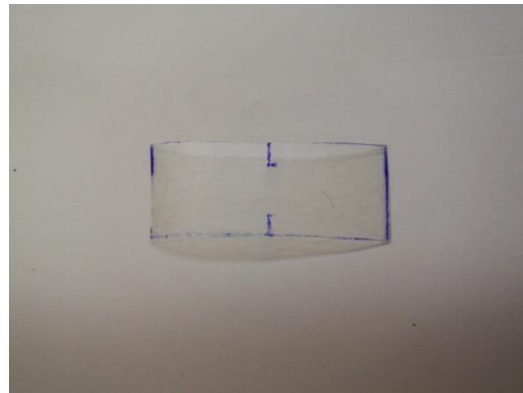
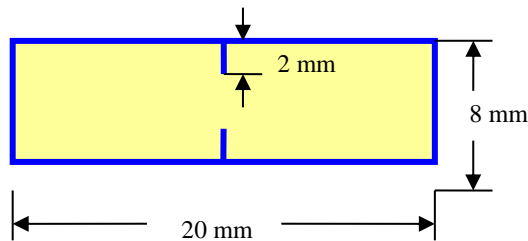


Figure 4.7: Specimen design of double edge notch test (left) and an experimental sample (right)

For selected specimen with $a = 2$ mm and $b = 4$ mm, the value of $F(a/b)$ was calculated as

$$F(a/b) = \sqrt{\frac{2b}{\pi a} \tan \frac{\pi a}{2b}}$$

$$= \sqrt{\frac{2(4)}{\pi(2)} \tan \frac{\pi(2)}{2(4)}} = \sqrt{\frac{4}{\pi} \tan \frac{\pi}{4}} = 1.128379$$

The value of Critical Stress Intensity Factor K_I was further calculated as

$$K_I = \sigma_{\max} \sqrt{\pi a} * F(a/b)$$

$$= \sigma_{\max} \sqrt{\pi * (2 * 10^{-3})} * F(a/b) = 0.089443 \sigma_{\max}$$

4.3.2 Tensile Testing

The tensile testing of nanofiber reinforcement composites specimens was performed using computerized MICROTTEST 200N tensile stage (Figure 4.8) by Deben UK Limited.

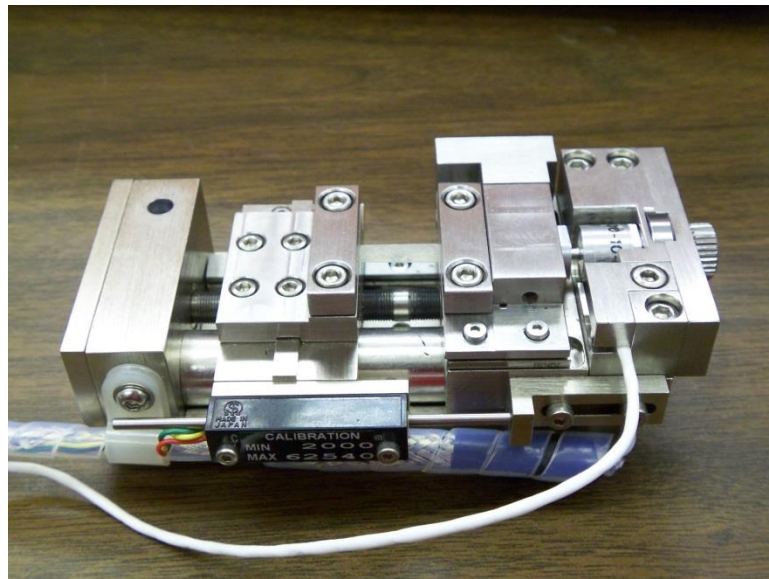


Figure 4.8: MICROTTEST 200N tensile stage

In this tensile testing, four materials were studied. Aligned PAN nanofiber reinforced composites were tested in two directions, i.e. with fibers oriented along the loading direction (0-degree or [0]) and in the perpendicular to loading direction (90-degree or [90]). The other two materials were random PAN nanofiber reinforced composites and pure epoxy made with the matrix used in of composites (Average thickness was 0.214 mm.).

4.3.3 Fracture Properties of Testing Materials

Fracture strength, Young's modulus and critical stress intensity factor were obtained from the tests.

4.3.3.1 [0] nanocomposites

At least 20 samples were tested to obtain average of fracture strength, Young's modulus and critical stress intensity factor.

	Fracture Strength (MPa)	Young's Modulus (MPa)	Critical Stress Intensity Factor (MPa*m ^{1/2})
Average	25.9	1273.9	2.3
Standard Deviation	8.3	437.2	0.8

Table 4.3: Fracture properties of [0] nanocomposites

Strain-stress curves of [0] nanocomposites (Figure 4.9) are shown below.

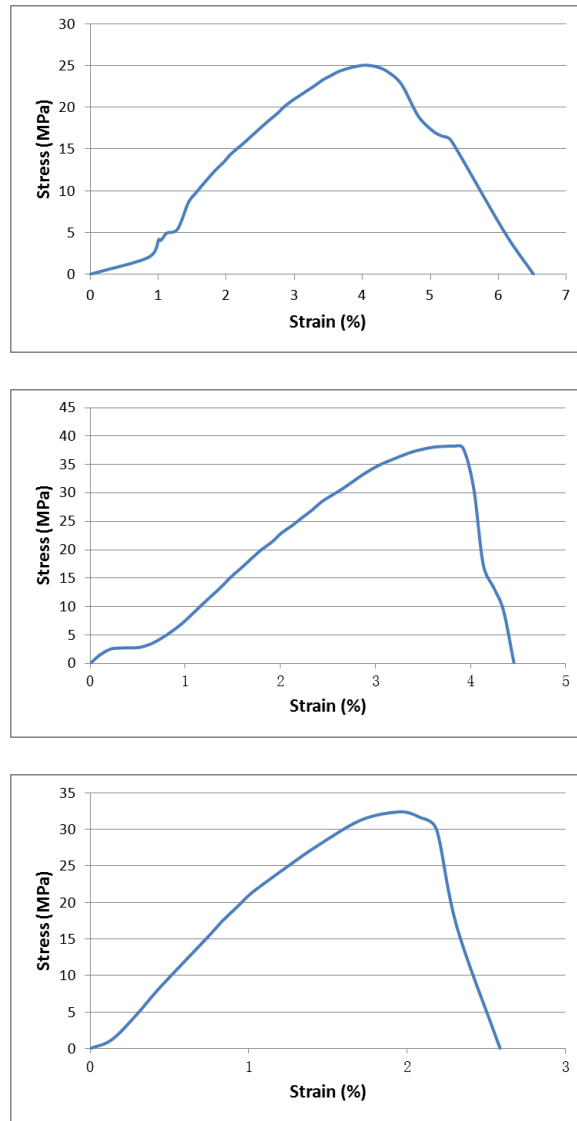


Figure 4.9: Representative strain-stress curves of [0] nanocomposites

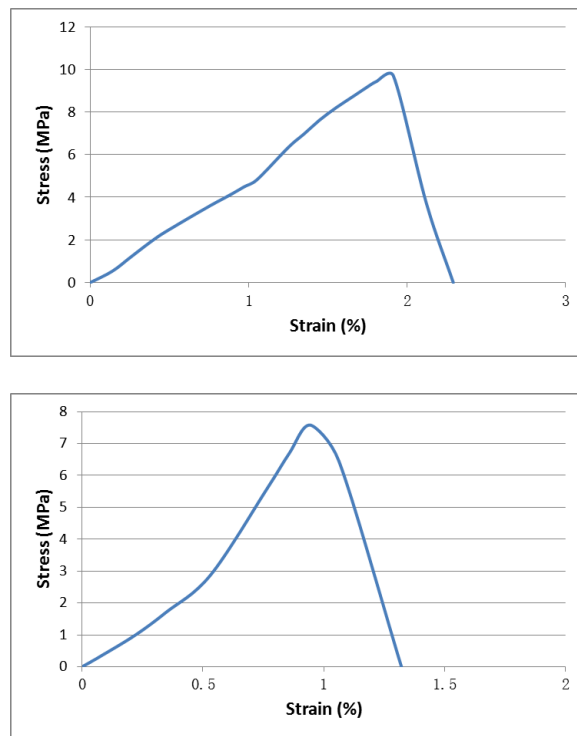
4.3.3.2 [90] nanocomposites

At least 20 samples were tested to obtain average of fracture strength, Young's modulus and critical stress intensity factor.

	Fracture Strength (MPa)	Young's Modulus (MPa)	Critical Stress Intensity Factor (MPa*m ^{1/2})
Average	10.8	583.1	1.0
Standard Deviation	2.9	348.4	0.3

Table 4.4: Fracture properties of [90] nanocomposites

Strain-stress curves of [90] nanocomposites (Figure 4.10) are shown below.



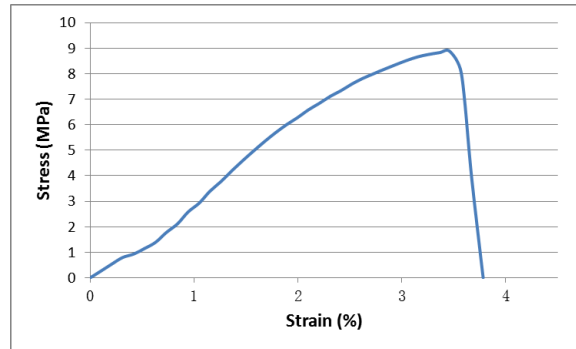


Figure 4.10: Representative strain-stress curves of [90] nanocomposites

4.3.3.3 Random Nanofiber Reinforced Composites

At least 20 samples were tested to obtain average of fracture strength, Young's modulus and critical stress intensity factor.

	Fracture Strength (MPa)	Young's Modulus (MPa)	Critical Stress Intensity Factor (MPa*m ^{1/2})
Average	20.1	971.4	1.8
Standard Deviation	4.5	246.8	0.4

Table 4.5: Fracture properties of random nanofiber reinforced composites

Strain-stress curves of random nanofiber reinforced composites (Figure 4.11) are shown below.

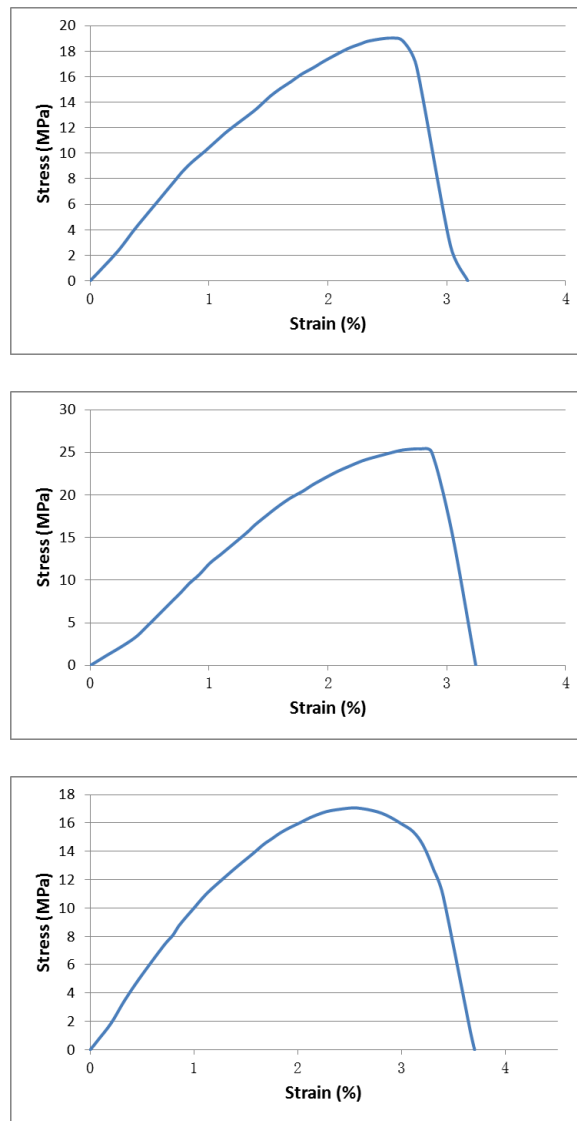


Figure 4.11: Representative strain-stress curves of random nanofiber reinforced composites

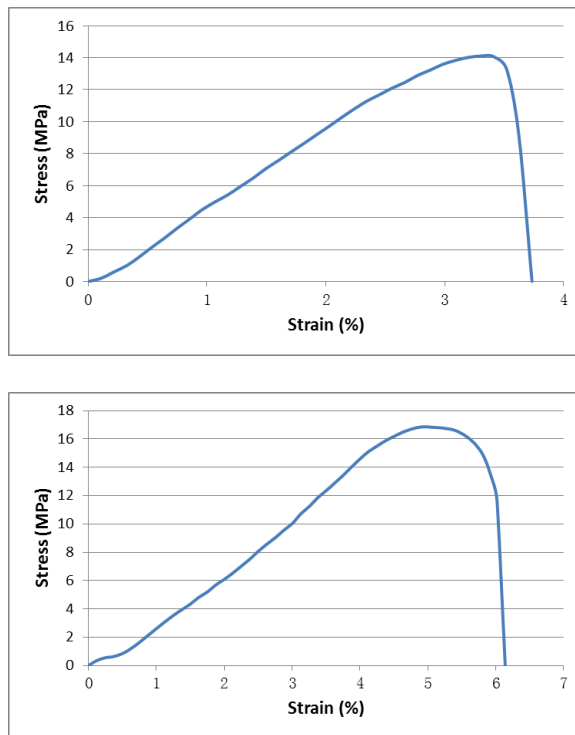
4.3.3.4 Pure Epoxy

At least 20 samples were tested to obtain average of fracture strength, Young's modulus and critical stress intensity factor.

	Fracture Strength (MPa)	Young's Modulus (MPa)	Critical Stress Intensity Factor (MPa*m ^{1/2})
Average	14.5	608.9	1.3
Standard Deviation	2.7	262.9	0.3

Table 4.6: Fracture properties of pure epoxy

Strain-stress curves of pure epoxy (Figure 4.12) are shown below.



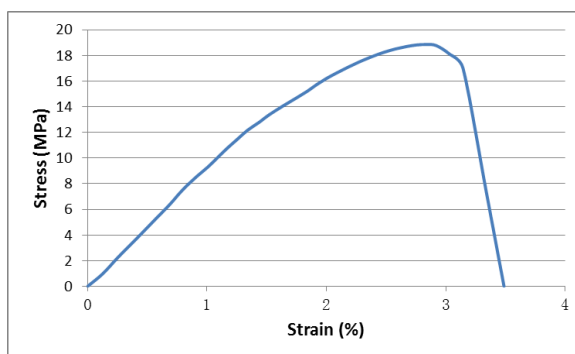


Figure 4.12: Representative strain-stress curves of pure epoxy

4.3.4 Data Summary and Analysis

All data for fracture properties of four materials are listed in Table 4.7 below. [0] nanofiber reinforced composite had the highest fracture properties of the four materials, i.e. it had the highest value of fracture strength, Young's modulus and critical stress intensity factor. However, the same composite tested in 90 direction (labeled [90] nanofiber reinforced composite) exhibited the lowest mechanical properties. This is similar to the existing advanced composites reinforced with conventional fibers. Their high mechanical anisotropy necessitates their application in the form of stacked composite laminates with unidirectional reinforced plies. Similar approach might be used with aligned nanofiber composites. Significant mechanical anisotropy of aligned nanofiber composites is demonstrated in this work for the first time. Random nanofiber reinforced composite had the second highest property values, which were better than the properties of the pure epoxy matrix.

Note that the mass fraction of nanofibers was very low in all nanofiber composites tested, compared to the typical high fraction of fibers in conventional composites. This

indicates that mechanical properties of nanofiber composites can be further significantly improved. In addition, use of optimized nanofibers such as the nanofibers with simultaneously high strength, modulus, and toughness that were recently developed by Dzenis' group, holds further promise for high-performance nanofiber reinforced composites.

	Fracture Strength (MPa)	Young's Modulus (MPa)	Critical Stress Intensity Factor (MPa*m ^{1/2})
[0]	25.9	1273.9	2.3
[90]	10.8	583.1	1.0
Random	20.1	971.4	1.8
Pure Epoxy	14.5	608.9	1.3

Table 4.7: Fracture properties of [0] nanocomposites, [90] nanocomposites, random nanofiber reinforced composites and pure epoxy

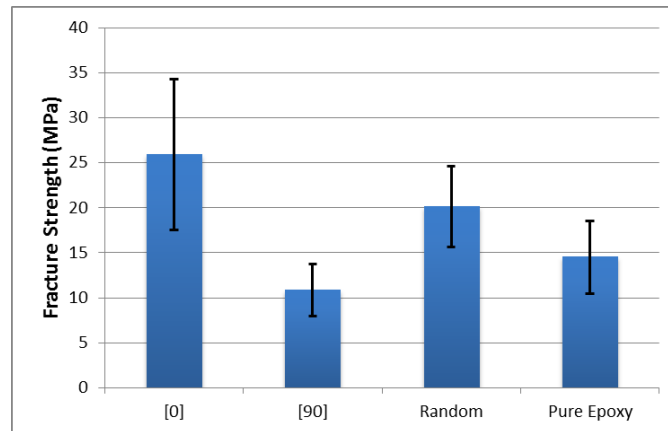


Figure 4.13: Fracture strength of [0] nanocomposites, [90] nanocomposites, random nanofiber reinforced composites and pure epoxy

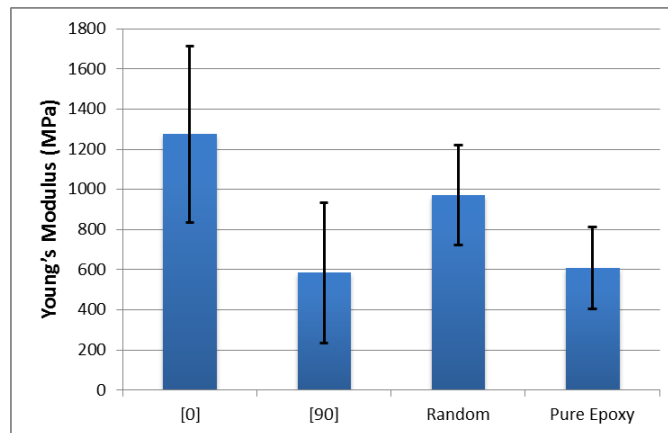


Figure 4.14: Young's Modulus of [0] nanocomposites, [90] nanocomposites, random nanofiber reinforced composites and pure epoxy

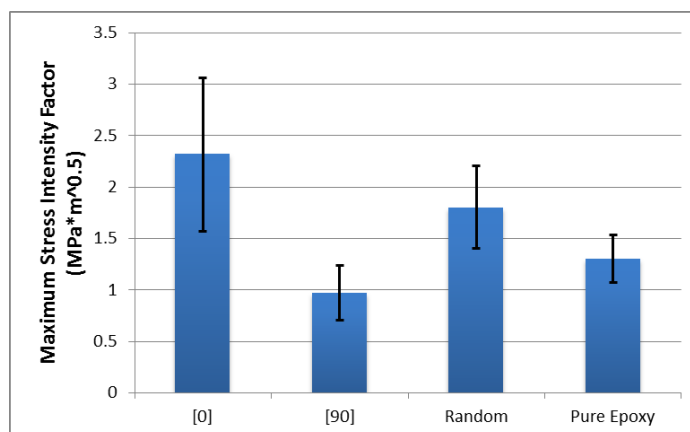


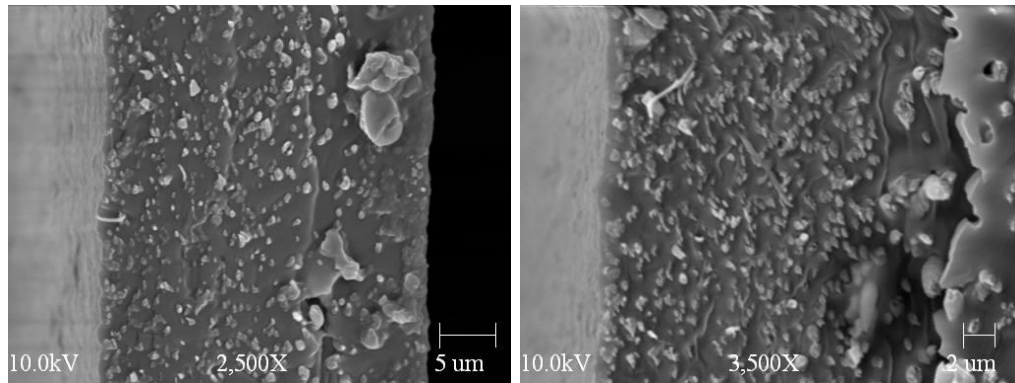
Figure 4.15: Critical stress intensity factor of [0] nanocomposites, [90] nanocomposites, random nanofiber reinforced composites and pure epoxy

4.3.5 SEM Images of Fracture Surface

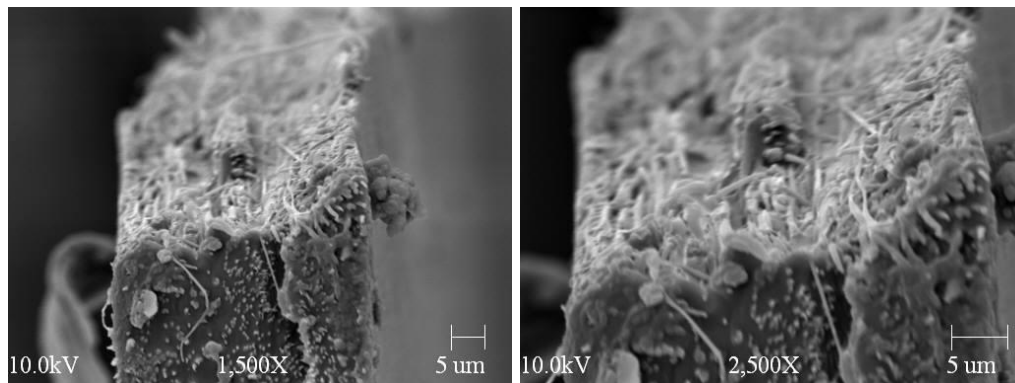
SEM images of fracture surface of [0] nanocomposites, [90] nanocomposites and random nanofiber reinforced composites are given in Figure 4.16 (a), (b); Figure 4.17 (a), (b) and Figure 4.18 (a), (b), respectively.

Figure 4.16 (a) shows nanofibers oriented perpendicular to fracture surface while Figure 4.17 (a) shows nanofibers mostly perpendicular to the fracture surface. SEM images of random nanofiber composite shown in Figure 4.18 (a) contain a mixture of nanofibers with different orientation.

In Figure 4.16 (b), Figure 4.17 (b) and Figure 4.18 (b), one can find that some nanofibers were pulled out from the matrix -- a possible mechanism of toughening.

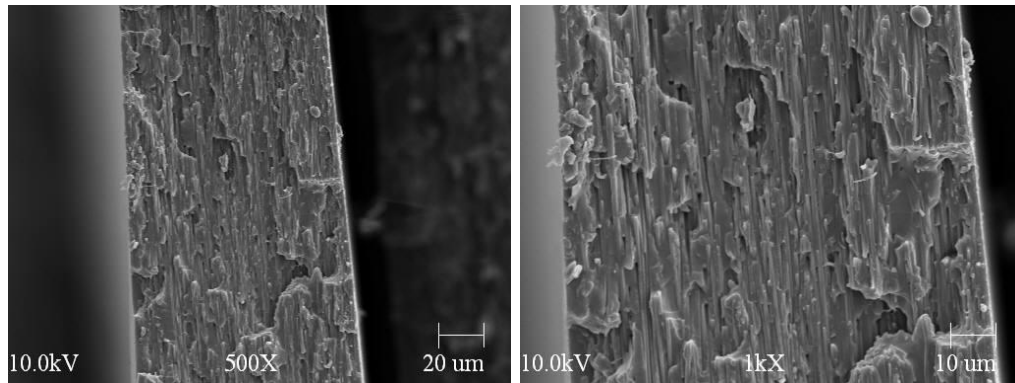


(a)

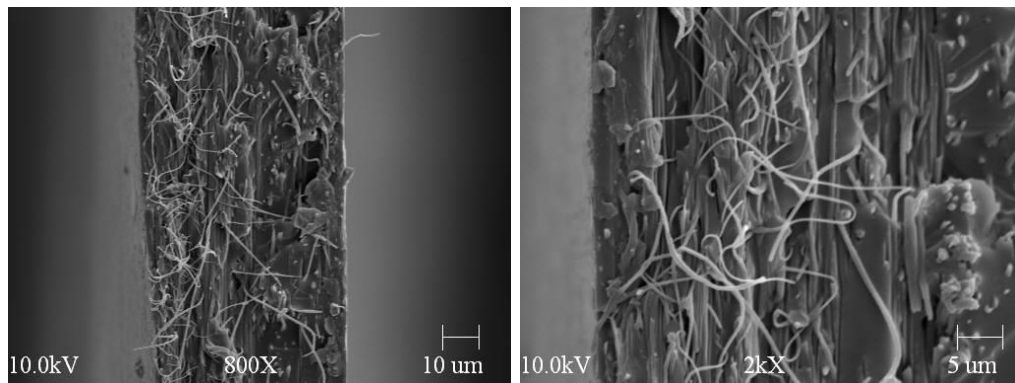


(b)

Figure 4.16: SEM images of fracture surface of [0] nanocomposites



(a)



(b)

Figure 4.17: SEM images of fracture surface of [90] nanocomposites

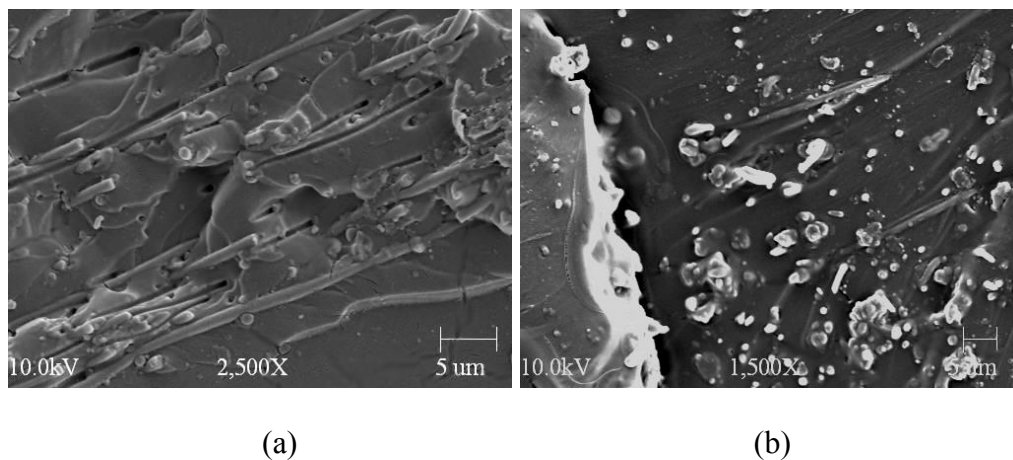


Figure 4.18: SEM images of fracture surface of random nanofiber reinforced composites

4.4 Conclusions

In this chapter, aligned and random PAN nanofiber reinforced composites were manufactured under the same manufacturing conditions. Fiber mass fraction was measured. Tensile tests were performed to investigate fracture properties of nanofiber reinforced composites. Main conclusions are as follows:

- Aligned PAN nanofiber reinforced composites had higher value of fiber mass fraction compared to random nanofiber composites.
- PAN nanofibers significantly increased mechanical properties of nanocomposites, especially along the fiber direction. All three measured mechanical parameters, i.e. strength, modulus, and critical stress intensity factor were the highest for the aligned sample in the fiber direction.
- Mechanical properties in the perpendicular to fiber direction were inferior to those

of random nanocomposite and pure matrix. Significant mechanical anisotropy of aligned nanofiber reinforced composites demonstrated in this work for the first time can be used for tailoring mechanical properties of future nanofiber composites and can lead to designs of nanocomposite laminates.

CHAPTER 5

SUMMARY AND CONCLUSIONS

Polymeric nanofibers are rapidly finding their place in nanomaterials technology. Electrospinning makes it easy to produce various kinds of nanofibers for many different applications.

In this study, continuous, uniform diameter polyacrylonitrile (PAN) nanofibers were produced using electrospinning technique. Qualitative and quantitative analysis of nanofiber diameters and morphology was conducted by SEM. The effects of the electrospinning process parameters on PAN nanofiber diameters were investigated. It was shown that higher applied voltage and lower PAN solution concentration resulted in electrospun nanofibers with finer diameters.

Aligned electrospun PAN nanofibers were produced by the gap method. Effects of process parameters on PAN nanofiber orientation were investigated. It was shown that smaller gap size and longer manufacturing duration led to decreased nanofiber alignment. The latter was attributed to the residual charge accumulation in poorly conductive nanofibers. Interestingly, the smaller gap size between the two collector parts has also led to finer nanofiber diameters.

Non-linear mechanical properties of single nanofibers, aligned and random nanofiber networks were investigated and compared. Aligned PAN nanofiber networks

had highest mechanical strength and modulus along the fiber direction. However, random network had highest toughness.

Aligned and random PAN nanofiber reinforced composites were fabricated. Better packing of aligned PAN nanofibers resulted in higher mass fraction of nanofibers in aligned reinforced composites. Anisotropic fracture properties of nanocomposites were evaluated experimentally for the first time. PAN nanofibers significantly improved mechanical properties of nanocomposites with very small fractions of nanoreinforcement.

The results of this study can be used for further electrospinning process optimization. Unique mechanical behavior of nanofibers, nanofiber networks, and nanofiber-reinforced composites analyzed and compared in this work for the first time will be beneficial to a broad variety of applications and can contribute to the development of the next generation structural nanocomposites.

BIBLIOGRAPHY

1. D. Vollath, Nanomaterials: An Introduction to Synthesis, Properties and Applications, Wiley-VCH Verlag GmbH & Co. KGaA Weinheim, (2008)
2. P. Gouma, Nanomaterials for chemical sensors and biotechnology, Singapore: Pan Stanford, (2010)
3. nisenet.org
4. Schmid et al., Nanotechnology: Assessment and Perspectives, Springer-Verlag Berlin Heidelberg, (2006)
5. A. Anderson, Nanotechnology, risk and communication, Basingstoke England, New York: Palgrave Macmillan, (2009)
6. J. M. Köhler, W. Fritzsche W, Nanotechnology :an introduction to nanostructuring techniques, Weinheim: Wiley-VCH, (2004)
7. P. Wei, L. Zhang, Y. Lu, N. Man, L. Wen, C60(Nd) nanoparticles enhance chemotherapeutic susceptibility of cancer cells by modulation of autophagy, Nanotechnology, 21(49):495101, (2010)
8. C. A. Haberzettl, Nanomedicine: destination or journey?, Nanotechnology, 13(4):R9, (2002)
9. Nelson, The potential of nanotechnology for molecular manufacturing, P.O. Box 2138 Santa Monica CA 90407-2138: Rand, (2005)
10. G. Cao, Nanostructures & nanomaterials :synthesis, properties & applications, London: Imperial College Press, (2004)
11. Xia Y, Yang P, Sun Y, Wu Y, Mayers B, Gates B, Yin Y, Kim F, Yan H. One-Dimensional Nanostructures: Synthesis, Characterization, an Applications, Adv Mater, 15(5):353, (2003)
12. D. Vollath, Nanomaterials: An Introduction to Synthesis, Properties and Applications, Wiley-VCH Verlag GmbH & Co. KGaA Weinheim, (2008)
13. Z. Guo, L. Tan, Fundamentals and Applications of Nanomaterials, Artech House Boston, (2009)
14. B. Cristina, P. Ivan, R. Kevin, Nanomaterials and Nanoparticles: Sources and

- Toxicity, (2007)
15. K. E. Drexler, Engines of Creation: The Coming Era of Nanotechnology, Doubleday, (1986)
 16. K. E. Drexler, Nanosystems: Molecular Machinery, Manufacturing, and Computation, New York: John Wiley & Sons, (1992)
 17. wikipedia.org
 18. R. Saini, S. Saini, S. Sharma, Nanotechnology: The Future Medicine, Journal of Cutaneous and Aesthetic Surgery, 3(1):32, (2010)
 19. Nanotechnology Information Center: Properties, Applications, Research, and Safety Guidelines, American Elements. Retrieved 13 May (2011)
 20. F. Allhoff, P. Lin, D. Moore, What is Nanotechnology and Why Does It Matter?: from science to ethics. John Wiley and Sons, (2010)
 21. A. J. Clarkson, D. A. Buckingham, A. J. Rogers, A. G. Blackman, C. R. Clark, Nanostructured Ceramics in Medical Devices: Applications and Prospects, 56 (10):38, (2004)
 22. Applications/Products, National Nanotechnology Initiative, Retrieved 19 Oct. 2007
 23. Z. Ghalanbor, S. A. Marashi, B. Ranjbar, Nanotechnology helps medicine: nanoscale swimmers and their future applications, Med Hypotheses, 65(1): 198, (2005)
 24. S. P. Leary, C. Y. Liu, M. L. Apuzzo, Toward the Emergence of Nanoneurosurgery: Part III-Nanomedicine: Targeted Nanotherapy, Nanosurgery, and Progress Toward the Realization of Nanoneurosurgery, Neurosurgery, 58(6):1009, (2006)
 25. Apply nanotech to up industrial, The Daily Star (Bangladesh), 17 April 2012
 26. C. Buzea, I. Pacheco, and K. Robbie, Nanomaterials and Nanoparticles: Sources and Toxicity, Biointerphases, 2(4), (2007)
 27. Nanomaterials, European Commission, Last updated 18 October 2011
 28. X. Wu, Fracture of Advanced Polymer Composites with Nanofiber Reinforced Interfaces, Ph.D. Dissertation, Department of Mechanical & Materials Engineering, University of Nebraska-Lincoln, 2003
 29. Y. Wen, Novel Continuous Carbon and Ceramic Nanofibers and Nanocomposites, Ph.D. Dissertation, Department of Mechanical & Materials Engineering,

University of Nebraska-Lincoln, 2004

30. X. Ren, Nanomanufacturing and Analysis of Novel Continuous Ferroelectric PVDF and P(VDF-TrFE) Nanofibers, Ph.D. Dissertation, Department of Mechanical & Materials Engineering, University of Nebraska-Lincoln, 2007
31. <http://www.news.cornell.edu/stories/May07/nanofibers.fashion.aj.html>
32. nano.gov
33. P.M. Ajayan, L.S. Schadler, P.V. Braun, Nanocomposite science and technology, Wiley, 2003
34. Y. Mai, Z. Yu, Polymer Nanocomposites, Woodhead Publ, (2006)
35. P. Knauth, J. Schoonman, Nanocomposites : Ionic Conducting Materials and Structural Spectroscopies, New York ; London, Springer, (2008)
36. P. Mukhopadhyay, R. K. Gupta, Graphite, Graphene, and Their Polymer Nanocomposites, Boca Raton, FL : CRC Press, (2013)
37. J. Ahmed, Starch-based Polymeric Materials and Nanocomposites : Chemistry, Processing, and Applications, Boca Raton : CRC Press, (2012)
38. O. Kamigaito, What can be improved by nanometer composites?, J. Jpn. Soc. Powder Metall, 38:315, (1991)
39. E. Gokdag, Static and Fatigue Interlaminar Fracture of Graphite-epoxy Composites with PAN Nonafiber Reinforcement at Interfaces, MS. Thesis, Department of Mechanical & Materials Engineering, University of Nebraska-Lincoln, 2001
40. F. Matthews, R. Rawlings, Composite Materials: Engineering and Science, 1999
41. <http://www.nanowerk.com/spotlight/spotid=23934.php>
42. J. Leng, A. Lau, Multifunctional Polymer Nanocomposites, CRC Press, (2011)
43. A. Kirecci, U. Ozkoc, H. I. Icoglu, Determination of Optimal Production Parameters for Polyacrylonitrile Nanofibers, Wiley Online Library, (2011)
44. Ziabicki, A. Fundamentals of Fiber Formation, John Wiley and Sons, London, 1976
45. T. Subbiah, G. S. Bhat, R. W. Tock, Electrospinning of Nanofibers, Journal of Applied Polymer Science, 96(23):557, (2005)
46. W. E. Teo, S. Ramakrishna, A Review on Electrospinning Design and Nanofibre

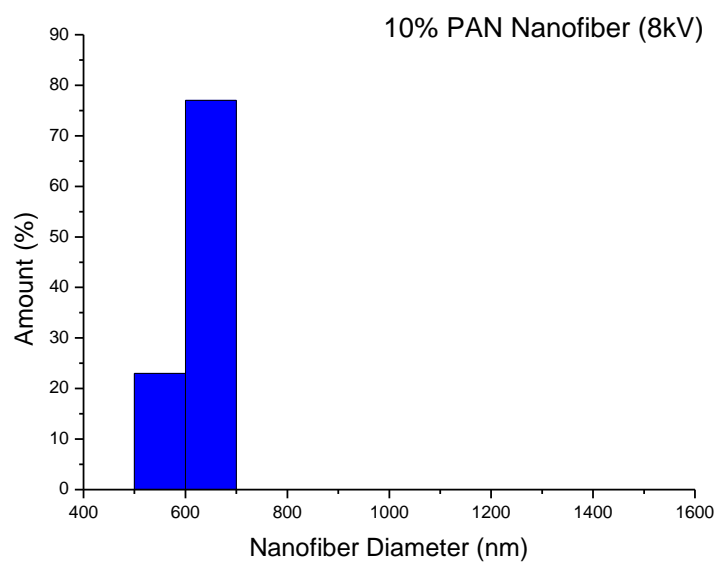
- Assemblies, *Nanotechnology*, 17:89, (2006)
47. N. Bhardwaj, S. C. Kundu, Electrospinning: A Fascinating Fiber Fabrication Technique, *Biotechnology Advances*, 28:325, (2010),
 48. Formhals, A., US Patent 1975504, 1934
 49. Formhals, A., US Patent 2109333, 1938
 50. Formhals, A., US Patent 2123992, 1938
 51. Formhals, A., US Patent 2160962, 1939
 52. Formhals, A., US Patent 2187306, 1940
 53. P. K. Baumgarten, Electrostatic spinning of acrylic microfibers, *J Colloid Interface Sci*, 36(1):71, (1971)
 54. T. Subbiah, G. S. Bhat, R. W. Tock, S. Parameswaran, S. S. Ramkumar, *Electrospinning of Nanofibers*, Wiley InterScience, (2004)
 55. J. Doshi, D. H. Reneker, Electrospinning Process and Applications of Electrospun Fibers, *J Electrostatics*, 35:151, (1995)
 56. Y. Dzenis , Spinning continuous fibers for nanotechnology, *Science*, 304(5679):1917, (2004)
 57. A. F. Spivak, Y. A. Dzenis, A Condition of the Existence of a Conductive Liquid Meniscus in an External Electric Field *Journal of Applied Mechanics*, 66(4):1026, (1999)
 58. X. Wu, Y. A. Dzenis, Collapse analysis of nanofibres *Nanotechnology*, 18(28):285702, (2007)
 59. X. Wu, Y. A. Dzenis, Electrohydrodynamic instability of thin conductive liquid films *J Phys D*, 38(16):2848, (2005)
 60. N. Bhardwaj, S. C. Kundu, Electrospinning: A Fascinating Fiber Fabrication Technique, *Biotechnology Advances*, 28:325, (2010)
 61. D. Li, Y. Xia, Electrospinning of Nanofibers: Reinventing the Wheel?, *Advanced Materials*, 16(4):1151, (2004)
 62. D. H. Reneker, I. Chun, Nanometre Diameter Fibres of Polymer, Produced by Electrospinning, *Nanotechnology*, 7:216, (1996)
 63. J. Doshi, D. H. Reneker, Electrospinning Process and Applications of Electrospun Fibers", *Journal of Electrostatics*, 35:151, (1995)

64. L. M. Bellan, H. G. Craighead, Nanomanufacturing Using Electrospinning, *Journal of Manufacturing Science and Engineering*, 131:34001, (2009)
65. F. L. Zhou, R. H. Gong, I. Porat, Needle and Needleless Electrospinning for Nanofibers, *Journal of Applied Polymer Science*, 115:2591, (2010)
66. T. Wang, S. Kumar, Electrospinning of Polyacrylonitrile Nanofibers, *Journal of Applied Polymer Science*, 102:1023, (2006)
67. A. Greiner, J. H. Wendorff, Electrospinning: A Fascinating Method for the Preparation of Ultrathin Fibers, *Angewandte Chemie International Edition*, 46:5670, (2007)
68. G. L. Wilkes, www.che.vt.edu/Wilkes/electrospinning/electrospinning.html. 2001
69. A. Baji, Y. M. Mai, S. C. Wong, Electrospinning of Polymer Nanofibers: Effects on Oriented Morphology, Structures and Tensile Properties, *Composites Science and Technology*, 70:703, (2010)
70. S. A. Theron, A. L. Yarin, E. Sussman, E. Kroll, Multiple Jets in Electrospinning: Experiment and Modeling, *Polymer*, 46:2889, (2005)
71. F. Cengiz, I. Krucinska, Comparative Analysis of Various Electrospinning Methods of Nanofibre Formation, *Fibres & Textiles in Eastern Europe*, (2009)
72. A. Frenot, I. S. Chronakis, Polymer Nanofibers Assembled by Electrospinning, *Current Opinion in Colloid & Interface Science*, 8, 64, (2003)
73. Z. M. Huang, Y. Z. Zhang, M. Kotaki, S. Ramakrishna, A Review on Polymer Nanofibers by Electrospinning and Their Applications in Nanocomposites, *Composites Science and Technology*, 63:2223, (2003)
74. D. H. Reneker, A. L. Yarin, H. Fong, S. Koomhongse, Bending Instability of Electrically Charged Liquid Jets of Polymer Solutions in Electrospinning, *Journal of Applied Physics*, 87:4531, (2000)
75. Y. M. Shin, M. M. Hohman, M. P. Brenner, G. C. Rutledge, Electrospinning: A Whipping Fluid Jet Generates Submicron Polymer Fibers, *Applied Physics Letters*, 78:1149, (2001)
76. A. L. Yarin, S. Koomhongse, D. H. Reneker, Bending Instability in Electrospinning of Nanofibers, *Journal of Applied Physics*, 90:4836, (2001)
77. Y. M. Shin, M. M. Hohman, M. P. Brenner, G. C. Rutledge, Experimental Characterization of Electrospinning: the Electrically Forced Jet and instabilities, *Polymer*, 42:9955, (2001)
78. S. R. Merritt, A. E. Agata, Z. Lee, H. A. von Recum, Electrospinning and

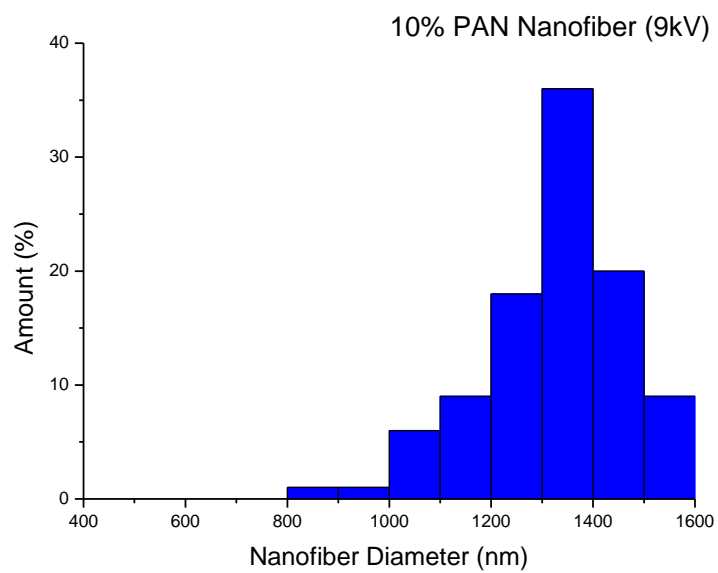
- Imaging, *Advanced Engineering Materials*, 14(5):B266, (2012)
79. E. P. S. Tan, C. T. Lim, Physical Properties of a Single Polymeric Nanofiber, *Appl. Phys. Lett.*, 84:1603, (2004)
 80. C. T. Lim, E. P. S. Tan, S. Y. Ng, Effects of Crystalline Morphology on the Tensile Properties of Electrospun Polymer Nanofibers. *Appl. Phys. Lett.*, 92:141908, (2008)
 81. A. Arinstein, M. Burman, O. Gendelman, E. Zussman, Effect of Supramolecular Structure on Polymer Nanofibre Elasticity, *Nat. Nanotechnol*, 2:59, (2007)
 82. M. K. Shin, et al, Size-dependent Elastic Modulus of Single Electroactive Polymer Nanofibers, *Appl. Phys. Lett.*, 89:231929, (2006)
 83. M. Naraghi, S. N. Arshad, I. Chasiotis, Molecular Orientation and Mechanical Property Size Effects in Electrospun Polyacrylonitrile Nanofibers, *Polymer* 52, 1612, (2011)
 84. C. T. Peterson, Hybrid Nanomanufacturing Process for High-Rate Polymer Nanofiber Production, MS. Thesis, Department of Mechanical & Materials Engineering, University of Nebraska-Lincoln, 2010
 85. W. Li, C. T. Laurencin, E. J. Caterson, R. S. Tuan, F. K. Ko, Electrospun Nanofibrous Structure: A Novel Scaffold for Tissue Engineering, *J Biomed Mater Res*, 60(4):613, (2002)
 86. H. S. Yoo, T. G. Kim, T. G. Park, Surface-functionalized Electrospun Nanofibers for Tissue Engineering and Drug Delivery, *Adv. Drug Deliv. Rev.*, 61(12):1033, (2009)
 87. C. J. Buchko, L. C. Chen, Y. Shen, D. C. Martin, Processing and Microstructural Characterization of Porous Biocompatible Protein Polymer Thin Films, *Polymer*, 40:7397, (1999)
 88. C. J. Buchko, K. M. Kozloff, D. C. Martin, Surface Characterization of Porous, Biocompatible Protein Polymer Thin Films, *Biomaterials*, 22:1289, (2001)
 89. T. J. Sill, H. A. von Recum, Electrospinning: Applications in Drug Delivery and Tissue Engineering, *Biomaterials*, 29(13):1989, (2008)
 90. Z. Huang, C. He, A. Yang, Y. Zhang, X. Han, J. Yin, Q. Wu, Encapsulating Drugs in Biodegradable Ultrafine Fibers Through Co-axial Electrospinning, *Journal of Biomedical Materials Research Part A*, 77A(1):169, (2006)
 91. P. W. Gibson, H. L. Schreuder-Gibson, D. Rivin, Electrospun Fiber Mats: Transport Properties, *Aiche Journal*, 45:190, (1999)

92. H. Schreuder-Gibson, P. Gibson, K. Senecal, M. Sennett, J. Walker, W. Yeomans, D. Ziegler, P. Tsai, Protective Textile Materials Based on Electrospun Nanofibers, *Journal of Advanced Materials*, 34:44, (2002)
93. X. Y. Wang, C. Drew, S. H. Lee, K. J. Senecal, J. Kumar, L. A. Sarnuelson, Electrospun Nanofibrous Membranes for Highly Sensitive Optical Sensors, *Nano Letters*, 2:1273, (2002)
94. L. Liu, Z.Y. Liu, H. W. Bai, D. D. Sun, Concurrent Filtration and Solar Photocatalytic Disinfection/degradation Using Hhigh-performance Ag/TiO₂ Nanofiber Membrane, *Water Research*, 46(4):1101, (2012)
95. Y. Dzenis, Structural Nanocomposites, *Science*, 319: 419, (2008)
96. S. F. Fennessey, R. J. Farris, Fabrication of Aligned and Molecularly Oriented Electrospun Polyacrylonitrile Nanofibers and The Mechanical Behavior of Their Twisted Yarns, *Polymer*, 45:4217, (2004)
97. E. Zussman, X. Chen, W. Ding, L. Calabri, D. A. Dikin, J. P. Quintana, R. S. Ruoff, Mechanical and Structural Characterization of Electrospun PAN-derived Carbon Nanofibers, *Carbon* 2005, 43:2175, (2005)
98. S. Y. Gu, J. Ren, Q. L. Wu, *Synth Metals*, 155:157, (2005)
99. S. Ramakrishna, K. Fujihara, W. E. Teo, T. C. Lim, Z. Ma, *An Introduction to Electrospinning and Nanofibers*, World Scientific: Singapore, 2005
100. Y. Ishii, H. Sakai, H. Murata, A New Electrospinning Method to Control the Number and Diameter of Uniaxially Aligned Polymer Fibers, *Materials Letters*, 62:3370, (2008)
101. D. Li, Y. L. Wang, Y. N. Xia, Electrospinning Nanofibers as Uniaxially Aligned Arrays and Layer-by-layer Stacked Films, *Advanced Materials*, 16:361, (2004)
102. D. Li, Y. L. Wang, Y. N. Xia, Electrospinning of Polymeric and Ceramic Nanofibers as Uniaxially Aligned Arrays, *Nano Letters*, 3:1167, (2003)
103. L. H. Liu, Studies on Deposition and Alignment of Electrospun Nanofiber Assemblies, Ph.D. Dissertation, Department of Mechanical & Materials Engineering, University of Nebraska-Lincoln, (2007)
104. A. A. Guseva, P. J. Hineb, I. M. Wardb, Fiber packing and elastic properties of a transversely random unidirectional glass/epoxy composite, *Composites Science and Technology*, 60:535, (2000)
105. S. Toll, Packing Mechanics of Fiber Reinforcements, *Polymer Engineering and Science*, 46(8):1337, (1998)

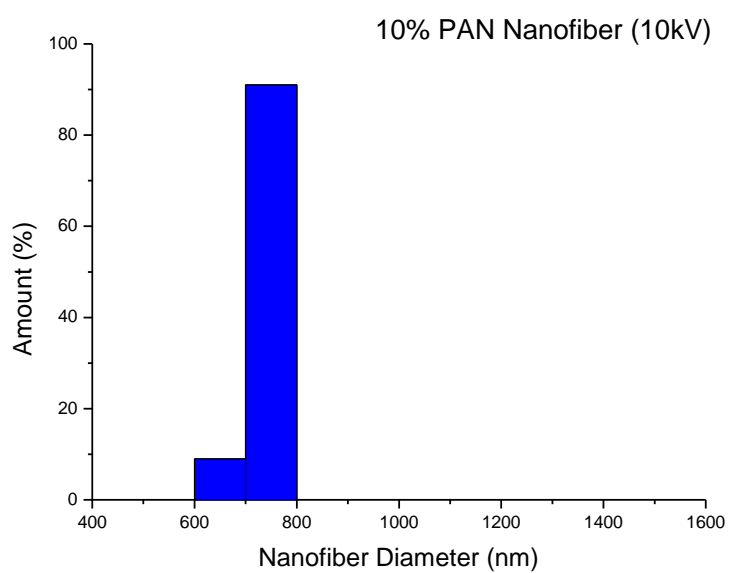
- 106.H. Tada, P. C. Paris, G. R. Irwin, The Stress Analysis of Cracks Handbook, Hellertown, Pa. Del Research Corp, (1973)
- 107.L. Liu, Y. A. Dzenis, Analysis of the Effects of the Residual Charge and Gap size on Electrospun Nanofiber Alignment in a Gap Method, Nanotechnology, 19, (2008)
- 108.D. Papkov, Y. Zou, M. N. Andalib, A. Goponenko, Z. D. Cheng, and Y. A. Dzenis, Simultaneously Strong and Tough Ultrafine Continuous Nanofibers, ACS Nano, 7:3324, (2013)
- 109.R. O. Ritchie, The Conflicts between Strength and Toughness, Nat. Mater., 10:817–822, (2011)

APPENDIX:**DIAMETER DISTRIBUTIONS OF PAN NANOFIBERS**

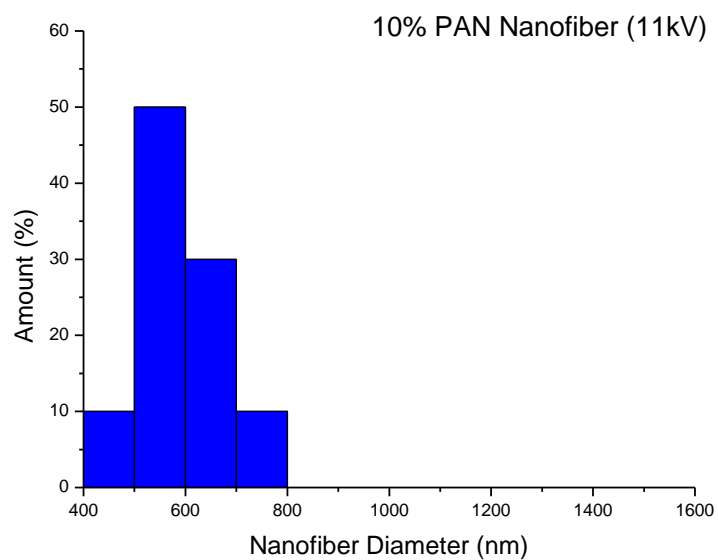
(a)



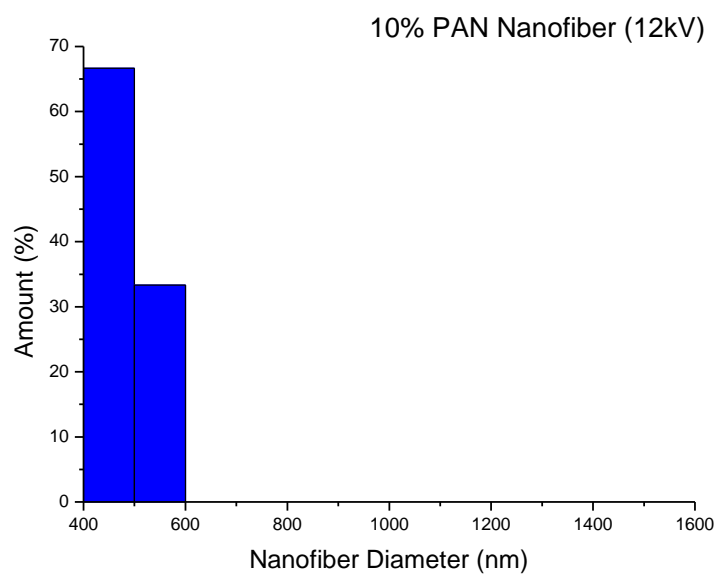
(b)



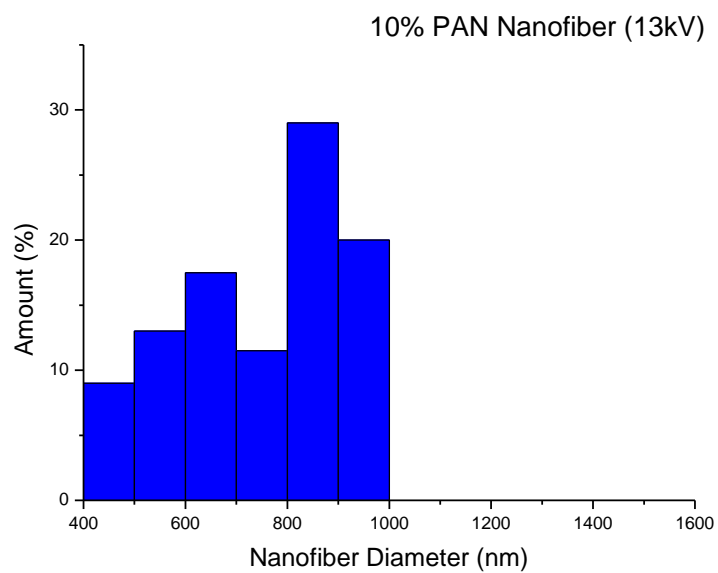
(c)



(d)

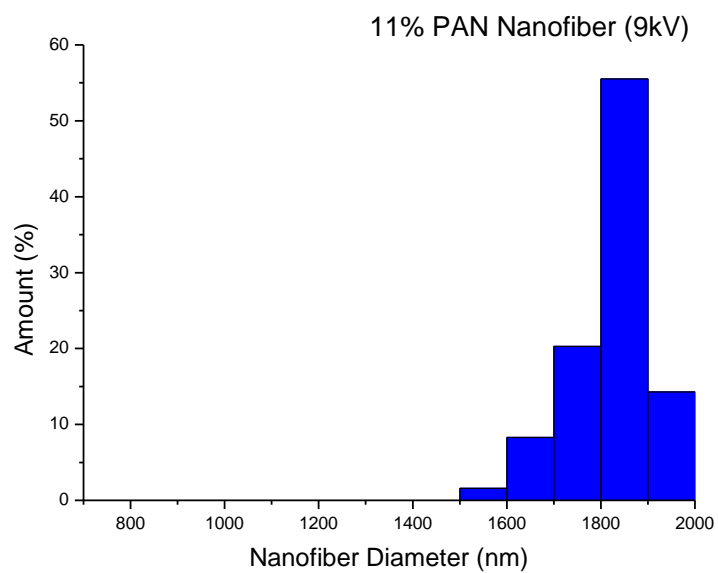


(e)

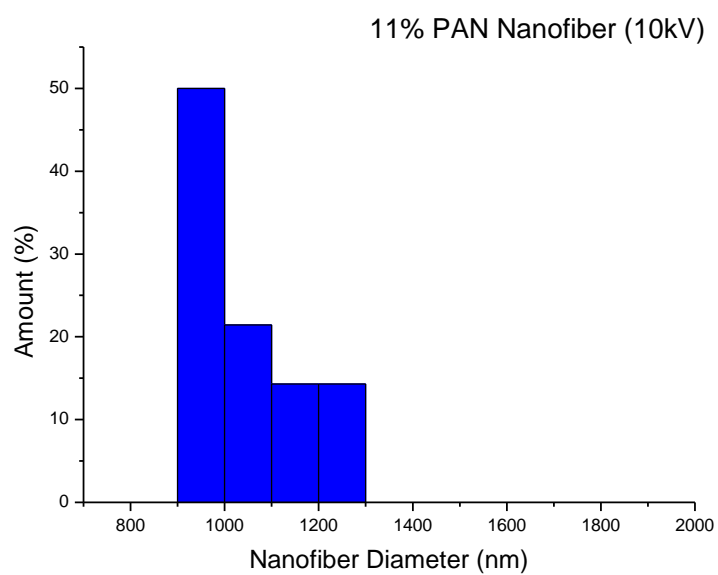


(f)

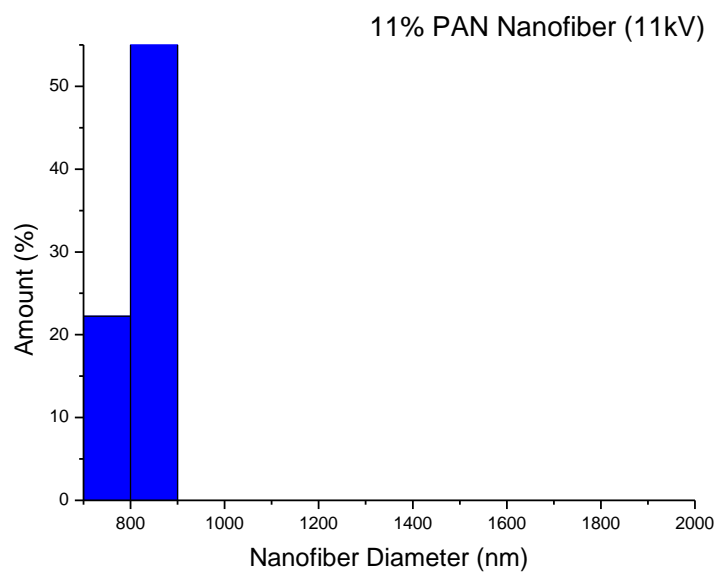
Figure 6.1: 10% PAN nanofibers manufactured in (a) 8kV; (b) 9kV; (c) 10kV; (d) 11kV; (e) 12kV; (f) 13kV



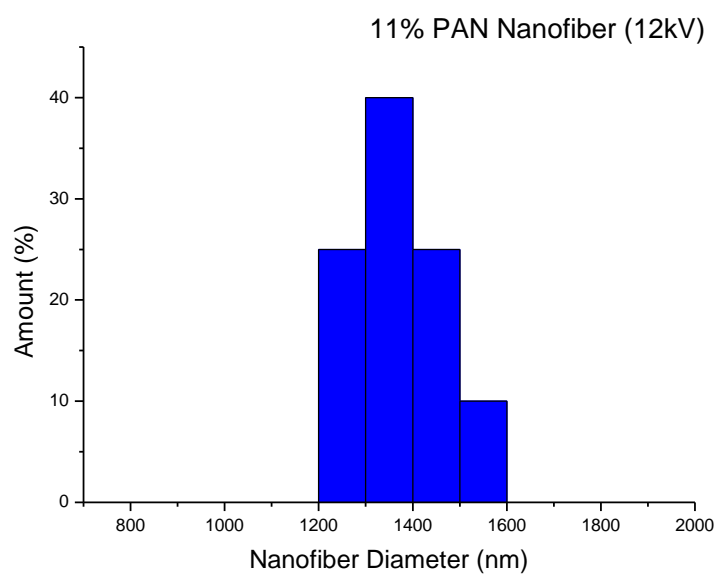
(a)



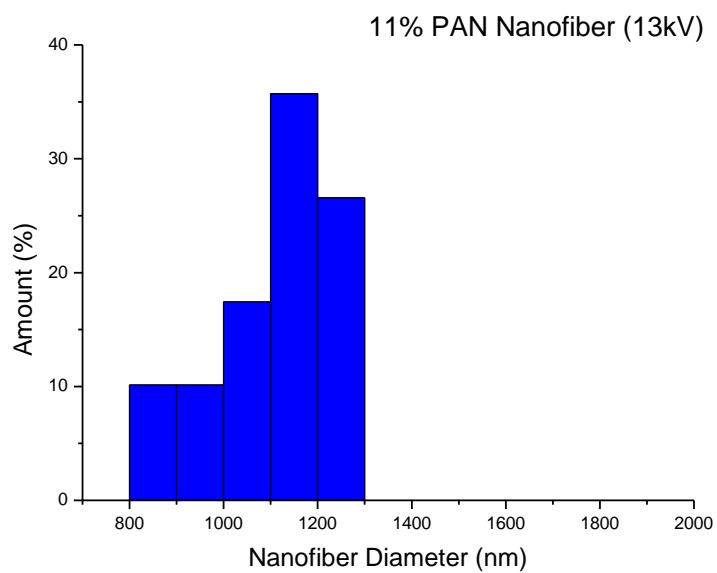
(b)



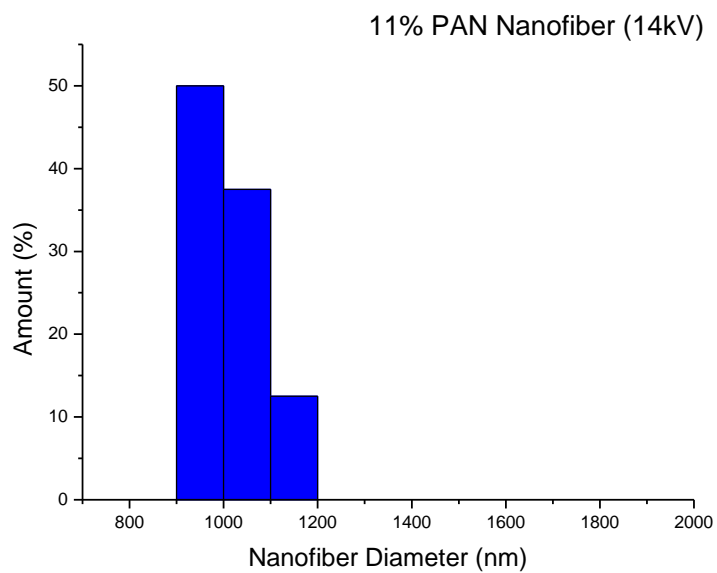
(c)



(d)



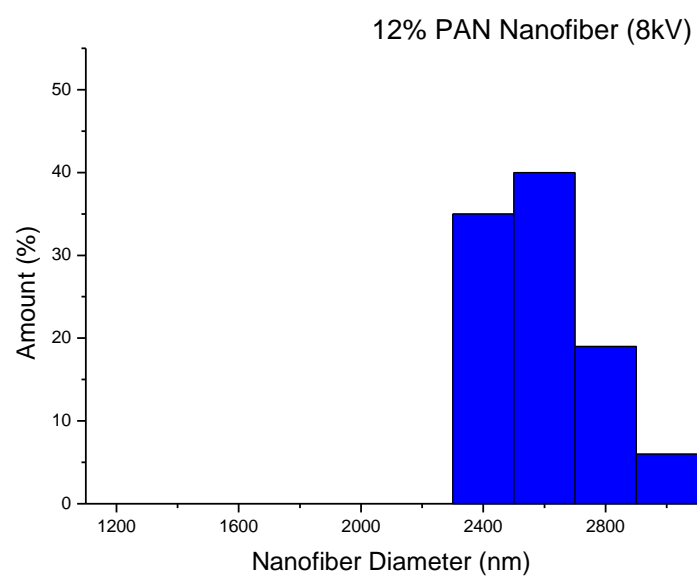
(e)



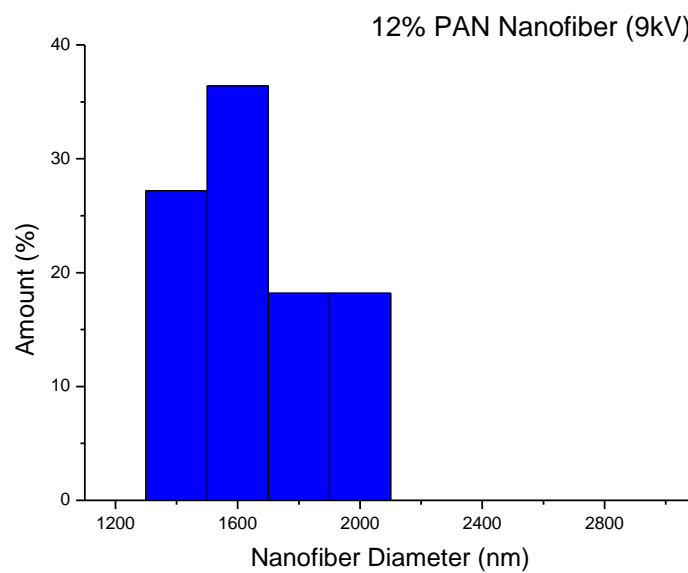
(f)

Figure 6.2: 11% PAN nanofibers manufactured in (a) 9kV; (b) 10kV; (c) 11kV; (d) 12kV;

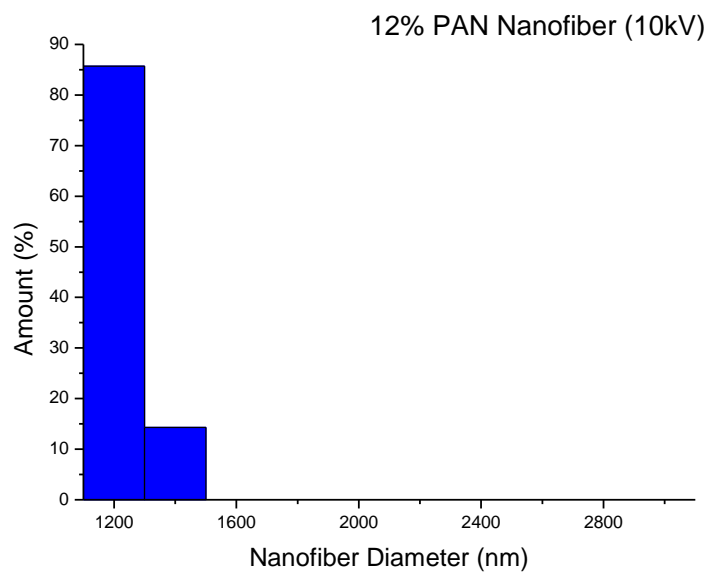
(e) 13kV; (f) 14kV



(a)

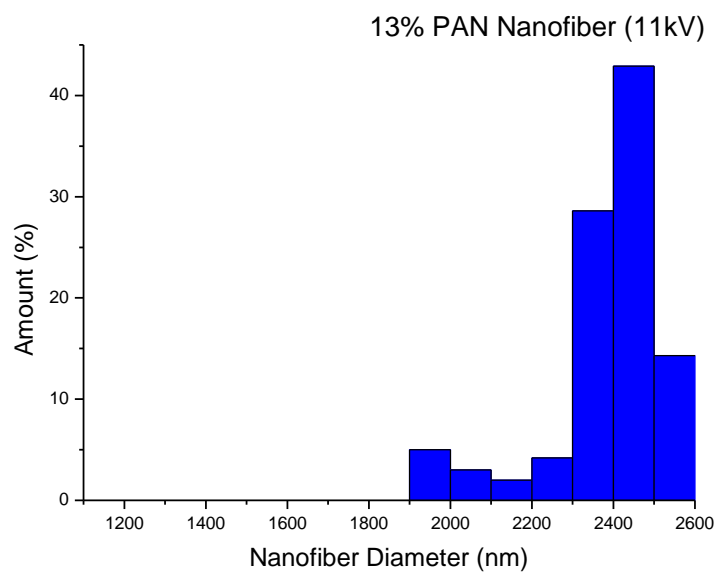


(b)

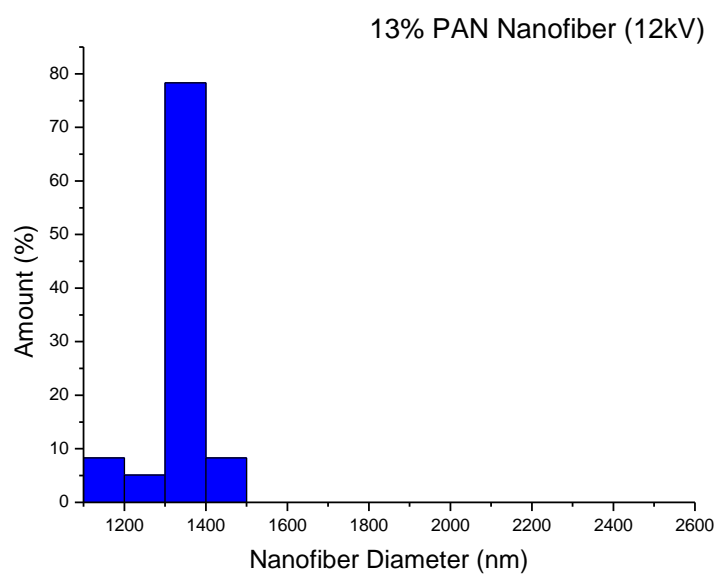


(c)

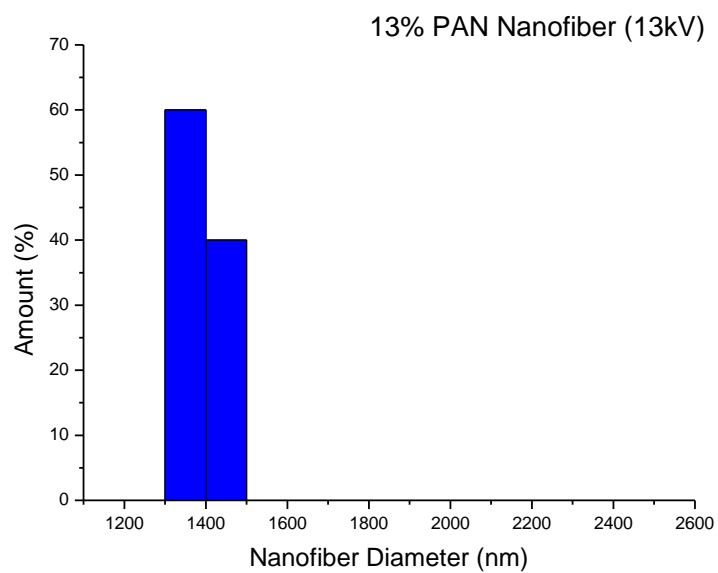
Figure 6.3: 12% PAN nanofibers manufactured in (a) 8kV; (b) 9kV; (c) 10k



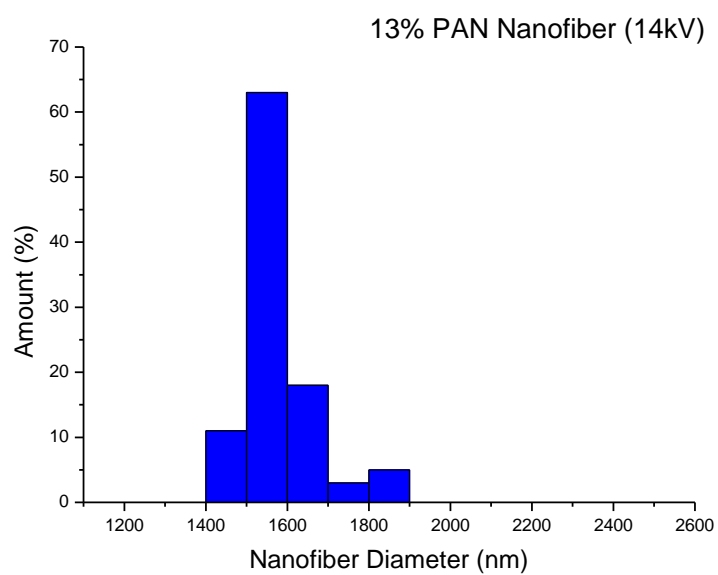
(a)



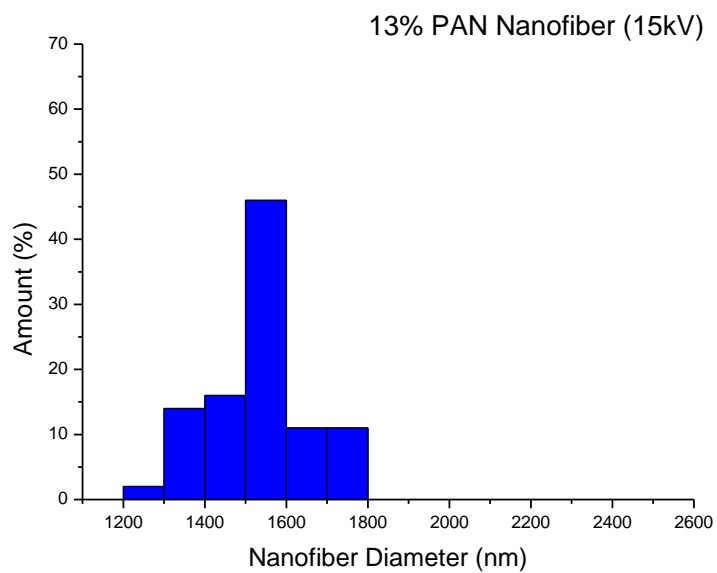
(b)



(c)

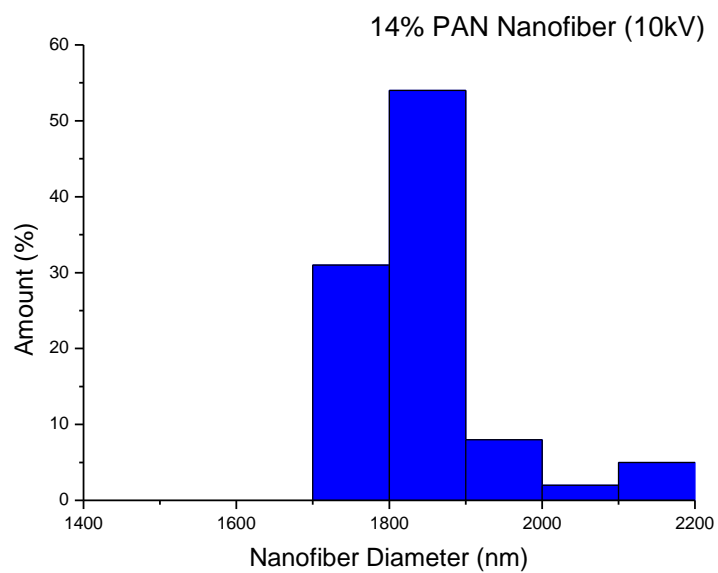


(d)

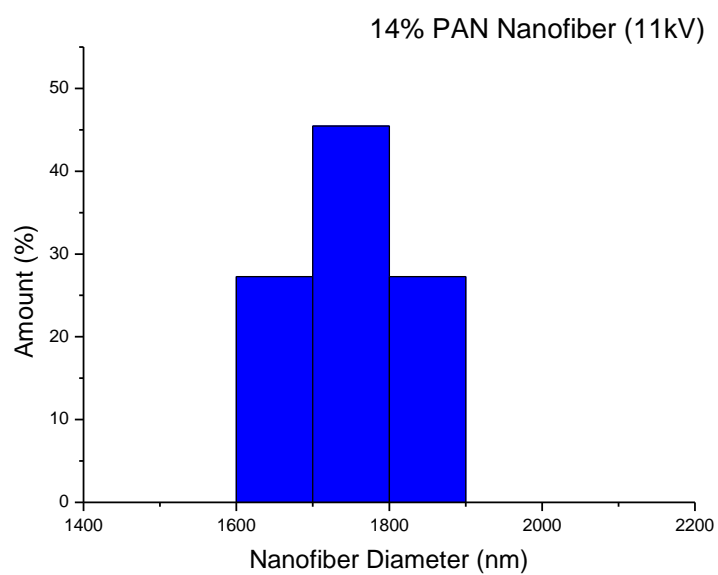


(e)

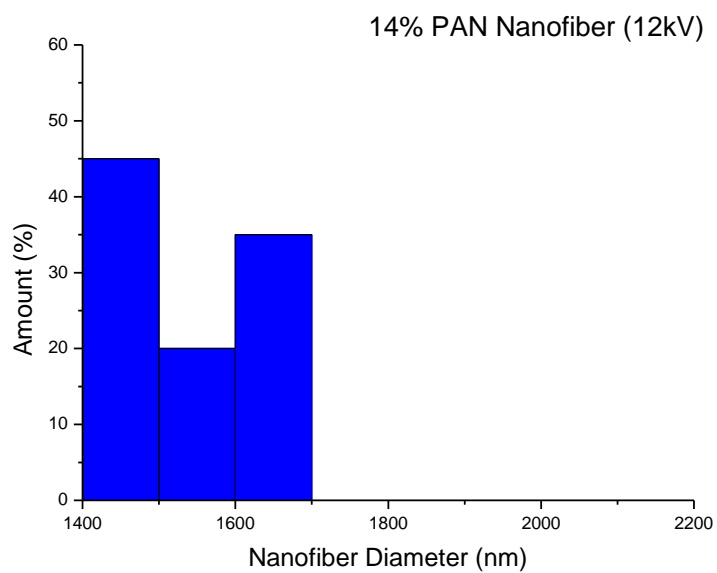
Figure 6.4: of 13% PAN nanofibers manufactured in (a) 11kV; (b) 12kV; (c) 13kV; (d) 14kV; (e) 15kV



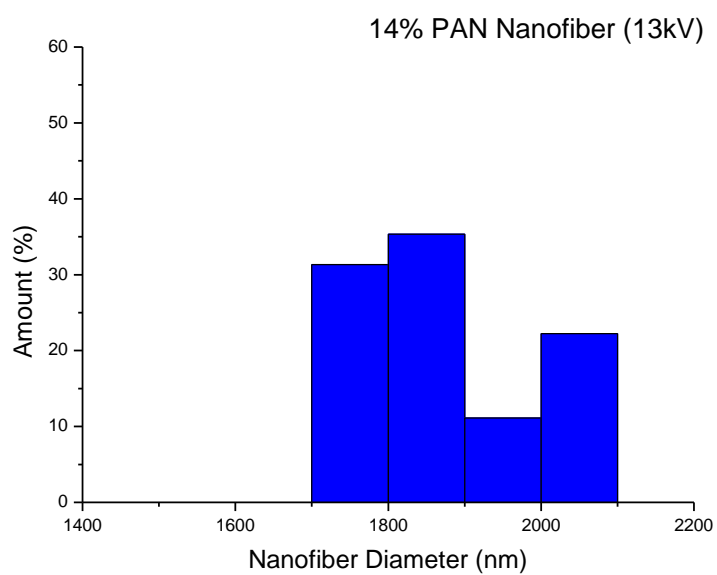
(a)



(b)



(c)



(d)

Figure 6.5: Diameter distribution of 14% PAN nanofibers manufactured in (a) 9kV; (b) 10kV; (c) 11kV; (d) 12kV